

University of New Hampshire

University of New Hampshire Scholars' Repository

Doctoral Dissertations

Student Scholarship

Spring 1997

Dynamic response of poroelastic materials containing Bingham fluid: Application to electrorheological fluids

Mete Kesan

University of New Hampshire, Durham

Follow this and additional works at: <https://scholars.unh.edu/dissertation>

Recommended Citation

Kesan, Mete, "Dynamic response of poroelastic materials containing Bingham fluid: Application to electrorheological fluids" (1997). *Doctoral Dissertations*. 1947.

<https://scholars.unh.edu/dissertation/1947>

This Dissertation is brought to you for free and open access by the Student Scholarship at University of New Hampshire Scholars' Repository. It has been accepted for inclusion in Doctoral Dissertations by an authorized administrator of University of New Hampshire Scholars' Repository. For more information, please contact Scholarly.Communication@unh.edu.

INFORMATION TO USERS

This manuscript has been reproduced from the microfilm master. UMI films the text directly from the original or copy submitted. Thus, some thesis and dissertation copies are in typewriter face, while others may be from any type of computer printer.

The quality of this reproduction is dependent upon the quality of the copy submitted. Broken or indistinct print, colored or poor quality illustrations and photographs, print bleedthrough, substandard margins, and improper alignment can adversely affect reproduction.

In the unlikely event that the author did not send UMI a complete manuscript and there are missing pages, these will be noted. Also, if unauthorized copyright material had to be removed, a note will indicate the deletion.

Oversize materials (e.g., maps, drawings, charts) are reproduced by sectioning the original, beginning at the upper left-hand corner and continuing from left to right in equal sections with small overlaps. Each original is also photographed in one exposure and is included in reduced form at the back of the book.

Photographs included in the original manuscript have been reproduced xerographically in this copy. Higher quality 6" x 9" black and white photographic prints are available for any photographs or illustrations appearing in this copy for an additional charge. Contact UMI directly to order.

UMI

**A Bell & Howell Information Company
300 North Zeeb Road, Ann Arbor MI 48106-1346 USA
313/761-4700 800/521-0600**

DYNAMIC RESPONSE OF POROELASTIC MATERIALS
CONTAINING BINGHAM FLUID: APPLICATION TO
ELECTRORHEOLOGICAL FLUIDS

BY

Mete Kesan

B.S.M.E., Middle East Technical University, 1989

M.S.M.E., Middle East Technical University, 1991

DISSERTATION

Submitted to the University of New Hampshire
in Partial Fulfillment of
the Requirements for the Degree of

Doctor of Philosophy

in

Engineering

May, 1997

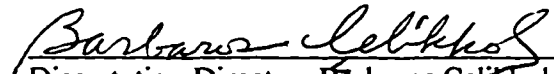
UMI Number: 9730830


UMI Microform 9730830
Copyright 1997, by UMI Company. All rights reserved.

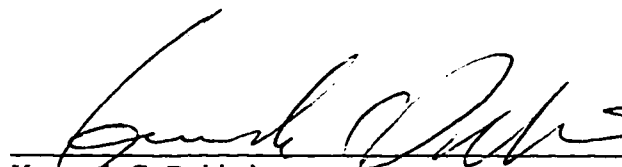
**This microform edition is protected against unauthorized
copying under Title 17, United States Code.**


UMI
300 North Zeeb Road
Ann Arbor, MI 48103

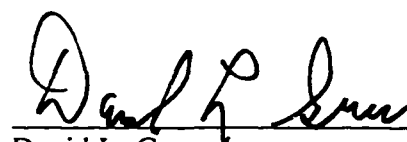
This dissertation has been examined and approved.


Dissertation Director, Barbaros Celikkol
Professor of Mechanical Engineering


M. Robinson Swift
Professor of Mechanical Engineering


Kenneth C. Baldwin
Associate Professor of Mechanical Engineering


Pedro A. De Alba
Professor of Civil Engineering


David L. Gress
Professor of Civil Engineering

May 02, 1997
Date

ACKNOWLEDGMENT

I would like to take this opportunity to express my deep gratitude and appreciation to my supervisor Prof. Barbaros Celikkol for his help, guidance and support during my study at UNH. I would also like to thank Dr. Kenneth Baldwin and Prof. Herbert Kingsbury for their help, encouragement and friendship.

My biggest thanks goes to my family for their patience, sacrifice and encouragement.

TABLE OF CONTENTS

ACKNOWLEDGMENT.....	iii
LIST OF TABLES	vii
LIST OF FIGURES.....	viii
ABSTRACT.....	xi
	<u>PAGE</u>
I. INTRODUCTION	1
II. BACKGROUND.....	5
2.1. Newtonian Fluids in Porous Media	5
2.2. Non-Newtonian Fluids in Porous Media	8
2.3. Electrorheological (ER) Fluids	13
III. THEORY OF POROELASTICITY.....	18
3.1. Biot's Formulation of the Equations of Poroelastic Media	18
3.2. Complex Modulus of a Poroelastic Material	25
3.3. Modified Darcy's Law.....	27
3.4. Governing Equations for Poroelastic Systems Containing Non-Newtonian Bingham Fluid	30
IV. FLOW OF BINGHAM FLUID THROUGH POROUS MEDIA	32
4.1. Finite Element Formulation	33

4.2. Problem Definition	42
4.3. Boundary Conditions.....	43
4.4. Verification of the Numerical Model.....	44
4.5. Results	46
V. INCORPORATING ELECTORRHEOLOGICAL FLUIDS IN POROUS MEDIA.....	53
5.1. Introduction	53
5.2. Electrorheological Fluid Characteristics.....	53
5.3. Electrorheological Fluid Behavior.....	56
5.4. Poroelastic Systems Incorporating ER Fluids.....	58
5.5. Field Dependency of Parameters.....	61
5.6. Results	64
VI. CONCLUSIONS.....	75
BIBLIOGRAPHY	80

APPENDICES	<u>PAGE</u>
A. GOVERNING EQUATIONS OF POROELASTIC SYSTEMS	90
A.1. Stress-Strain Equations	91
A.2. Strain-Displacement Equations.....	94
A.3. Equilibrium Equations	95
A.4. Darcy's Law.....	96
B. GALERKIN WEIGHTED-RESIDUAL METHOD	98

C. ELEMENTAL COEFFICIENT MATRICES AND RIGHT-HAND-SIDE VECTORS	100
C.1. Derivation of $[K_e^u]$	101
C.2. Derivation of $[K_e^{P1}]$	102
C.3. Derivation of $[K_e^{P2}]$	103
C.4. Derivation of $[M_e^u]$	105
C.5. Derivation of $[M_e^{\dot{p}}]$	106
C.6. Derivation of $\{F_e^1\}$	107
C.7. Derivation of $\{F_e^2\}$	108
D. NUMERICAL CODE	110

LIST OF TABLES

<u>TABLE</u>	<u>PAGE</u>
4.1. Material properties used for the verification of the numerical model ..	44
4.2. Material properties used in the calculations	47
5.1. Material Properties of the poroelastic material and ER fluids.....	61

LIST OF FIGURES

<u>FIGURE</u>	<u>PAGE</u>
2.1. Variation of storage modulus and loss factor of a fluid-filled foam with frequency	7
2.2. Variation of shearing stress with rate of shearing strain for several types of fluids.....	10
2.3. Idealized constitutive shear behavior of ER materials	14
3.1. Relation between fluid velocity and pressure gradient for non-Newtonian Bingham fluid flow in porous medium	28
4.1. Linear trial function $N_j(y)$ and the derivatives $N_j'(y)$	36
4.2. Linear trial functions defined for an element	38
4.3. Poroelastic column subjected to harmonic surface displacement ...	43
4.4. Comparison of the numerical results with analytical results for solid displacement.....	45
4.5. Comparison of the numerical results with analytical results for fluid pressure	46
4.6. Variation of apparent viscosity along y-direction.....	48
4.7. Solid-phase displacements in y-direction	49
4.8. Variation of fluid pressure along y-direction.....	49

4.9	Variation of pressure gradient along y-direction	50
4.10	Storage modulus of the poroelastic material containing Bingham fluid.....	51
4.11	Loss tangent of the poroelastic material containing Bingham fluid.....	51
5.1.	Development of the chainlike structure in a model ER fluid with increasing DC electric field	55
5.2.	ER fluid-filled poroelastic column subjected to harmonic surface displacement.....	59
5.3.	Electric field dependency of yield stress (ERF I)	62
5.4.	Electric field dependency of plastic viscosity (ERF I)	62
5.5.	Electric field dependency of yield stress (ERF II)	63
5.6.	Electric field dependency of plastic viscosity (ERF II).....	63
5.7.	Variation in the apparent viscosity of ERF I along y-direction for (a) $E=0$ kV/mm, (b) $E=1$ kV/mm, (c) $E=2$ kV/mm.....	65
5.8.	Variation in the apparent viscosity of ERF II along y-direction for (a) $E=0$ kV/mm, (b) $E=2$ kV/mm, (c) $E=5$ kV/mm.....	66
5.9.	Variation of solid displacement with electric field (ERF I).....	68
5.10.	Variation of solid displacement with electric field (ERF II).....	68
5.11.	Variation of fluid pressure with electric field (ERF I)	69
5.12.	Variation of fluid pressure with electric field (ERF II).....	69
5.13.	Variation of pressure gradient with electric field (ERF I).....	70

5.14. Variation of pressure gradient with electric field (ERF II)	70
5.15. Storage modulus calculated at different electric fields (ERF I).....	71
5.16. Loss tangent calculated at different electric fields (ERF I)	72
5.17. Storage modulus calculated at different electric fields (ERF II)	72
5.18. Loss tangent calculated at different electric fields (ERF II).....	73
C.1. Variation of apparent viscosity over the element Ω_e	103

ABSTRACT

DYNAMIC RESPONSE OF POROELASTIC MATERIALS CONTAINING BINGHAM FLUID: APPLICATION TO ELECTRORHEOLOGICAL FLUIDS

by

Mete Kesan

University of New Hampshire, May, 1997

This work examines the dynamic response to harmonic loading of a disk of poroelastic material containing non-Newtonian Bingham fluid which exhibits a yield stress. Biot's poroelasticity equations and modified Darcy's law for non-Newtonian fluids exhibiting a yield stress are combined together to obtain the governing equations of the system for quasi-static case. Dissipation due to friction arising from the flow of fluid relative to the solid is taken into account but inertia effects are neglected. The response and the complex modulus of the system are calculated using the finite element method taking into account the nonlinear nature of Bingham fluid. As an application of the model developed, the behavior of electrorheological (ER) fluids in poroelastic media is investigated. The storage modulus and loss tangent are obtained for different electric field strengths. The results suggest that ER fluid-porous solid

device can be tuned to provide optimum stiffness and damping as excitation or resonant frequencies change.

CHAPTER I

INTRODUCTION

Even though most studies conducted on flow and transport in porous media deal with Newtonian fluids, a tremendous effort has also been devoted to developing quantitative analysis of flow of non-Newtonian fluids through porous media. The theoretical investigations carried out in this field have concentrated mainly on single-phase non-Newtonian fluid flow, while the experimental attempts have been designed to provide flow analysis with rheological models for non-Newtonian fluids and porous materials of interest.

In order to apply Darcy's law which is an empirical relation between the flow velocity and pressure gradient, to the flow of non-Newtonian fluids in porous media, apparent viscosities are needed for use in the Darcy equation. A significant amount of laboratory studies has been performed by many investigators in an effort to develop correlations for apparent viscosities of non-Newtonian fluids in porous media. In almost all of these studies, a power-law viscosity model has been used exclusively to approximate the flow behavior of non-Newtonian fluids. However, there is considerable evidence from laboratory experiments that certain fluids in porous media exhibit a Bingham-type non-Newtonian behavior. For these fluids, flow takes place

only after the pressure gradient exceeds a certain minimum value which is called as “threshold gradient”. Analogous to Darcy’s law which is developed for Newtonian fluids, modified Darcy’s law is developed for the flow of non-Newtonian Bingham type fluids which exhibit a yield stress, in porous media. Dynamic behavior of Bingham fluid in porous media is highly nonlinear because of the yield stress of the fluid. Bingham fluids behave like a solid as long as the pressure gradient is less than the threshold gradient. Once the threshold gradient is overcome, the flow starts and Bingham material behaves like a non-Newtonian viscous fluid. There are only a few studies in the literature on the flow of Bingham fluid in porous media. In some of these studies, considering that a portion of the fluid will flow, the location of the yield surface is predicted at each time step and the solution is obtained for the yielded portion of the Bingham fluid. On the contrary, Lipscomb and Denn (1984) showed that yield surfaces cannot exist in confined, complex geometries, and flow must occur at all interior points.

The petroleum industry has received most of the attention with regard to the research on the flow of non-Newtonian Bingham fluid in porous media. However, a new type of fluids called electrorheological (ER) fluids which exhibit Bingham type of fluid behavior are also studied by many researchers in this area in the past 30 years. Electrorheological (ER) fluids are suspensions of fine particles in a non-conducting oil. They are distinctive because, when subjected to an electric field, they solidify and behave like a non-Newtonian Bingham fluid. They exhibit a yield stress which is proportional to the applied voltage. By varying the applied voltage, the yield stress and

the viscosity of ER fluid can be altered. One of the most important reason for the lack of commercially available devices employing ER fluids is the low strength characteristics of ER fluids. There is significant amount of research going on to find new particle/fluid combinations that can withstand higher stresses. On the other hand, incorporating ER fluids in a poroelastic structure can increase the material strength considerably even with the current ER fluids and can still provide controllable stiffness and damping characteristics.

It is the goal of this work to develop a theory to investigate the dynamic response to harmonic loading of poroelastic materials containing non-Newtonian Bingham fluid which exhibits a yield stress. As an application of the theory developed, the use of combinations of electrorheological fluids and porous deformable solids to construct active vibration control devices will be explored.

Chapter 2 reviews the literature on the experimental and theoretical studies of Newtonian and non-Newtonian fluid flow through porous media and electrorheological fluids.

In Chapter 3, Biot's theory of poroelasticity is reviewed first. Then, Biot's theory of poroelasticity is combined with the modified Darcy's law which is developed for non-Newtonian Bingham fluids, to obtain the modified governing equations describing the flow of Bingham fluid in poroelastic media.

Chapter 4 is devoted to the development of a numerical model for the solution of nonlinear governing equations. A model problem is defined, boundary conditions are specified and the solution is obtained by using the numerical model developed. The

results obtained from the numerical model are also compared with the exact solution in Chapter 4.

Chapter 5 explains the brief theory of electrorheological fluids. The model developed is modified for the analysis of ER fluid flow in poroelastic media. Also, field dependencies of ER fluid parameters are investigated and the results obtained from the numerical model for the problem defined are presented and interpreted in this chapter.

Finally, the conclusion of this work is given in Chapter 6. Several important conclusions are drawn considering the results obtained from the model developed. The results suggests that electrorheological fluid-filled poroelastic systems can be used as an active vibration isolation devices to provide optimum stiffness and damping as excitation or resonant frequencies change.

CHAPTER II

BACKGROUND

2.1. Newtonian Fluids in Porous Media

The theory of poroelastic media has its origins in the one-dimensional theory of consolidation formulated by Terzaghi (1925, 1943) for use in soil mechanics where settling of water-soaked soils under load is called consolidation. Beginning in 1941, M.A. Biot published a series of papers dealing with a general theory of behavior of what are now termed poroelastic materials [Biot (1941, 1955, 1956)]. Biot's poroelastic materials are two-phase solid-fluid-filled systems. The porous-solid skeleton is linearly elastic and undergoes small deformations while the flow of fluid produced by deformation of the material is governed by Darcy's law. In his first paper, the isotropic poroelastic material is studied [Biot (1941)]. Then, he generalized the theory to anisotropic materials [Biot (1955)] and obtained the general solutions to the poroelasticity equations [Biot (1956)].

A mathematical treatment to predict the fluid damping of open-cell foams was proposed by Rush (1965) and by Gent and Rush (1966). In their analysis, a rectangular block of Newtonian fluid-filled foam which is sinusoidally compressed, is considered. The fluid inside the foam specimen is forced to flow through the sides of the matrix.

The pressure distribution was determined and the average compressive stress in the cross-section of the specimen was calculated. This stress was added to the compressive stress of the foam matrix and an equivalent complex modulus of open-cell foam was derived. They predicted the frequency dependence of the complex modulus to be qualitatively as shown in Fig. 2.1.

The complex modulus of a viscoelastic material is basically defined from the ratio of the stress to the strain. For a harmonic loading, the stress and strain will both vary sinusoidally, but the strain lags behind the stress. The real part of the modulus is often called the *storage modulus* because it defines the energy stored in the specimen due to the applied strain. The imaginary part of the modulus, which is out of phase with the strain, defines the dissipation of energy and is often called the *loss modulus*. Also, the ratio of the loss modulus to the storage modulus usually named as the *loss factor*.

Another typical behavior of viscoelastic materials is the *rubber to glass transition behavior*. Typically at low frequencies viscoelastic materials are soft and flexible while at high frequencies they are stiff. These two types of behavior are called rubbery and glassy, respectively. There is a certain range of frequency called rubber to glass transition frequency over which the behavior of viscoelastic materials changes rapidly from rubbery to glassy. Since the region is usually quite narrow, specific values of frequency called the rubber to glass transition frequency are often quoted in literature.

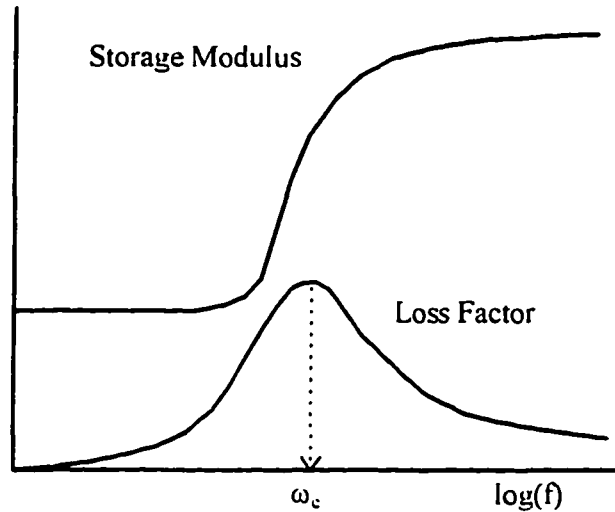


Fig. 2.1. Variation of storage modulus and loss factor of a fluid-filled foam with frequency

As the frequency is increased, the fluid flow resistance increases, resulting in increased material stiffness and loss factor. At high frequencies, the interaction force between the fluid and the solid matrix becomes so large that the solid and fluid move together and there is no fluid flow. At these frequencies the loss factor becomes zero and the storage modulus becomes its maximum. Thus, as the frequency increases, the loss factor starts to increase and reaches its maximum at a “critical” frequency ω_c , and then reduces to the matrix loss factor again. Similarly, the storage modulus starts to increase from the matrix storage modulus and approaches its maximum value as the frequency goes to infinity.

The model of Gent and Rusch explains the effects of the material constants and the specimen geometry on the fluid damping. The validity of their analysis has been

well proven by extensive experiments. However, the method cannot be applied to different deformation modes and/or flow boundary conditions.

In order to analyze the fluid damping in more general deformation modes and fluid flow conditions, it is essential to have constitutive equations for the fluid-solid system. Wijesinghe and Kingsbury (1979) used Biot's poroelastic theory to describe a theoretical complex modulus of the poroelastic material containing Newtonian viscous fluid. In their analysis, the dynamic response of a porous material subjected to harmonic surface displacement was considered. The resulting theoretical complex modulus shows a frequency response similar to the one shown in Fig. 2.1.

2.2. Non-Newtonian Fluids in Porous Media

Flow of non-Newtonian fluids through porous media occurs in many systems and has found applications in certain technological areas. Previous studies on the flow of fluids through porous media were limited for the most part to Newtonian fluids. Since the 1950's, the flow of non-Newtonian fluids through porous media has received a significant amount of attention because of its important industrial applications. Most of the research on non-Newtonian fluid flow is related to the petroleum industry. Non-Newtonian fluids, especially polymer solutions, are often injected into reservoirs in various enhanced oil recovery processes. There exist a considerable amount of literature and reports on the use of polymeric and chemical additives in oil recovery processes.

In contrast with classical fluid mechanics developed for Newtonian fluids, the theory of non-Newtonian fluid dynamics is a very new branch of applied sciences. The increasing importance of non-Newtonian fluids has been recognized in those fields dealing with materials whose flow behavior of stress and shear rate cannot be characterized by Newton's law of viscosity. In a broad sense, fluids are divided into two main categories: (1) Newtonian, and (2) non-Newtonian. Newtonian fluids follow Newton's law of viscous resistance and possess a constant viscosity. Non-Newtonian fluids deviate from Newton's law of viscosity, and exhibit variable viscosity. The behavior of non-Newtonian fluids is generally represented by a rheological model, or correlation of shear stress and shear rate. Although there are many rheological models available for different non-Newtonian fluids in the literature, the simplest and most common are shown in Fig. 2.2. The slope of shearing stress vs. rate of shearing strain graph is denoted as apparent viscosity, μ_a . For Newtonian fluids the apparent viscosity is the same as the viscosity and is independent of shear rate.

For shear thinning fluids the apparent viscosity decreases with increasing shear rate - the harder the fluid is sheared, the less viscous it becomes. Many colloidal suspensions and polymer solutions are shear thinning. For shear thickening fluids the apparent viscosity increases with increasing shear rate - the harder the fluid is sheared, the more viscous it becomes. Common examples of this type of fluid include water-corn starch mixture and water-sand mixtures.

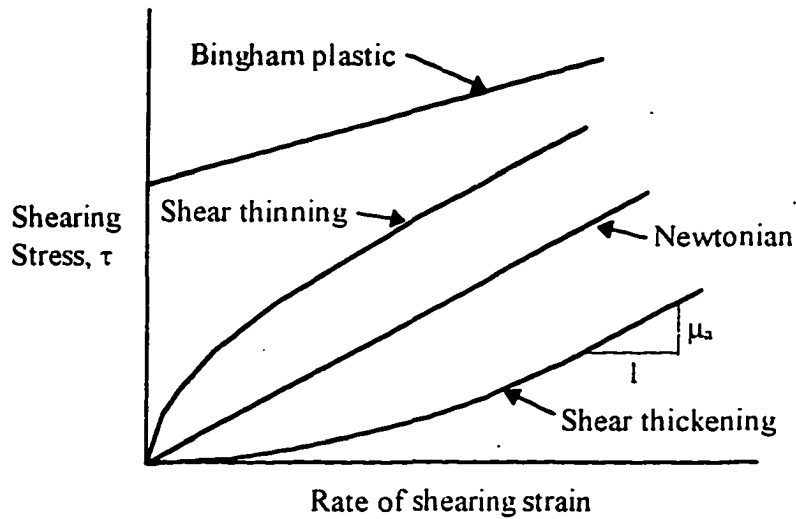


Fig. 2.2. Variation of shearing stress with rate of shearing strain for several types of fluids.

The other type of behavior indicated in Fig. 2.2 is that of a Bingham plastic. Such material can withstand a finite shear stress without motion, but once the yield stress is exceeded it flows like a fluid. The characteristics of these fluids are defined by two constants: the yield stress τ_y , which is the stress that must be exceeded for flow to begin, and the plastic viscosity μ_0 , which is the slope of the straight line in Fig. 2.2. The rheological equation for a Bingham plastic is then,

$$\tau = \tau_y + \mu_0 \dot{\gamma} \quad (2.1)$$

in which τ is the shearing stress and $\dot{\gamma}$ is the rate of shearing strain.

To date the power-law model is the most widely used rheological model for the flow problems in porous media. Originally formulated from an empirical curve-fitting function, the power-law model is represented by,

$$\tau = H\dot{\gamma}^n \quad (2.2)$$

where n is the power-law index and H is called the consistence coefficient. For $n=1$, the fluid becomes Newtonian.

Compared with studies conducted on flow of non-Newtonian power-law fluids, there are only a few publications dealing with flow problems in porous media involving non-Newtonian Bingham fluids.

A series of papers on the non-Newtonian fluid flow through porous medium is published by Pascal (1981, 1983, 1984, 1985, 1986, 1989). He has analyzed theoretically the application of Darcy's law to Bingham fluid flow by introducing the effect of the yield value in a so-called "threshold gradient". He has investigated the effect of the threshold gradient in steady and unsteady state flow through porous media and has obtained solutions for well flow test analyses [Pascal (1981)]. He also extended the theory for nonsteady flow of power-law fluids with a yield stress through a porous medium. In his analyses, the approximate solutions in a closed form were obtained by using the integral method [Pascal (1983)]. His next study was the investigation of the rheological behavior effect of non-Newtonian fluids on the dynamic of moving interface in porous media by using Muskat's model which

describes the flow of two immiscible fluids, separated by an interface, in oil displacement mechanisms from a porous medium [Pascal (1984)]. He recently published a paper [Pascal (1989)] which presents a mathematical model for describing approximately the viscoelastic effect in non-Newtonian steady flows through a porous medium.

Al-Fariss and Pinder (1987) used the modified, more general form of Darcy's law which describes the flow through porous media of homogeneous fluids whose flow behavior can be characterized by power-law model. In their analysis, a more general Reynolds number for flow through porous media, which includes a fluid yield value was developed. They also verified their model with the experimental results obtained from the flow of crude oil in packed beds of sand.

Lipscomb and Denn (1984) studied the flow of Bingham fluid in complex geometries. They concluded that Bingham fluids cannot contain yield surfaces in complex, confined geometries and flow must occur at all interior points.

Wu (1990) presented a theoretical study on the flow and displacement of Bingham fluid in porous media. He developed an integral method of analyzing the single-phase flow of this type of fluid and confirmed the accuracy of the approximate analytical solution developed by comparison with numerical solutions.

Vradis et al. (1993) derived macroscopic equations of motion in saturated porous media for non-Newtonian Bingham fluids. They used "capillary tubes" as well as the "resistance to flow" models which are modified to account for the effects of the

yield stress. In addition, the minimum static head gradient required for the initiation of flow in porous medium is predicted using the two models developed.

2.3. Electrorheological (ER) Fluids

ER fluids are suspensions of fine particles in non-conducting oil. They are distinctive because, when subjected to an electric field, they instantly turn into a gel-like solid. When the current is removed, they revert to the liquid state. This change in state can occur in 0.0001 to 0.001 second.

ER fluids were discovered in 1947 by Willis M. Winslow who patented them [Winslow (1947)], and published the first paper regarding them [Winslow (1949)]. In fact, originally the term “Winslow effect” was used to describe the unique action of ER fluids.

When an electric field is applied across the ER fluid, positive and negative charges on the suspended particles respond by separating such that each particle has a positive and a negative end. The particles are then attracted to each other forming chains between the electrodes - similar to the way iron filings align themselves in a magnetic field. When the electric field is removed, charges no longer separate on the particles, and the fluid returns to its original no-field flow characteristics in a fully reversible manner. The gelling is proportional to field strength, so by varying the voltage, any rheological state from liquid to solid and back again can be smoothly and instantly selected. Upon jelling, when a shearing force is applied the gel reacts as a solid with a measurable stiffness. Upon increasing the force, a critical value is reached

whereupon the material flows. This critical force per unit area is termed the yield stress. Normally, the yield stress is proportional to the applied voltage, and increases with particle volume fraction.

The carrier fluids can be based on almost any type of oil and the particles which are typically in the range of 1-10 μm can consist of either organic materials like starch and cellulose or inorganics like ceramics, glass, and a variety of polymers. The carrier fluids must be good insulators as well as be compatible with the materials they contact. Today, silicone oil, mineral oil and chlorinated paraffin are mostly used as carrier fluids. Density matching between the particles and carrier fluid is very desirable to reduce the sedimentation.

The typical constitutive behavior of an ER fluid in shear is shown in Fig. 2.3 where shear stress is plotted as a function of shear strain and shear rate, respectively.

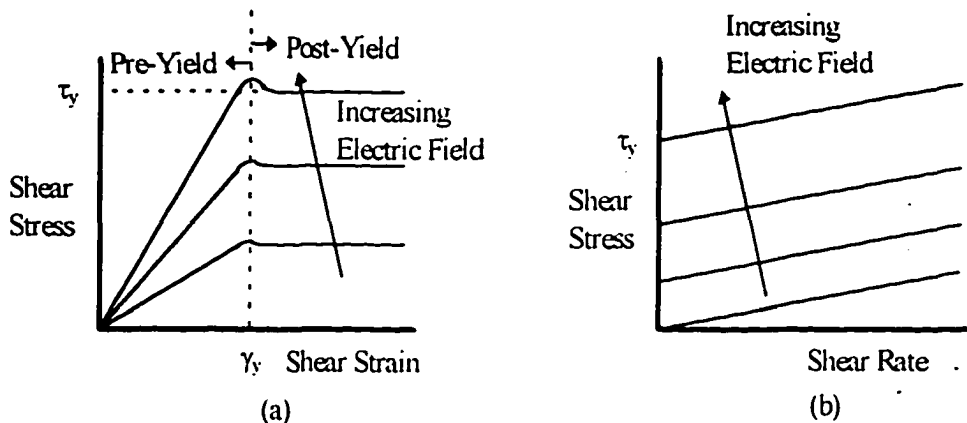


Fig. 2.3. Idealized constitutive shear behavior of ER materials

As shown in Fig. 2.3, ER material behavior can be divided into pre-yield and post-yield regions. These materials under a non-zero field can be described as

viscoelastic solids below a certain yield stress or yield strain (pre-yield region) and as non-Newtonian viscous liquids for stresses at or above the yield stress or strains equal or greater than the yield strain (post-yield region). Controllable devices are based on the post-yield behavior depicted in Fig. 2.3b. For post-yield situations the constitutive shear behavior of ER materials is often modeled using the Bingham plastic approximation.

Since their discovery in 1947, ER fluids received only minor research attention in the 1960's and 1970's. Serious research began in the 1980's. Klass and Martinek (1967) investigated the effect of many parameters such as composition, shear rate, frequency and temperature on the apparent viscosity of electroviscous fluid.

Gamota and Filisko (1991a) experimentally studied the response of an ER material to sinusoidally oscillating shear strains at moderate frequencies. They discussed the response of material in terms of three rheological regions; pre-yield, yield and post-yield. Furthermore, the energy dissipated by the ER material is analyzed as related to strain amplitude and electric field. They also extended their analysis for the frequencies in the range of 300-400 Hz and measured the storage and loss factor of the ER material for various electric field strengths [Gamota and Filisko (1991b)].

Xu and Liang (1991) developed a new type of semiconducting polymer-based ER suspension. They measured the rheological properties such as yield stress, complex viscosity, dynamic modulus as functions of electric field, particle concentration, water content and temperature.

Coulter et al. (1992) discussed the usage of ER materials in controllable devices such as anti-vibration mounts, clutches, and dampers. They summarized the models which have been developed to simulate the response of such structures with an attempt to identify current and future key areas of research and development in ER material applications technology.

Williams et al. (1992) worked on the mathematical modeling of ER fluids when used in oscillating squeeze-flow mode; in a prototype automotive engine mount. They found a solution for the situation in which the non-Newtonian behavior of the fluid is represented by a bi-viscous characteristic.

Fujita et al. (1993) measured the viscosity of electro-rheological (ER) and magneto-rheological (MR) fluids under electric and magnetic fields, respectively and concluded that the electric field was more effective than the magnetic field in increasing the viscosity.

Weiss et al. (1994) examined the transition area between the elastic and viscous behavior for the electro-rheological and magneto-rheological fluids. Both ER and MR fluids were observed to yield at a strain level of less than 1% in their measurements. They suggested that the research efforts should be focused in development of ER and MR fluids that yield at a higher level of strain.

Kudallar et al. (1994) discussed the use of pre-yield rheological behavior of an ER fluid in a mount structure for precision applications to demonstrate tunable stiffness and damping in a changing environment. They modeled the ER fluid as a

simple linear viscoelastic model. Their preliminary design analysis of the mount structure showed that damping and stiffness control is feasible.

Over the last 20 years, a significant amount of effort has been directed towards the development of ER material applications. The controllable rheological nature of these materials has been evaluated for a wide range of application concepts. Significant advancements in the development and understanding of ER material controllable devices have been realized, with the primary proposed device types being valves, mounts, clutches, and dampers. In addition, during the past several years the new potential ER application area of adaptive structures has emerged. Proof of concept studies in this area have been completed, but the theoretical understanding of ER adaptive structures requires further development.

CHAPTER III

THEORY OF POROELASTICITY

3.1. Biot's Formulation of the Equations of Poroelastic Media

Biot's poroelastic materials are two phase solid-fluid filled systems. The porous solid skeleton is linearly elastic and undergoes small deformations while the flow of fluid produced by the deformations of the material is governed by Darcy's law. He developed the theory for isotropic and anisotropic poroelastic materials and obtained the general solutions to the poroelasticity equations for quasi-static case. A dynamic theory for such systems is also developed by Biot, for the study of wave propagation. In this chapter, Biot's quasi-static formulation which includes the dissipation but neglects the fluid inertia is presented.

The quasi-static poroelastic theory as presented by Biot is based on several fundamental assumptions. The two-phase poroelastic material is considered to be comprised of a solid material forming a framework possessing a statistical distribution of small pores filled with, in general, a Newtonian viscous, compressible fluid. The bulk material is assumed to be homogeneous on a microscopic scale and the pores to be all interconnected. The deformation of the solid and fluid are taken to be reversible

with the solid skeleton being linearly elastic and undergoing small deformations. The fluid is assumed to follow Darcy's law and the stresses in the bulk material are assumed to be smoothly divided between the solid and the fluid. In the quasi-static theory the inertia effects, considered in the dynamic theory, are neglected. The sign convention used in this work assumes that tensile stresses are positive and compressive stresses are negative.

The porosity "n" of a poroelastic material is defined as the ratio of pore volume to the volume of the bulk material. It can also be defined as the ratio of the void area to the total area of any cross section of the bulk material.

Several different measures of stress are defined by Biot. Let F_{T_i} be the x_i component of the total force acting on a small surface of area A with outward normal x_i of a fluid-filled porous solid. If F_{s_i} is the corresponding force component acting on the solid phase of the material and F_{f_i} is the force component on the fluid phase (normal component only) then,

$$F_{T_i} = F_{s_i} + F_{f_i} \quad (3.1)$$

The total stress (τ_{ij}), the average solid stress (σ_{ij}) and the average fluid stress (σ) are defined, respectively as

$$\tau_y = \frac{F_{T_i}}{A} \quad (3.2)$$

$$\sigma_{ij} = \frac{F_s}{A} \quad (3.3)$$

$$\sigma = \frac{F_f}{A} \quad (3.4)$$

so that

$$\tau_{ij} = \sigma_{ij} + \sigma \delta_{ij} \quad (3.5)$$

where δ_{ij} is the Kronecker delta. The actual stresses, $\tilde{\sigma}_{ij}$, acting on the solid phase material of area A_s and the fluid pressure, P , acting on the fluid area A_f are given by

$$\tilde{\sigma}_{ij} = \frac{F_s}{A_s} \quad (3.6)$$

$$P = \frac{-F_f}{A_f} \quad (3.7)$$

where the minus sign indicates that pressure is a negative normal stress.

Since $A_f = nA$ and $A_s = (1-n)A$, the average and actual solid and fluid phase stresses are related by

$$\sigma_{ij} = (1-n)\tilde{\sigma}_{ij} \quad (3.8)$$

$$\sigma = -nP \quad (3.9)$$

Then, the total stress can be defined in terms of actual solid and fluid stresses as

$$\tau_{ij} = (1-n)\tilde{\sigma}_{ij} - nP\delta_{ij} \quad (3.10)$$

Biot has postulated several forms of a linear relationship between the seven stress components and seven strain components for the fluid-filled poroelastic systems.

The most general of those [Biot (1955)] may be expressed as

$$\begin{Bmatrix} \sigma_{xx} \\ \sigma_{yy} \\ \sigma_{zz} \\ \sigma_{yz} \\ \sigma_{zx} \\ \sigma_{xy} \\ \sigma \end{Bmatrix} = \begin{bmatrix} C_{11} & C_{12} & C_{13} & C_{14} & C_{15} & C_{16} & C_{17} \\ & C_{22} & C_{23} & C_{24} & C_{25} & C_{26} & C_{27} \\ & & C_{33} & C_{34} & C_{35} & C_{36} & C_{37} \\ & & & C_{44} & C_{45} & C_{46} & C_{47} \\ & & & & C_{55} & C_{56} & C_{57} \\ & & & & & C_{66} & C_{67} \\ & & & & & & C_{77} \end{bmatrix} \begin{Bmatrix} e_{xx} \\ e_{yy} \\ e_{zz} \\ 2e_{yz} \\ 2e_{zx} \\ 2e_{xy} \\ \varepsilon \end{Bmatrix} \quad (3.11)$$

where σ_{ij} are the average solid stresses, σ is the average fluid stress, and e_{ij} are the solid strains which can be defined as

$$e_{ij} = \frac{1}{2} \left(\frac{\partial u_i}{\partial x_j} + \frac{\partial u_j}{\partial x_i} \right) \quad (3.12)$$

Similarly, the solid dilatation, e , and the fluid dilatation, ε , are defined in terms

of the average solid phase displacements, u_i , and the average fluid phase displacements, U_i , as

$$e = \frac{\partial u_i}{\partial x_i} \quad \text{or} \quad e = e_{xx} + e_{yy} + e_{zz} \quad (3.13)$$

$$\varepsilon = \frac{\partial U_i}{\partial x_i} \quad \text{or} \quad \varepsilon = \varepsilon_{xx} + \varepsilon_{yy} + \varepsilon_{zz} \quad (3.14)$$

For the isotropic poroelastic material, only four of the coefficients in Equation (3.11) are independent. Then, the stress-strain relationship which employs the total stress τ_{ij} [Biot (1957)] can be written as

$$\begin{pmatrix} \tau_{xx} \\ \tau_{yy} \\ \tau_{zz} \\ \tau_{yz} \\ \tau_{zx} \\ \tau_{xy} \\ P \end{pmatrix} = \begin{bmatrix} 2\mu^* + \lambda^* + \alpha^2 M & \lambda^* + \alpha^2 M & \lambda^* + \alpha^2 M & 0 & 0 & 0 & -\alpha M \\ \lambda^* + \alpha^2 M & 2\mu^* + \lambda^* + \alpha^2 M & \lambda^* + \alpha^2 M & 0 & 0 & 0 & -\alpha M \\ \lambda^* + \alpha^2 M & \lambda^* + \alpha^2 M & 2\mu^* + \lambda^* + \alpha^2 M & 0 & 0 & 0 & -\alpha M \\ 0 & 0 & 0 & \mu^* & 0 & 0 & 0 \\ 0 & 0 & 0 & 0 & \mu^* & 0 & 0 \\ 0 & 0 & 0 & 0 & 0 & \mu^* & 0 \\ -\alpha M & -\alpha M & -\alpha M & 0 & 0 & 0 & M \end{bmatrix} \begin{pmatrix} e_{xx} \\ e_{yy} \\ e_{zz} \\ 2e_{yz} \\ 2e_{zx} \\ 2e_{xy} \\ \zeta \end{pmatrix} \quad (3.15)$$

or in index notation

$$\tau_{ij} = 2\mu^* e_{ij} + [(\lambda^* + \alpha^2 M)e - \alpha M \zeta] \delta_{ij} \quad (3.16)$$

$$P = -\alpha M e + M \zeta \quad (3.17)$$

in which

μ^* , λ^* : Lamé's constants of the skeleton

α : Solid-phase compressibility coefficient

M : Modified bulk modulus which is defined as

$$M = \frac{1}{n(c - \delta) + \alpha\delta} \quad (3.18)$$

c : Fluid compressibility

δ : Compressibility of the solid comprising the skeleton

ζ : Increment of fluid content in porous material during a deformation which is defined as

$$\zeta = n(e - \varepsilon) \quad (3.19)$$

These parameters are usually determined experimentally. Combining Equations (3.16) and (3.17), the isotropic stress-strain relation becomes

$$\tau_{ij} = 2\mu^* e_{ij} + (\lambda^* e - \alpha P) \delta_{ij} \quad (3.20)$$

In the absence of body forces, the stress equilibrium equations are

$$\frac{\partial \tau_{ij}}{\partial x_j} = 0 \quad (3.21)$$

Combining Equations (3.20) and (3.21) gives the first governing equation as

$$\mu^* u_{i,kk} + (\lambda^* + \mu^*) u_{k,ki} - \alpha P_{,i} = 0 \quad (3.22)$$

At this point there are seven unknown stress components, seven unknown strain components, and six unknown displacement components giving a total of twenty unknowns. Also, there are seven stress-strain equations, seven strain-displacement equations and three equilibrium equations that make a total of seventeen equations (see Appendix A). The discrepancy between the number of equations and unknowns is rectified by the use of an empirical physical principle; Darcy's law which relates the flow velocity to the pressure gradient of the fluid, to complete the theory. Darcy's law is given as

$$\frac{\partial}{\partial t}(U_i - u_i) = \frac{-k}{\mu_v} \left(\frac{\partial P}{\partial x_i} \right) \quad (3.23)$$

Taking the divergence of Equation (3.23) and combining with Equation (3.17) yields the second governing equation as

$$P_{,kk} = \frac{\partial}{\partial t} (\beta_1 u_{i,i} + \beta_2 P) \quad (3.24)$$

in which

$$\beta_1 = \frac{\mu_0 \alpha}{n k} \quad , \quad \beta_2 = \frac{\mu_0}{M n k}$$

Equations (3.22) and (3.24) are the constitutive equations governing the flow and deformation of poroelastic media containing Newtonian fluid. In case of one dimensional problem, the governing equations can be written as

$$(\lambda^* + 2\mu^*) \frac{\partial^2 u_y}{\partial y^2} - \alpha \frac{\partial P}{\partial y} = 0 \quad (3.25)$$

$$\frac{\partial^2 P}{\partial y^2} - \frac{\partial}{\partial t} \left(\beta_1 \frac{\partial u_y}{\partial y} + \beta_2 P \right) = 0 \quad (3.26)$$

3.2. Complex Modulus of a Poroelastic Material

Using the isotropic stress-strain relation given by Equation (3.20) the total stress in y-direction can be written as

$$\tau_{yy} = 2\mu^* e_{yy} + (\lambda^* e - \alpha P) \quad (3.27)$$

For one-dimensional problem, e_{xx} and e_{zz} will be negligible. Then, the stress in y-direction will be equal to

$$\tau_{yy} = (\lambda^* + 2\mu^*) \frac{\partial u_y}{\partial y} - \alpha P \quad (3.28)$$

The complex modulus $K(\omega)$ is defined as the ratio of normal surface stress to a dimensionless surface displacement as

$$K(\omega) = \frac{\tau_{yy}|_{y=d}}{\left(\frac{V_0}{d}\right)} \quad (3.29)$$

where V_0 is the amplitude of the harmonic surface displacement and d is the height of the poroelastic material. Substituting stress equation (3.28) in Equation (3.29) the complex modulus can be obtained in terms of the solid displacement u_y and the fluid pressure P as

$$K(\omega) = \left[(\lambda^* + 2\mu^*) \frac{\partial u_y}{\partial y} \Big|_{y=d} - \alpha P(d) \right] \left(\frac{V_0}{d} \right)^{-1} \quad (3.30)$$

Then, the storage modulus $K_s(\omega)$ and the loss factor $\eta(\omega)$ is defined by

$$K(\omega) = K_s(\omega)[1 + i\eta(\omega)] \quad (3.31)$$

3.3. Modified Darcy's Law

Darcy's law is an empirical relationship between the fluid velocity v and the pressure drop ΔP in the steady flow of a Newtonian fluid through a porous medium and can be written, in most general form, as

$$v = -\frac{k}{\mu_0} \cdot \Delta P \quad (3.32)$$

Nevertheless, Darcy's law cannot be applied for the flow through a porous medium of non-Newtonian fluids with a yield stress. A modified Darcy's law to take into account the non-Newtonian rheological effect is required. Pascal (1983) obtained the modified Darcy's law as the relationship between the flow velocity and pressure gradient for non-Newtonian Bingham fluids exhibiting a yield stress as

$$v = -\frac{k}{\mu_0} \cdot \left(\Delta P - \alpha_0 \frac{\Delta P}{|\Delta P|} \right) \quad (3.33)$$

or in a second form which employs the apparent viscosity μ_a

$$v = -\frac{k}{\mu_a} \cdot \Delta P \quad (3.34)$$

which is valid provided that

$$\begin{aligned} |\Delta P| \geq \alpha_0 & ; v \neq 0 \\ |\Delta P| < \alpha_0 & ; v = 0 \end{aligned}$$

In Fig. 3.1, fluid velocity v is plotted as a function of pressure gradient ΔP for the flow of non-Newtonian Bingham fluid through porous media as described by modified Darcy's law.

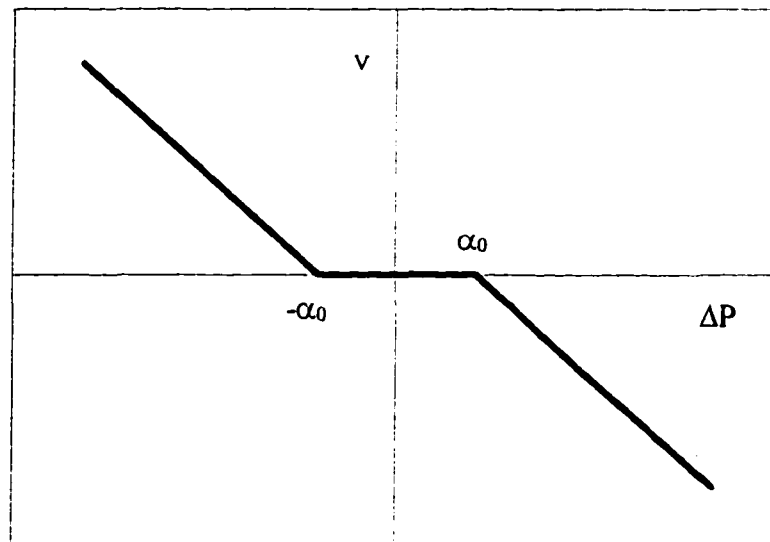


Fig. 3.1. Relation between fluid velocity and pressure gradient for non-Newtonian Bingham fluid flow in porous medium

As shown in Fig. 3.1, Bingham fluid in a poroelastic system exhibits a nonlinear behavior because of the threshold gradient α_0 . Flow will not start until the pressure gradient is equal or greater than the threshold gradient α_0 .

For the purposes of numerical analysis, it is possible to represent the flow of Bingham fluids through porous media by a constant viscosity μ_0 and a threshold gradient α_0 as in Equation (3.33). However, it is more convenient to treat Bingham fluids as having a pressure gradient dependent apparent viscosity as in Equation (3.34). In this case the apparent viscosity can be defined as

$$\begin{aligned} \mu_a &= \frac{\mu_0}{1 - \frac{\alpha_0}{|\Delta P|}} & \text{for } |\Delta P| \geq \alpha_0 \\ \mu_a &= \infty & \text{for } |\Delta P| < \alpha_0 \end{aligned} \quad (3.35)$$

in which the threshold gradient α_0 is related to the yield stress τ_y by the relation

$$\alpha_0 = \frac{\beta \cdot \tau_y}{\sqrt{k}} \quad (3.36)$$

where k is the permeability of the porous medium and β is a coefficient to be determined experimentally.

3.4. Governing Equations for Poroelastic Systems Containing Non-Newtonian Bingham Fluid

In this section, one-dimensional constitutive equations developed for Newtonian fluid flow through porous media will be modified to govern the flow and deformation of poroelastic systems employing non-Newtonian Bingham fluid with a yield stress.

As shown in Fig. 2.2, stress vs. shear-rate plot for Bingham fluid does not pass through the origin. Therefore, Bingham fluids exhibit an apparent viscosity due to the yield stress of the fluid. The apparent viscosity depends on two parameters. The fluid attains higher apparent viscosity as the fluid yield stress increases. Also, the apparent viscosity decreases as the shear-rate (or pressure gradient) increases. This common behavior is referred to as the Bingham plastic (fluid) model.

The shear-rate dependent apparent viscosity needs to be included in the formulation. Therefore, the second form of the modified Darcy's law given by Equation (3.34) is used with the apparent viscosity defined in Equation (3.35). The modified Darcy's law can be re-written in the form

$$\frac{\partial}{\partial t}(U_y - u_y) = -\frac{k}{\mu_a} \cdot \left(\frac{\partial P}{\partial y} \right) \quad (3.37)$$

Taking the divergence of Equation (3.37) and combining with Equation (3.17) yields the modified second governing equation as

$$\left[\frac{\partial}{\partial y} \left(\frac{1}{\mu_a} \right) \right] \frac{\partial P}{\partial y} + \left(\frac{1}{\mu_a} \right) \frac{\partial^2 P}{\partial y^2} - \frac{\partial}{\partial t} \left(\beta_1 \frac{\partial u_y}{\partial y} + \beta_2 P \right) = 0 \quad (3.38)$$

where

$$\beta_1 = \frac{\alpha}{nk} \quad , \quad \beta_2 = \frac{1}{Mnk}$$

The first governing equation will be the same for the flow of Newtonian fluids and non-Newtonian Bingham fluids in poroelastic material. Therefore, Equations (3.25) and (3.38) are the constitutive equations governing the flow and deformation of poroelastic material employing non-Newtonian Bingham fluid with shear-thinning apparent viscosity. Equation (3.38) is valid as long as the condition $\Delta P \geq \alpha_0$ is satisfied over the entire flow field. In other words, the minimum threshold gradient should be exceeded and the flow should occur everywhere.

CHAPTER IV

FLOW OF BINGHAM FLUID THROUGH POROUS MEDIA

Compared with the progress made in analyzing the flow of power-law fluids through porous media, the flow behavior of Bingham plastic fluid in porous media is very poorly understood. To date research on Bingham fluid has been conducted mainly in laboratory experiments and field tests, from which a modified Darcy's law, given by Equation (3.33), has been derived. There are only a few quantitative analyses published on Bingham fluid flow in porous media.

In this chapter, a numerical model is constructed for the investigation of Bingham fluid flow in a poroelastic material. The response and complex modulus of the system are calculated using the finite element method taking into account the nonlinear nature of the Bingham fluid. It is assumed that the porous solid skeleton is linearly elastic and undergoes small deformations while the flow of fluid produced by the deformation of the material is governed by modified Darcy's law. The quasi-static theory including dissipation due to friction arising from the flow of fluid relative to the solid within the material, but neglecting inertia effects is used in the formulation.

For Bingham fluids, flow takes place only after the pressure gradient exceeds the threshold gradient. In this work, it is assumed that the minimum threshold gradient is exceeded and flow occurs everywhere. This assumption is the result of two considerations. First, Lipscomb and Denn (1984) showed that yielding and flow must occur everywhere for the flow of Bingham fluids in confined, complex geometries. Also the yielding of electrorheological fluids which are analyzed as the application of the theory developed here, occurs at relatively low levels of strains (<1%).

4.1. Finite Element Formulation

In order to solve the coupled and time-dependent governing equations given by Equations (3.25) and (3.38), a finite element model is constructed. Galerkin weighted-residual method which is summarized in Appendix B, is used in the formulation in which solid-phase displacement and fluid pressure are the primary variables. A linear variation of apparent viscosity is assumed over each element because of the non-Newtonian shear-thinning nature of the fluid.

Let's recall the governing equations for the one-dimensional flow of Bingham fluid in poroelastic media.

$$(\lambda^* + 2\mu^*) \frac{\partial^2 u}{\partial y^2} - \alpha \frac{\partial P}{\partial y} = 0 \quad (4.1)$$

$$\left[\frac{\partial}{\partial y} \left(\frac{1}{\mu_s} \right) \right] \frac{\partial P}{\partial y} + \left(\frac{1}{\mu_s} \right) \frac{\partial^2 P}{\partial y^2} - \frac{\partial}{\partial t} \left(\beta_1 \frac{\partial u}{\partial y} + \beta_2 P \right) = 0 \quad (4.2)$$

The following approximate solutions are assumed for the solid-phase displacements, u , and the fluid pressure, P , in y -direction;

$$u(y,t) = \sum_{j=1}^n N_j(y) \cdot u_j(t) \quad \text{or} \quad u = \sum_{j=1}^n N_j \cdot u_j \quad (4.3)$$

$$P(y,t) = \sum_{j=1}^n N_j(y) \cdot P_j(t) \quad \text{or} \quad P = \sum_{j=1}^n N_j \cdot P_j \quad (4.4)$$

where u_j 's and P_j 's are the solid-phase displacements and fluid pressures at the nodal points, respectively. Also, derivatives of u and P can be written as

$$\frac{\partial u}{\partial y} = \sum_{j=1}^n \frac{dN_j}{dy} u_j \quad (4.5)$$

$$\frac{\partial P}{\partial y} = \sum_{j=1}^n \frac{dN_j}{dy} P_j \quad (4.6)$$

$$\frac{\partial}{\partial t} \left(\frac{\partial u}{\partial y} \right) = \sum_{j=1}^n \frac{dN_j}{dy} \frac{du_j}{dt} \quad (4.7)$$

$$\frac{\partial}{\partial t} (P) = \sum_{j=1}^n N_j \frac{dP_j}{dt} \quad (4.8)$$

where N_j 's are the linear trial functions defined by

$$N_j(y) = \begin{cases} \frac{y - y_{j-1}}{h_j} & \text{for } y_{j-1} \leq y \leq y_j \\ \frac{y_{j+1} - y}{h_{j+1}} & \text{for } y_j \leq y \leq y_{j+1} \\ 0 & \text{for } y < y_{j-1} \text{ or } y > y_{j+1} \end{cases} \quad (4.9)$$

where $h_i = y_i - y_{i-1}$ is the length of an element. The first derivatives are then

$$N'_j(y) = \begin{cases} \frac{1}{h_j} & \text{for } y_{j-1} \leq y \leq y_j \\ \frac{-1}{h_{j+1}} & \text{for } y_j \leq y \leq y_{j+1} \\ 0 & \text{for } y < y_{j-1} \text{ or } y > y_{j+1} \end{cases} \quad (4.10)$$

The trial functions $N_j(y)$ and the derivatives $N'_j(y)$ are also plotted for the j 'th nodal point in Fig. 4.1.

Applying Galerkin method,

$$\int_0^d N_i \left\{ (\lambda^* + 2\mu^*) \frac{\partial^2 u}{\partial y^2} - \alpha \frac{\partial P}{\partial y} \right\} dy = 0 \quad (4.11)$$

$$\int_0^d N_i \left\{ \left[\frac{\partial}{\partial y} \left(\frac{1}{\mu_a} \right) \right] \frac{\partial P}{\partial y} + \left(\frac{1}{\mu_a} \right) \frac{\partial^2 P}{\partial y^2} - \frac{\partial}{\partial t} \left(\beta_1 \frac{\partial u}{\partial y} + \beta_2 P \right) \right\} dy = 0 \quad (4.12)$$

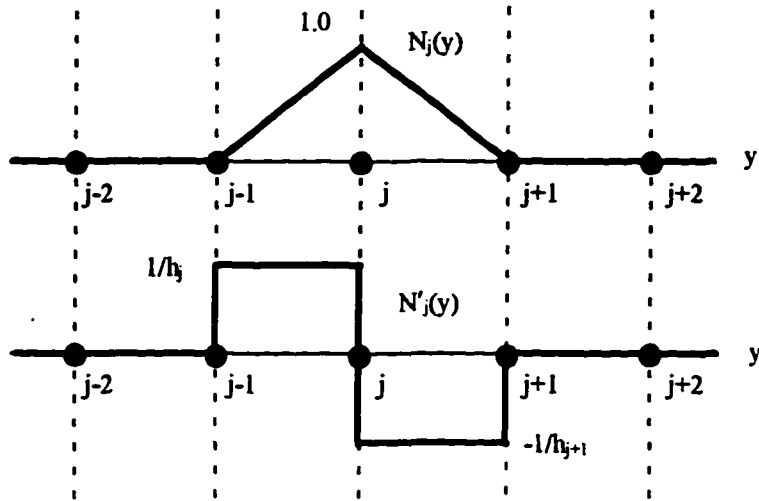


Fig. 4.1. Linear trial function $N_j(y)$ and the derivatives $N_j'(y)$

Expanding Equations (4.11) and (4.12),

$$\int_0^d N_i (\lambda^* + 2\mu^*) \frac{\partial^2 u}{\partial y^2} dy - \int_0^d N_i \alpha \frac{\partial P}{\partial y} dy = 0 \quad (4.13)$$

$$\int_0^d N_i \left[\frac{\partial}{\partial y} \left(\frac{1}{\mu_a} \right) \right] \frac{\partial P}{\partial y} dy + \int_0^d N_i \left(\frac{1}{\mu_a} \right) \frac{\partial^2 P}{\partial y^2} dy - \frac{\partial}{\partial t} \int_0^d N_i \left(\beta_1 \frac{\partial u}{\partial y} + \beta_2 P \right) dy = 0 \quad (4.14)$$

Using the property,

$$N_i \frac{\partial^2 H}{\partial y^2} = \frac{\partial}{\partial y} \left(N_i \frac{\partial H}{\partial y} \right) - \frac{dN_i}{dy} \frac{\partial H}{\partial y} \quad (4.15)$$

Equations (4.13) and (4.14) can be written as

$$\int_0^d \left\{ (\lambda^* + 2\mu^*) \frac{dN_i}{dy} \frac{\partial u}{\partial y} + \alpha N_i \frac{\partial P}{\partial y} \right\} dy = (\lambda^* + 2\mu^*) N_i \frac{\partial u}{\partial y} \Big|_0^d \quad (4.16)$$

$$\int_0^d \left\{ \frac{dN_i}{dy} \frac{\partial P}{\partial y} - \left[\mu_a \frac{\partial}{\partial y} \left(\frac{1}{\mu_a} \right) \right] N_i \frac{\partial P}{\partial y} + [\mu_a] \frac{\partial}{\partial t} \left(\beta_1 N_i \frac{\partial u}{\partial y} + \beta_2 N_i P \right) \right\} dy = N_i \frac{\partial P}{\partial y} \Big|_0^d \quad (4.17)$$

Substituting Equations (4.3)-(4.8) in Equations (4.16) and (4.17),

$$\sum_{j=1}^n \int_0^d \left\{ (\lambda^* + 2\mu^*) \frac{dN_i}{dy} \frac{dN_j}{dy} u_j + \alpha N_i \frac{dN_j}{dy} P_j \right\} dy = (\lambda^* + 2\mu^*) N_i \frac{\partial u}{\partial y} \Big|_0^d \quad (4.18)$$

$$\sum_{j=1}^n \int_0^d \left\{ \left[\frac{dN_i}{dy} \frac{dN_j}{dy} - \left(\mu_a \frac{\partial}{\partial y} \left(\frac{1}{\mu_a} \right) \right) N_i \frac{dN_j}{dy} \right] P_j + [\mu_a] \beta_1 N_i \frac{dN_j}{dy} \frac{\partial u_j}{\partial t} + [\mu_a] \beta_2 N_i N_j \frac{\partial P_j}{\partial t} \right\} dy = N_i \frac{\partial P}{\partial y} \Big|_0^d \quad (4.19)$$

Considering Equations (4.18) and (4.19), the coefficient matrices and right-hand-side (RHS) vectors can be defined as

$$[K_{ij}^u] = \int_0^d (\lambda^* + 2\mu^*) \frac{dN_i}{dy} \frac{dN_j}{dy} dy \quad (4.20)$$

$$[K_{ij}^{P1}] = \int_0^d \alpha N_i \frac{dN_j}{dy} dy \quad (4.21)$$

$$[K_{ij}^{P2}] = \int_0^d \left[\frac{dN_i}{dy} \frac{dN_j}{dy} - \left(\mu_a \frac{\partial}{\partial y} \left(\frac{1}{\mu_a} \right) \right) N_i \frac{dN_j}{dy} \right] dy \quad (4.22)$$

$$[M_{ij}^{\dot{u}}] = \int_0^d [\mu_a] \beta_1 N_i \frac{dN_j}{dy} dy \quad (4.23)$$

$$[M_{ij}^{\dot{P}}] = \int_0^d [\mu_a] \beta_2 N_i N_j dy \quad (4.24)$$

$$\{F_i^1\} = (\lambda^* + 2\mu^*) N_i \frac{\partial u}{\partial y} \Big|_0^d \quad (4.25)$$

$$\{F_i^2\} = N_i \frac{\partial P}{\partial y} \Big|_0^d \quad (4.26)$$

The elemental coefficient matrices and RHS vectors are obtained using the linear trial functions defined for the element Ω_e shown in Fig. 4.2.

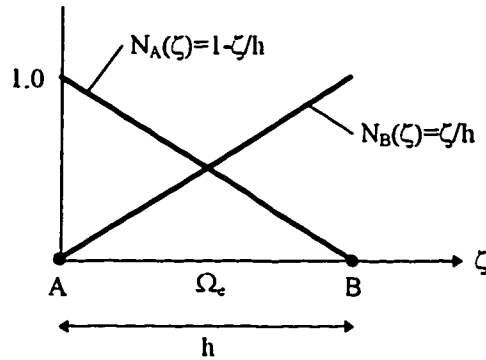


Fig. 4.2. Linear trial functions defined for an element

The elemental coefficient matrices and RHS vectors are calculated as

$$[K_e^u] = (\lambda^* + 2\mu^*) \begin{bmatrix} 1/h & -1/h \\ -1/h & 1/h \end{bmatrix} \quad (4.27)$$

$$[K_e^{P1}] = \alpha \begin{bmatrix} -1/2 & 1/2 \\ -1/2 & 1/2 \end{bmatrix} \quad (4.28)$$

$$[K_e^{P2}] = \begin{bmatrix} \frac{1}{h} + \frac{\mu_B^2 - 2\mu_A^2 + \mu_A\mu_B}{6h} & -\frac{1}{h} - \frac{\mu_B^2 - 2\mu_A^2 + \mu_A\mu_B}{6h} \\ -\frac{1}{h} - \frac{\mu_A^2 - 2\mu_B^2 + \mu_A\mu_B}{6h} & \frac{1}{h} + \frac{\mu_A^2 - 2\mu_B^2 + \mu_A\mu_B}{6h} \end{bmatrix} \quad (4.29)$$

$$[M_e^{\ddot{u}}] = \frac{-\beta_1}{6} \begin{bmatrix} (2\mu_A + \mu_B) & -(2\mu_A + \mu_B) \\ (2\mu_B + \mu_A) & -(2\mu_B + \mu_A) \end{bmatrix} \quad (4.30)$$

$$[M_e^{\dot{P}}] = \frac{\beta_2 h}{12} \begin{bmatrix} (3\mu_A + \mu_B) & (\mu_A + \mu_B) \\ (\mu_B + \mu_A) & (3\mu_B + \mu_A) \end{bmatrix} \quad (4.31)$$

$$\{F_e^1\} = \begin{Bmatrix} -(\lambda^* + 2\mu^*) N_i \frac{\partial u}{\partial y} \Big|_{y=0} \\ (\lambda^* + 2\mu^*) N_i \frac{\partial u}{\partial y} \Big|_{y=d} \end{Bmatrix} \quad (4.32)$$

$$\{F_e^2\} = \begin{Bmatrix} -N_i \frac{\partial P}{\partial y} \Big|_{y=0} \\ N_i \frac{\partial P}{\partial y} \Big|_{y=d} \end{Bmatrix} \quad (4.33)$$

The derivations of these elemental matrices and RHS vectors are given in Appendix C.

The coefficient matrices and RHS vectors defined by Equations (4.20)-(4.26) are assembled from the elemental coefficient matrices and RHS vectors. Then, the master coefficient matrices and RHS vector are constructed and the system matrix equation is generated in the form

$$\begin{bmatrix} [K_{ij}^u] & [K_{ij}^{P1}] \\ [0] & [K_{ij}^{P2}] \end{bmatrix} \cdot \begin{pmatrix} \{u_i\} \\ \{P_i\} \end{pmatrix} + \begin{bmatrix} [0] & [0] \\ [M_{ij}^{\dot{u}}] & [M_{ij}^{\dot{P}}] \end{bmatrix} \cdot \begin{pmatrix} \{\dot{u}_i\} \\ \{\dot{P}_i\} \end{pmatrix} = \begin{pmatrix} \{F_i^1\} \\ \{F_i^2\} \end{pmatrix} \quad (4.34)$$

Equation (4.34) is the matrix equation representing the discrete analog of the governing equations. The resulting matrix equation can be written in a more general form as

$$[K_{ij}] \cdot \begin{pmatrix} \{u_i\} \\ \{P_i\} \end{pmatrix} + [M_{ij}] \cdot \begin{pmatrix} \{\dot{u}_i\} \\ \{\dot{P}_i\} \end{pmatrix} = (F_i) \quad (4.35)$$

In order to deal with the time-dependency of Equation (4.35) two-point recurrence scheme is used. All of the recurrence formulas which are used for the solution of equations similar to Equation (4.35), can be summarized in one convenient equation as

$$\begin{aligned} [[M_{ij}] + \theta [K_{ij}] \Delta t] \cdot \begin{pmatrix} \{u_{i+1}\} \\ \{P_{i+1}\} \end{pmatrix} &= [[M_{ij}] - (1 - \theta) [K_{ij}] \Delta t] \cdot \begin{pmatrix} \{u_i\} \\ \{P_i\} \end{pmatrix} \\ &+ [(1 - \theta)(F_i) + \theta(F_{i+1})] \Delta t \end{aligned} \quad (4.36)$$

where the parameter θ takes the values of 0, $1/2$, and 1 for the forward, central, and backward difference schemes based on the finite difference method, respectively. When the weighted-residual finite element method is used for the solution of Equation (4.35), the parameter θ can be defined as

$$\theta = \frac{\int_0^1 W\xi d\xi}{\int_0^1 Wd\xi} \quad (4.37)$$

where W is the weighting function. The weighting functions for Galerkin method are taken to be the trial functions themselves. Hence, it is possible to use either

$$W = N_A(\xi) = 1 - \frac{\xi}{h} \quad (4.38)$$

or

$$W = N_B(\xi) = \frac{\xi}{h} \quad (4.39)$$

It can be easily shown that if Equation (4.38) is substituted in Equation (4.37), the value of θ becomes $1/3$, whereas if Equation (4.39) is used in Equation (4.37), the parameter θ takes the value of $2/3$. The latter, $\theta=2/3$, is particularly useful because it is more accurate than the backward difference scheme ($\theta=1$) and more stable than the

central difference scheme ($\theta=1/2$). Therefore, $\theta=2/3$ is used in the numerical model such that Equation (4.36) can be arranged in the form

$$\begin{aligned} \left[[M_{ij}] + \frac{2}{3} \Delta t [K_{ij}] \right] \cdot \begin{pmatrix} \{u_{i+1}\} \\ \{P_{i+1}\} \end{pmatrix} &= \left[[M_{ij}] - \frac{1}{3} \Delta t [K_{ij}] \right] \cdot \begin{pmatrix} \{u_i\} \\ \{P_i\} \end{pmatrix} \\ &+ \left[\frac{1}{3} \Delta t (F_i) + \frac{2}{3} \Delta t (F_{i+1}) \right] \end{aligned} \quad (4.40)$$

Then, the solution is computed in an iterative way by

- (i) assuming a (variable) viscosity at all points in the material,
- (ii) calculating, using the finite element model, displacement and pressure values,
- (iii) recalculating the viscosity at all points using Equation (3.35),
- (iv) repeating the above steps until convergence (or divergence) occurs.

4.2. Problem Definition

The numerical model developed is capable of calculating the dynamic response of the poroelastic systems containing non-Newtonian Bingham fluid. In this section, a model problem is selected for the verification of the numerical model developed. A column of poroelastic material undergoing harmonic compression, as shown in Fig. 4.3, is considered.

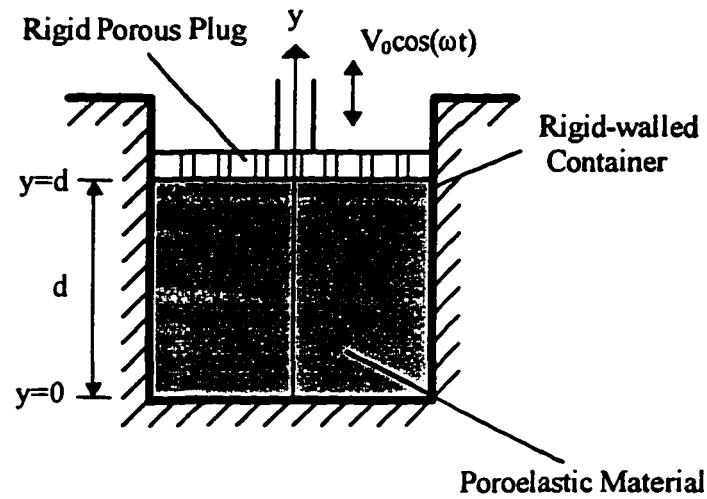


Fig. 4.3. Poroelastic column subjected to harmonic surface displacement

The poroelastic material is perfectly bounded at the bottom and side surfaces while a harmonic displacement input is applied at the top surface through a freely draining porous plug. Therefore, the deformation and flow occur only in y -direction.

4.3. Boundary Conditions

The boundary conditions imposed are those of a harmonic displacement input applied to the top surface in which the fluid flows in and out of the specimen through a rigid porous plug. Other surfaces are perfectly bounded and impermeable. The boundary conditions can be written as

$$u_y(0) = 0 \quad (4.41)$$

$$u_y(d) = V_0 \cos(\omega t) \quad (4.42)$$

$$\left. \frac{\partial P}{\partial y} \right|_{y=0} = 0 \quad (4.43)$$

$$P(d) = 0 \quad (4.44)$$

4.4. Verification of the Numerical Model

In this section, the accuracy of the numerical solution is examined and confirmed by comparison with an exact solution. The material properties used for this purpose are summarized in Table 4.1.

Table 4.1. Material properties used for the verification of the numerical model.

$$\lambda^* = 1.29 \times 10^5 \text{ kPa}$$

$$\mu^* = 9.79 \times 10^4 \text{ kPa}$$

$$n = 0.48$$

$$k = 3.62 \times 10^{-8} \text{ cm}^2$$

$$M = 5.58 \times 10^5 \text{ kPa}$$

$$\alpha = 0.98$$

$$d = 2.54 \text{ cm}$$

$$\mu_0 = 0.05 \text{ Pa-s}$$

The solid displacements and the fluid pressure values obtained from the finite element model are compared with the analytical solution derived by Wijesinghe and Kingsbury (1979). Since the analytical solution is available for Newtonian viscous fluid

with no yield stress, the yield stress value is taken as zero in the numerical model. For the special case of minimum threshold gradient $\alpha_0=0$, Bingham fluid becomes Newtonian, and the available analytical solution can be used to check the accuracy of the numerical model. In this case, the apparent viscosity will be constant and equal to the plastic viscosity because of the zero threshold gradient.

The results are obtained for $\omega=2\pi$ rad/s and 20 elements are used in the finite element model. As shown in Fig. 4.4 and 4.5, the numerical results are in good agreement with the analytical results.

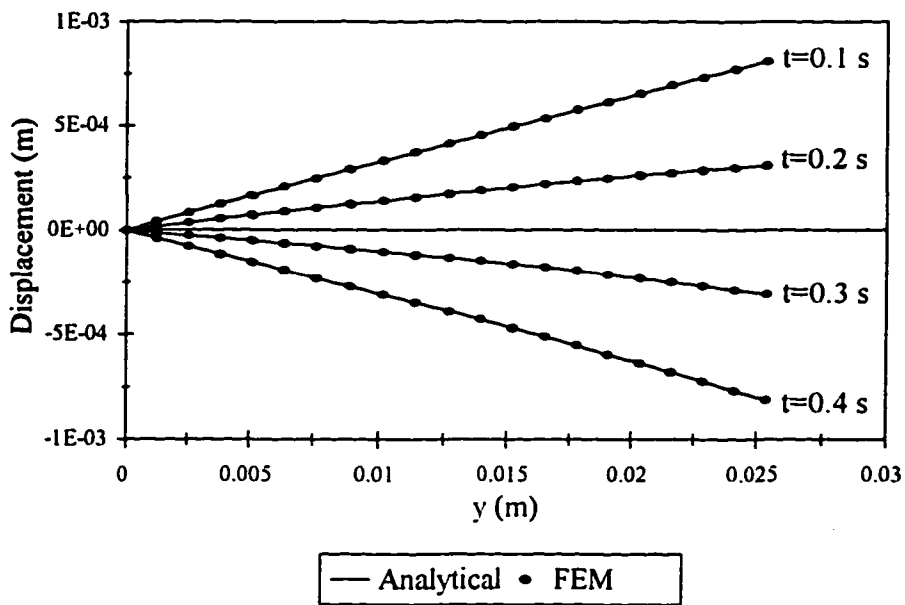


Fig. 4.4. Comparison of the numerical results with the analytical results for solid displacement

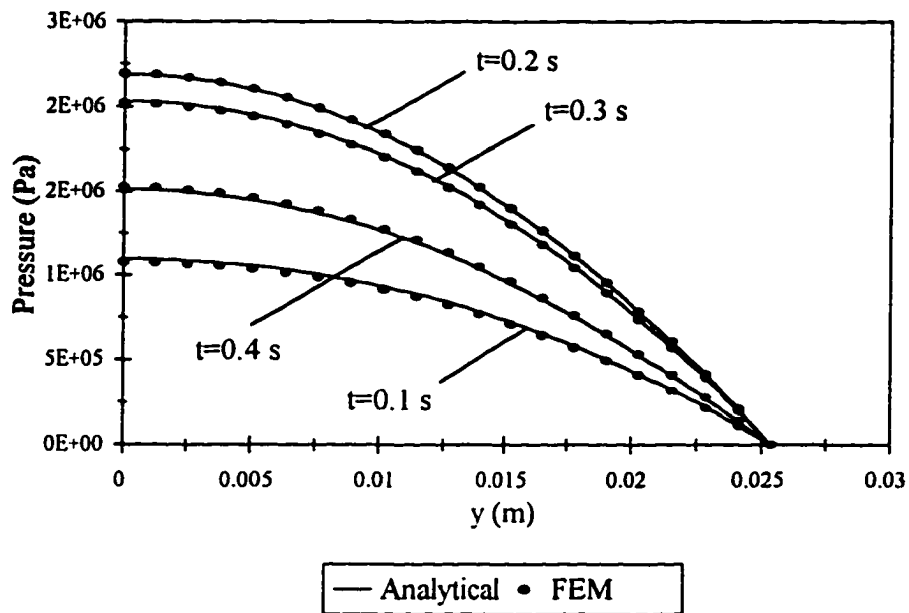


Fig. 4.5. Comparison of the numerical results with analytical results for fluid pressure

4.5. Results

After verifying the accuracy of the numerical model by comparing with the analytical solution of Wijesinghe and Kingsbury (1979) for the flow of Newtonian viscous fluid through poroelastic media, the results obtained from the finite element model for the flow of Bingham fluid with a certain yield stress in a poroelastic media are presented in this section.

As shown in Fig. 4.4. and 4.5, the finite element model gives accurate results for 20 elements although it is possible to increase the accuracy further by increasing the number of elements. Therefore, 20 elements are used in all calculations in this section. The material properties used in the analyses are given in Table 4.2.

Table 4.2. Material properties used in the calculations.

$\lambda^{\circ} = 1.29 \times 10^5$ kPa
$\mu^{\circ} = 9.79 \times 10^4$ kPa
$n = 0.48$
$k = 3.62 \times 10^{-8}$ cm ²
$M = 5.58 \times 10^5$ kPa
$\alpha = 0.98$
$d = 2.54$ cm
$\mu_0 = 0.00454$ Pa-s
$\tau_y = 412$ Pa
$\alpha_0 = 216542$ Pa/m
$\beta = 0.001$

In Fig. 4.6, the variation of apparent viscosity along the flow field is plotted for $\omega=20\pi$ rad/s and $t=0.05$ sec. For the flow of Bingham fluid in porous medium, the apparent viscosity is defined by Equation (3.35). The variation in the apparent viscosity is due to the non-Newtonian effect caused by the existence of a yield stress in the fluid. This variation is determined by the ratio $\frac{\alpha_0}{|\Delta P|}$. In fact, it would be better to examine the variation of the apparent viscosity in terms of the pressure gradient, ΔP , since the threshold gradient, α_0 , is constant. When the pressure gradient increases the fluid velocity will also increase as described by Darcy's law. Then, the ratio $\frac{\alpha_0}{|\Delta P|}$ will decrease and the apparent viscosity will get lower (shear-thinning effect). As the ratio goes to zero the apparent viscosity will be equal to the plastic viscosity μ_0 .

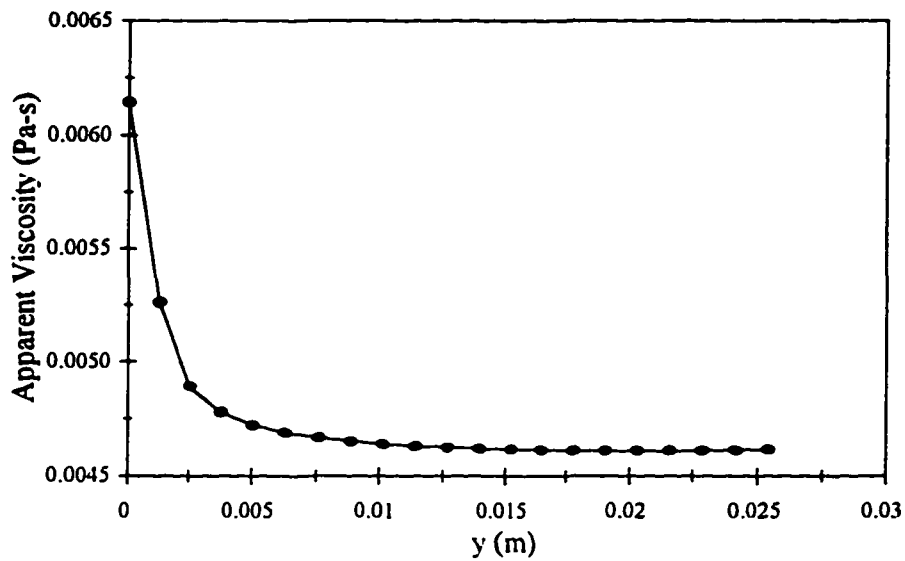


Fig. 4.6. Variation of apparent viscosity along y-direction

In Fig. 4.7, the solid-phase displacement along y-direction is plotted for $\omega=20\pi$ rad/s at six different times within a period. The solid deforms linearly at each time step as shown in Fig. 4.7.

The fluid pressure along y-direction is also plotted for various time steps in Fig. 4.8. The pressure which is maximum at the bottom surface drops gradually along y-direction and becomes zero at the free surface. A similar trend is observed at each time step as shown in Fig. 4.8. The pressure gradient values calculated from the pressure data by means of forward, central and backward difference numerical schemes are also given in Fig. 4.9.

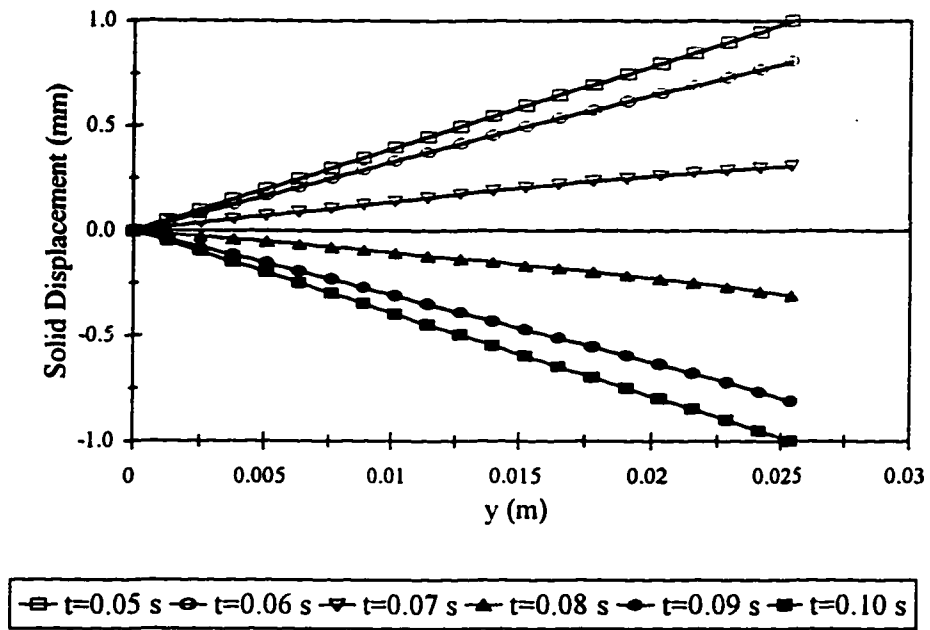


Fig. 4.7. Solid-phase displacements in y-direction

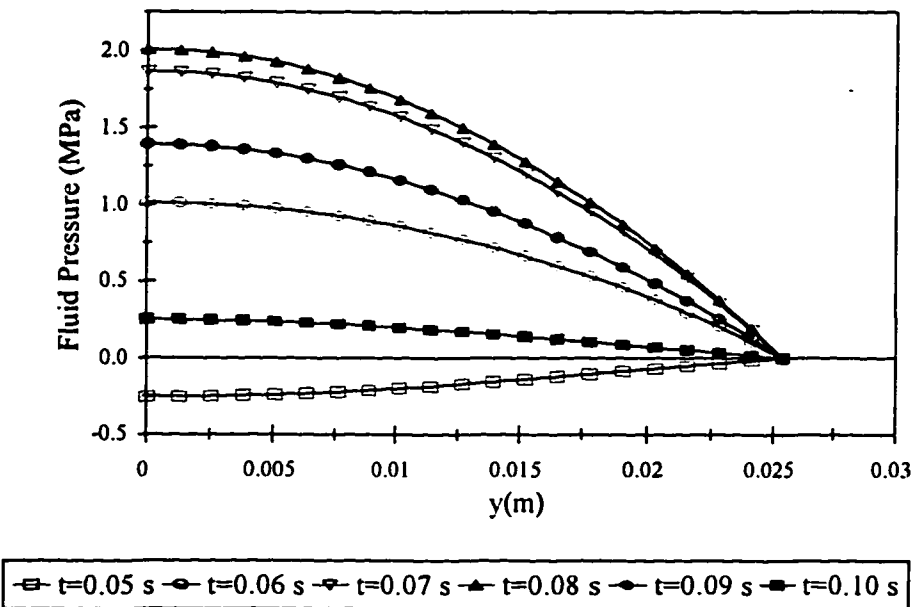


Fig. 4.8. Variation of fluid pressure along y-direction

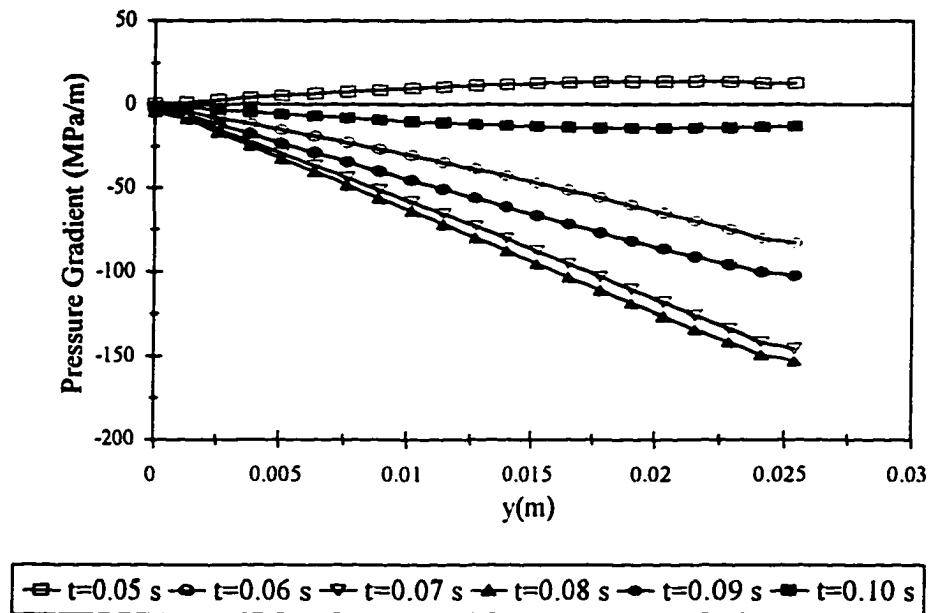


Fig. 4.9. Variation of pressure gradient along y-direction

As shown in Fig. 4.6 and 4.9, the apparent viscosity is maximum at $y=0$ at which the pressure gradient is minimum. Then, the apparent viscosity decreases due to the increasing pressure gradient or fluid velocity along y-direction. At the surface the pressure gradient becomes maximum and the ratio $\alpha_0/|\Delta P|$ reaches its minimum. Hence, the apparent viscosity becomes almost equal to the plastic viscosity at the nodes close to the surface.

The complex modulus of a poroelastic system as defined by Equation (3.30) is also calculated at various frequencies. The storage modulus and the loss factor are plotted against frequency in Fig. 4.10 and 4.11, respectively.

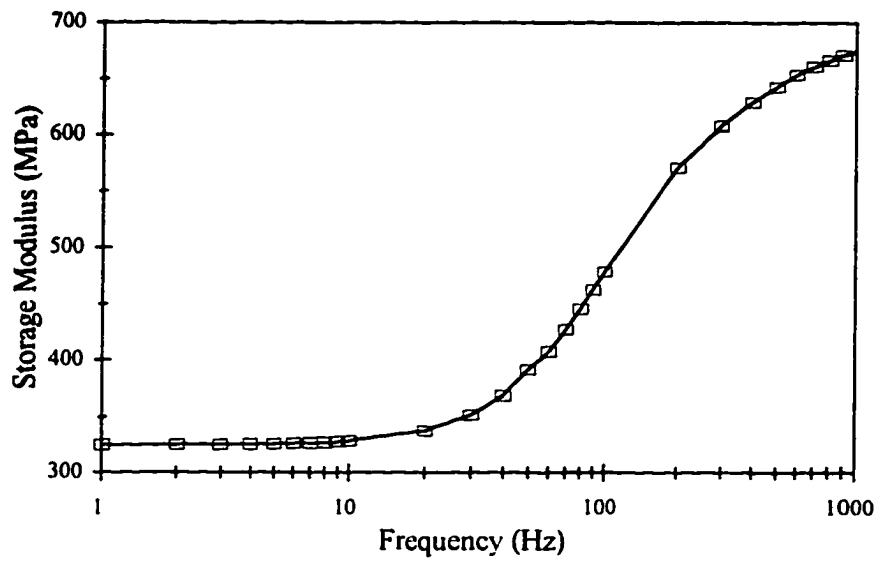


Fig. 4.10. Storage modulus of the poroelastic material containing Bingham fluid

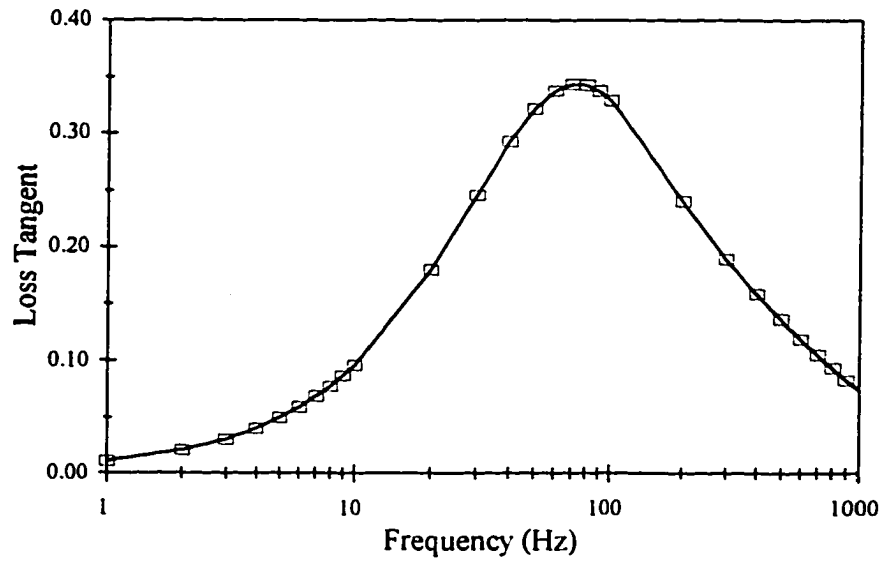


Fig. 4.11. Loss factor of the poroelastic material containing Bingham fluid

It is observed that the loss factor starts to increase from zero and reaches its maximum at a critical frequency ω_c and then gradually decreases to zero again. Over the latter range of frequencies the storage modulus is seen to suffer a somewhat sudden increase after which it begins to level off at higher frequencies. This behavior is due to the fact that as the frequency increases the relative motion between the fluid and the solid increases and this in turn yields increased dissipation. However, beyond the peak in the loss factor, the fluid drag on the solid is so great that the fluid and the solid move together in the interior (except at the draining boundaries) and the dissipation decreases.

CHAPTER V

INCORPORATING ELECTORRHEOLOGICAL FLUIDS IN POROUS MEDIA

5.1. Introduction

The ability to control the rheology of a material with an applied electric field is of interest to both industrial and academic communities. The development of theories and models to explain this electrorheological (ER) phenomenon has been fueled by the multi-million dollar market potential for this technology. Unfortunately, the primary barriers to establishing a commercial ER business have been an inadequate understanding of the ER phenomenon and lack of satisfactory materials. There are vast amount of research going on to find new particle/fluid combinations that can withstand higher stresses. On the other hand, incorporating ER fluids in a poroelastic structure can increase the material strength considerably and can still provide controllable stiffness and damping characteristics.

5.2. Electrorheological Fluid Characteristics

ER fluids consist of suspensions of fine polarizable particles in a dielectric liquid, which upon application of an electric field take on the characteristics of a solid.

This occurs reversibly, and in times of the order of milliseconds, and in general with low power requirements. Some examples of suspensions which exhibit ER behavior include corn starch in corn oil, silica gel in mineral oil, cellulose in transformer oil, and zeolite in silica oil.

Upon application of an electric field the particles in an ER fluid align along the direction of the field in a chainlike or fibrous structure. The increased strength of the fluid is attributed to the force required to rupture the chains or fibers. Practically all known ER fluids exhibit this characteristic chainlike or fibrous structure. The development of the chainlike structure with increasing electric field in a model ER fluid (0.2 vol. fraction of 27- μm beads in silicone oil), as given by Conrad and Sprecher (1991), is illustrated in Fig. 5.1.

At small electric fields the particles begin to cluster, with a tendency to align along the field. This clustering increases with field until at $E=0.5$ kV/mm complete chains first form across the gap between the electrodes. Further increase in electric field leads to an increase in the number of complete chains and thickness of the chains.

One of the greatest problems in designing devices that use ER fluids is overcoming the tendency of the particles to settle out if the fluid stands quietly for a length of time. Depending on the particular particle/fluid combination, the device configuration, and other factors, the time period can range from hours to weeks. Settling can be controlled somewhat by adjusting particle size and by using surfactant that inhibit particle interaction and the tendency to clump together. Another stabilization technique is to match the base-liquid density to that of the particles.

Although density matching is good in principle, it is difficult in practice because it severely limits the choice of particles that can be used in specific carrier fluids. Also, because thermal expansion coefficients of the particles are usually different from those of carrier fluids, density matching only operates well over a small temperature range.

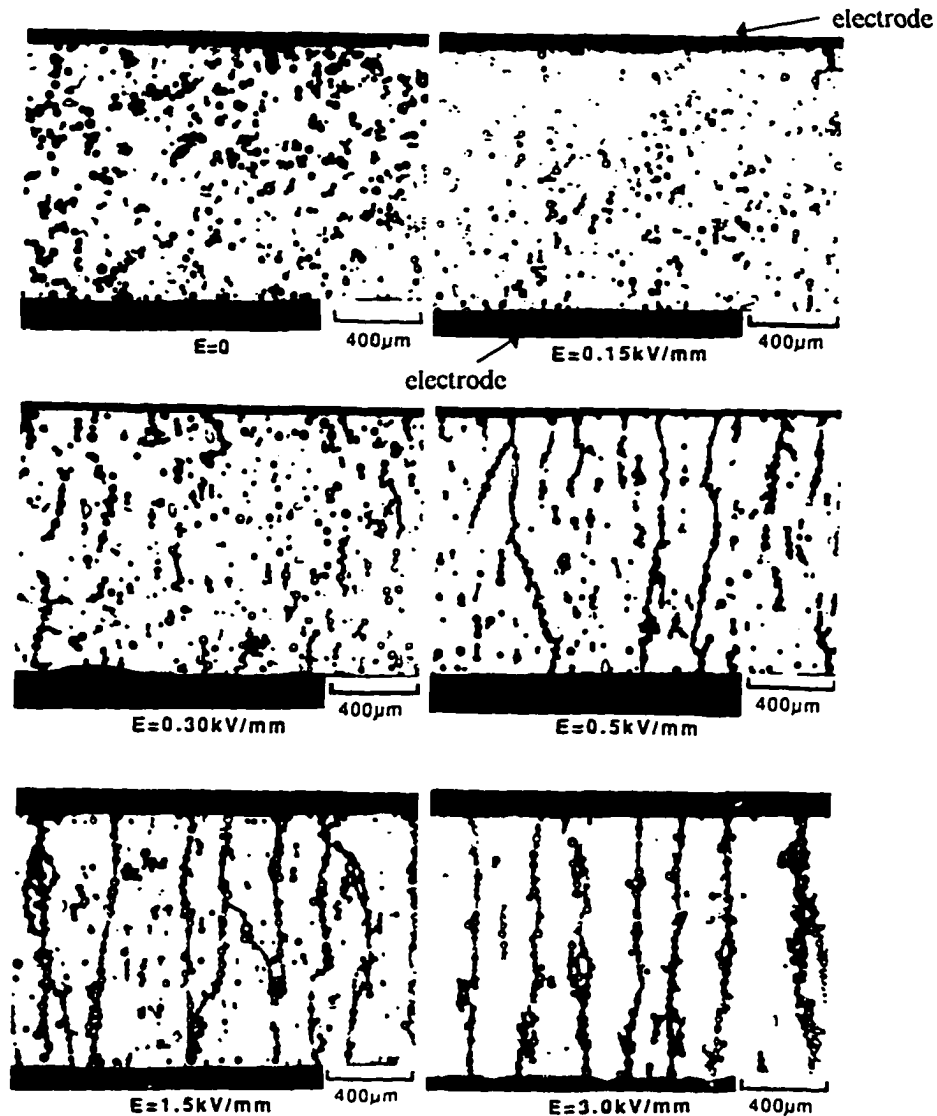


Fig. 5.1. Development of the chainlike structure in a model ER fluid with increasing DC electric field.

5.3. Electrorheological Fluid Behavior

The electrorheological effect initially was defined as the apparent change in viscosity observed in the materials developed by Winslow (1949). Although from a macroscopic point of view, a change in apparent or effective viscosity does occur, the actual plastic viscosity of the material remains approximately constant as the applied electric field is varied. In this situation the parameter that changes is the amount of shear stress needed to initiate flow.

A Bingham plastic model, as described by Equation (5.1), can often provide a sufficiently accurate description of the observed post-yield behavior to be used for the designing of ER material devices. The electric-field-induced yield stress, τ_y , and viscosity, μ_0 , are the two most significant parameters used in designing electroactive devices where flow properties or post-yield properties are essential. For post-yield situations the constitutive shear behavior of ER materials is often modeled using the Bingham plastic approximation described as

$$\begin{aligned} \tau &= \tau_y + \mu_0 \dot{\gamma} & \text{for} & \quad |\tau| \geq \tau_y \\ \dot{\gamma} &= 0 & \text{for} & \quad 0 < |\tau| < \tau_y \end{aligned} \quad (5.1)$$

where τ_y is the dynamic yield stress, μ_0 is the plastic (or zero-field) viscosity and $\dot{\gamma}$ is the shear rate. The yield stress is a strong function of electric field. The effect of electric field strength E on yield stress generally fits an equation of the form

$$\tau_y = AE^n \quad (5.2)$$

where A and n may be fluid and field dependent constants. The value of n is usually between 1 and 2.5. Although usually assumed constant, the plastic viscosity μ_0 is also a function of electric field; however, its electric field dependency is not as strong as the electric field dependency of the yield stress. Stangroom (1991) measured the yield stress and the plastic viscosity of two different ER fluids as a function of electric field. He observed that while the plastic viscosity was a weak function of electric field for one fluid, it was a strong function of the electric field for the other.

In Bingham plastic model, the apparent viscosity μ_a is related to the plastic viscosity μ_0 and the yield stress τ_y as

$$\mu_a = \frac{\tau_y}{\dot{\gamma}} + \mu_0 \quad (5.3)$$

where $\dot{\gamma}$ is the shear rate. On the other hand, the apparent viscosity of ER fluid in a porous medium can be expressed analogous to the apparent viscosity of Bingham fluid in a porous medium given by Pascal (1986) by the relation

$$\mu_a = \mu_0 + \frac{\alpha_0 k}{|v|} \quad (5.4)$$

where k is the permeability of the porous medium and v is the fluid velocity. The threshold gradient α_0 is related to the yield stress τ_y by the relation

$$\alpha_0 = \frac{\beta \tau_y}{\sqrt{k}} \quad (5.5)$$

where β is a coefficient determined experimentally.

Substituting the modified Darcy's law given by Equation (3.34) in Equation (5.4) yields a more convenient form of apparent viscosity of ER fluids in porous medium as

$$\mu_a = \frac{\mu_0}{1 - \frac{\alpha_0}{|\Delta P|}} \quad (5.6)$$

where ΔP is the pressure gradient.

5.4. Poroelastic Systems Incorporating ER Fluids

As explained in the previous sections, Bingham plastic model can provide an accurate description of the post-yield behavior of the ER fluids. The theory of non-Newtonian Bingham fluid flow in poroelastic media is developed and the governing equations are derived in Chapter 3. Therefore, the constitutive equations given by

Equations (3.25) and (3.33) can also be applied to the flow and deformation of poroelastic materials employing ER fluids as long as the condition $\Delta P \geq \alpha_0$ is satisfied over the entire flow field. However, some of the parameters like yield stress, plastic viscosity and fluid bulk modulus, will be electric field dependent because of the ER phenomenon.

The problem defined in Chapter 4 is modified such that the dynamic response of ER fluid-filled poroelastic column subjected to harmonic displacement input applied to the top surface through a freely draining porous plug and a perfectly bounded impermeable surface at the bottom will be obtained. The electric field is provided through the metal screens placed within the poroelastic material as shown in Fig. 5.2.

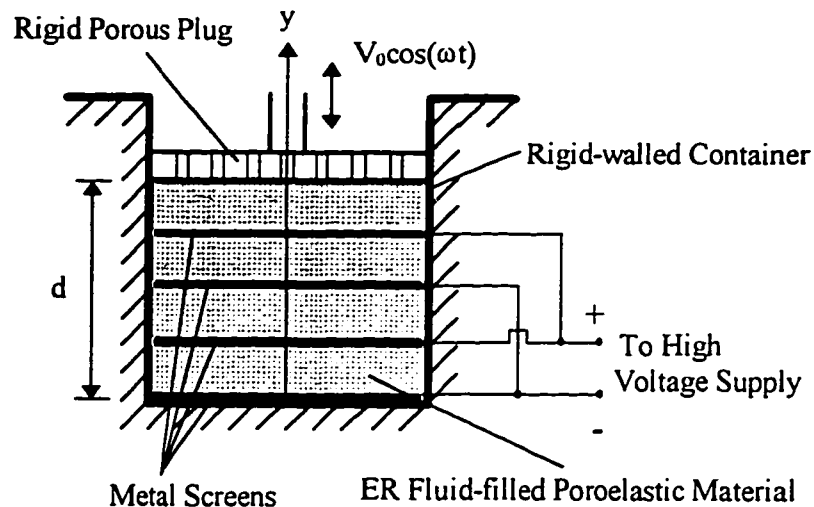


Fig. 5.2. ER fluid-filled poroelastic column subjected to harmonic surface displacement

Although ER fluids are anisotropic solids in pre-yield region, the theory developed here considers the post-yield behavior (fluid phase) of ER fluids by assuming that the yield stress is exceeded at every point within the material, at any time. There will always be a regime where the stresses are below the yield stress because of the harmonic loading. This regime must be passed through during each cycle. However, this regime is not considered in the analysis by assuming that the duration of this regime will be very short compared to the duration of each cycle. This assumption is made considering the fact that yielding of ER fluid in a poroelastic material is desired as soon as possible in each cycle to obtain maximum dissipation and this criteria can be achieved with the proper selection of ER fluid-poroelastic material combination.

The material properties used in the analysis are summarized in Table 5.1. The field-dependent properties of the ER fluids are obtained from the experimental data reported by Stangroom (1991). He used two different ER fluids: 30% lithium polymethacrylate suspended in fluorosilicone oil (ERF I) and 30% condensed aromatic ketone suspended in chlorophenyl chlorotoly methane (ERF II). He obtained the yield stress values for the shear mode. Although the yield stress values for tension-compression mode will be different than the yield stress values for shear mode for the same ER fluid, the yield stress values for shear mode are used in the analysis due to the lack of yield stress data obtained for tension-compression mode in literature. On the other hand, this doesn't create any problem since this is a parametric investigation of ER fluids in poroelastic media.

Table 5.1. Material properties of the poroelastic material and ER fluids.

Poroelastic system	ER fluid I (ERF I)	ER fluid II (ERF II)
$\lambda^* = 1.29 \times 10^5$ kPa	$\tau_y = 103 \times E^2$ (Pa)	$\tau_y = 80 \times E^2 + 180 \times E$ (Pa)
$\mu^* = 9.79 \times 10^4$ kPa	$\mu_0 = 0.05 - 0.0227 \times E$ (Pa-s)	$\mu_0 = 0.125 - 0.008 \times E$ (Pa-s)
$n = 0.48$		
$k = 3.62 \times 10^{-8}$ cm ²		
$M = 5.58 \times 10^5$ kPa		
$\alpha = 0.98$		
$d = 2.54$ cm		

5.5. Field Dependency of Parameters

The ER fluid properties which are most affected by electric field are yield stress, plastic viscosity and fluid compressibility. Most of the researchers assume the plastic viscosity to be constant since its field dependency is small compared to the field dependency of yield stress. On the other hand, Stangroom (1991) showed that, for some ER fluids, plastic viscosity changes considerably with electric field. He measured yield stress and plastic viscosity for two different ER fluids (ERF I and ERF II) at different electric fields. The functions fitted to his data are given in Table 5.1 and also plotted in Fig. 5.3, 5.4, 5.5, and 5.6.

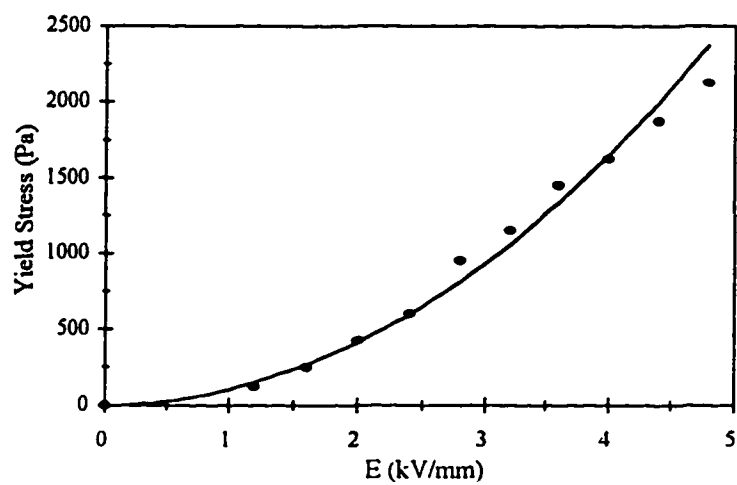


Fig. 5.3. Electric field dependency of yield stress (ERF I)

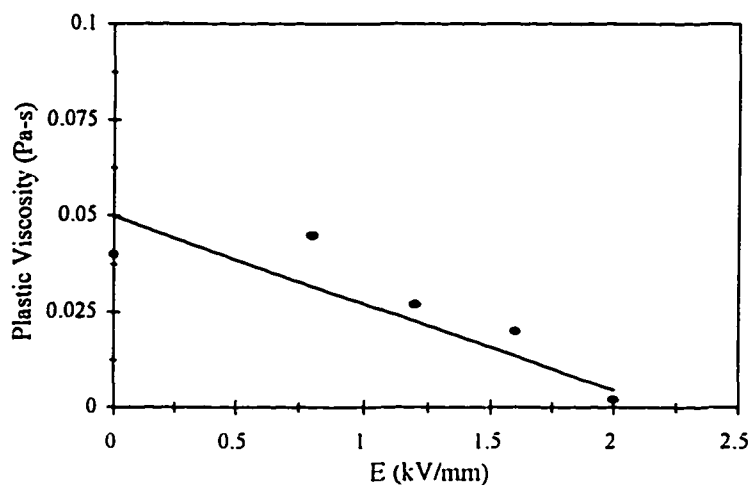


Fig. 5.4. Electric field dependency of plastic viscosity (ERF I)

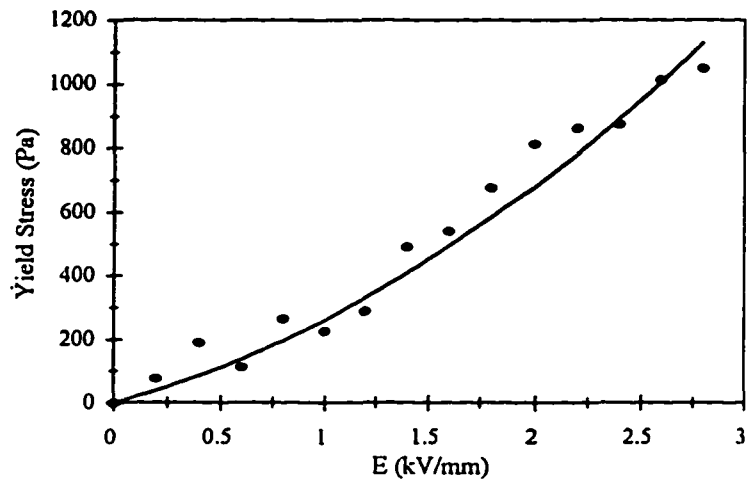


Fig. 5.5. Electric field dependency of yield stress (ERF II)

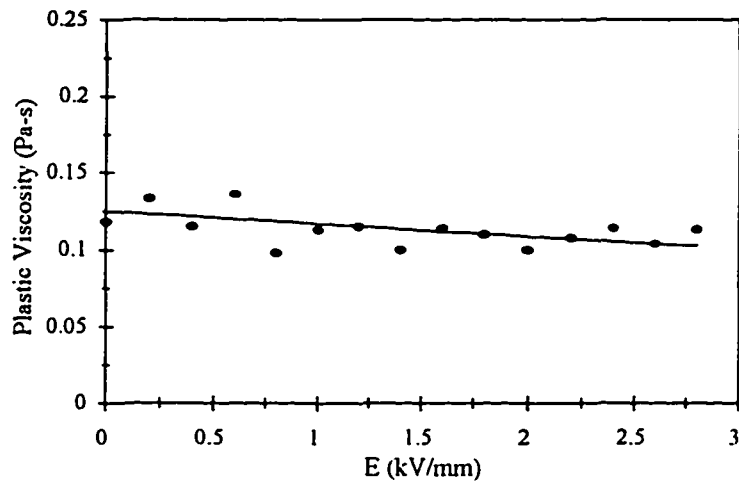


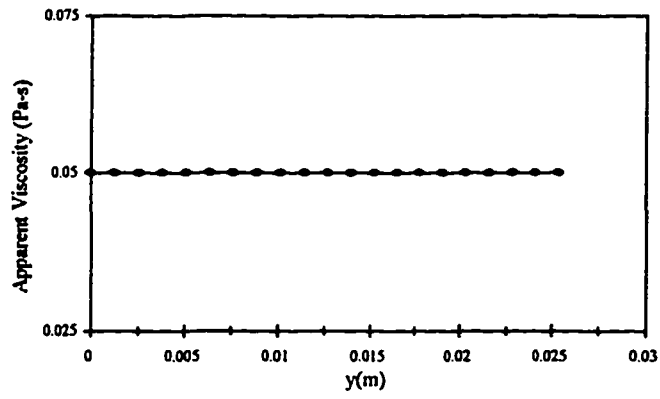
Fig. 5.6. Electric field dependency of plastic viscosity (ERF II)

Song *et al.* (1991) developed general correlating equations for the prediction of the compressibility of mineral oil-based lubricants, and silicone fluids as a function of viscosity. These equations are combined with the viscosity functions given in Table 5.1 to predict the electric field dependency of the compressibility for mineral oils and silicone fluids. It is observed from the obtained results that the variations of the compressibility of mineral oils and silicone fluids with electric field are very small, therefore, fluid compressibility is assumed field-independent.

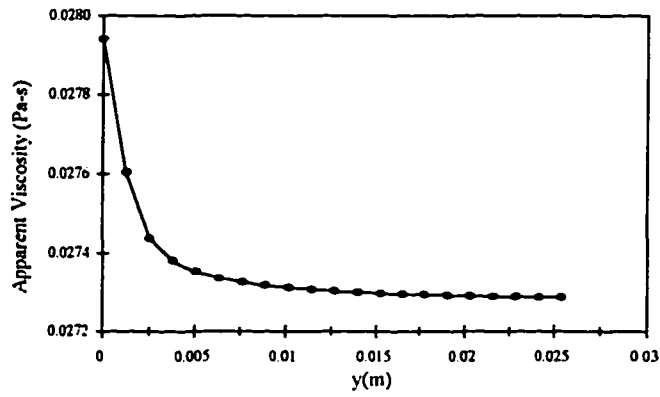
5.6. Results

In this section, the response and the complex modulus of the poroelastic material employing two different ER fluids are calculated by using the numerical model developed. The geometry is shown in Fig. 5.2 and the material properties are given in Table 5.1. The results are obtained for different electric field strengths in order to investigate the effect of electric field strength on various parameters.

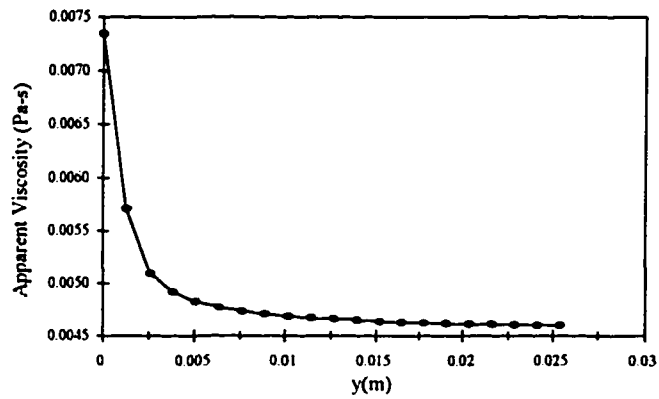
In Fig. 5.7 and 5.8, the apparent viscosity is calculated in the presence of different electric fields and plotted along y -direction for ERF I and ERF II fluids, respectively. Under zero electric field, the apparent viscosity becomes equal to the plastic viscosity since ER fluids do not possess a yield stress at zero electric field. Upon the application of an electric field the particles in the ER fluid align along y -direction in a chainlike structure and the fluid exhibits a yield stress. Changing the electric field strength will effect the apparent viscosity, defined by Equation (5.4), in two ways. First, the plastic viscosity will change as the electric field is varied. Second,



(a)

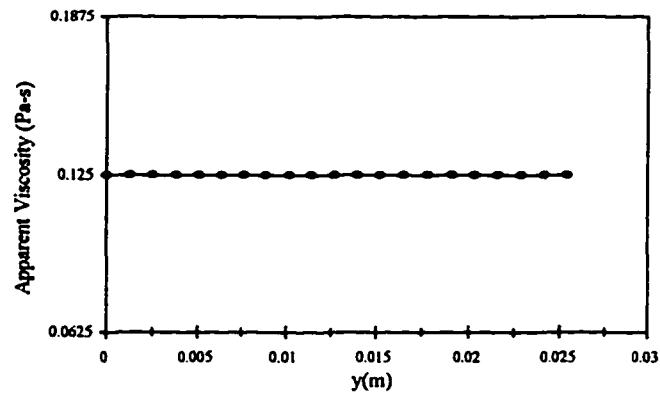


(b)

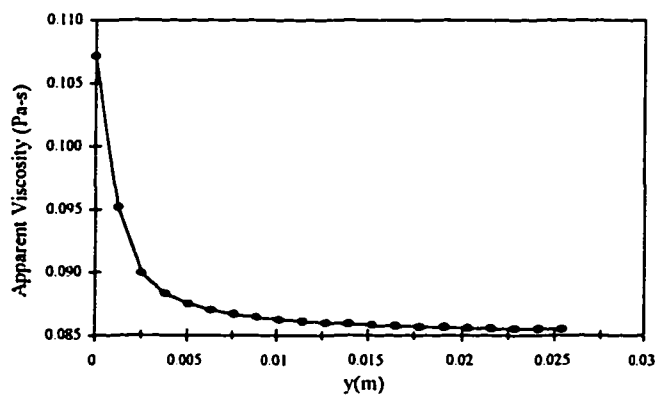


(c)

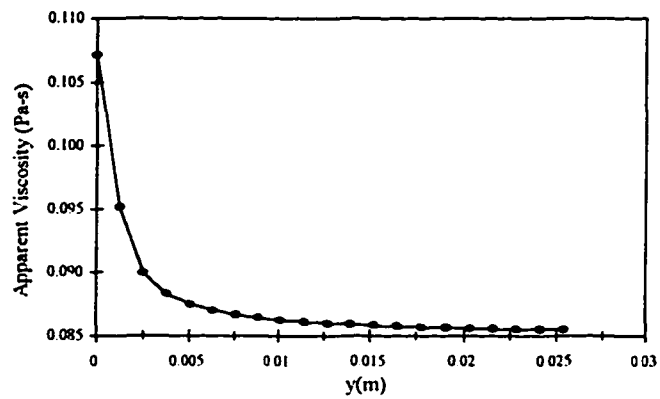
Fig. 5.7. Variation in the apparent viscosity of ERF I along y-direction for
 (a) E=0 kV/mm, (b) E=1 kV/mm, (c) E=2 kV/mm.



(a)



(b)



(c)

Fig. 5.8. Variation in the apparent viscosity of ERF II along y-direction for

(a) $E=0$ kV/mm, (b) $E=2$ kV/mm, (c) $E=5$ kV/mm.

the threshold gradient α_0 , defined by Equation (5.5), is affected by the electric field.

As shown in Fig. 5.7 and 5.8, the apparent viscosity drops along the y-direction with a similar trend for both ERF I and ERF II as the ER fluid flows through the poroelastic material. It is observed that the total amount of change in the apparent viscosity of ERF I is higher than that of ERF II. This is because ERF I has strong electric field dependent parameters (yield stress and plastic viscosity) compared to ERF II as shown in Fig. 5.3, 5.4, 5.5, and 5.6.

For different field strengths, solid displacement, fluid pressure, and pressure gradient are calculated at each node for the poroelastic system having ERF I and ERF II fluids, at $\omega=2\pi$ rad/s and $t=0.2$ sec. In Fig. 5.9 and 5.10 solid displacements, in Fig. 5.11 and 5.12 fluid pressures, and in Fig. 5.13 and Fig. 5.14 pressure gradient values are plotted along y-direction for three different values of electric field. It is observed that a considerable change occurs in all these variables as the electric field is varied. As a matter of fact, the variations in all these variables due to the electric field changes are the result of the variation of the apparent viscosity as a function of electric field. For ERF I, the electric field dependency of the apparent viscosity is strong compared to ERF II. Hence, the effect of electric field changes on solid displacement, fluid pressure, and pressure gradient are more pronounced in ERF I system compared to ERF II system. As the electric field is increased the apparent viscosity decreases, as shown in Fig. 5.7 and 5.8, resulting in a reduced fluid drag on the solid. Therefore, solid deforms more uniformly and fluid pressure drops at every point within the material. For ERF I system the fluid pressure at the bottom drops from -2.0 MPa to

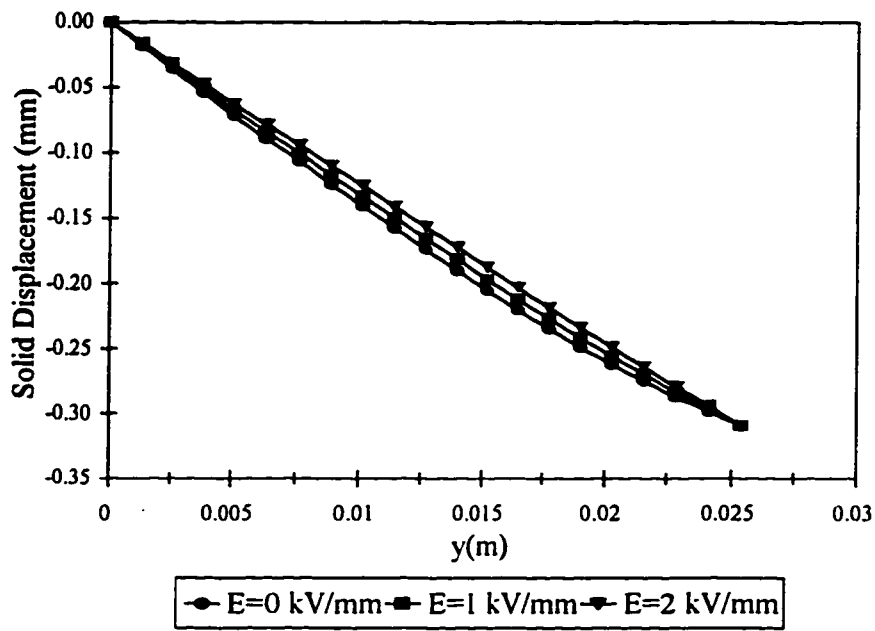


Fig. 5.9. Variation of solid displacement with electric field (ERF I)

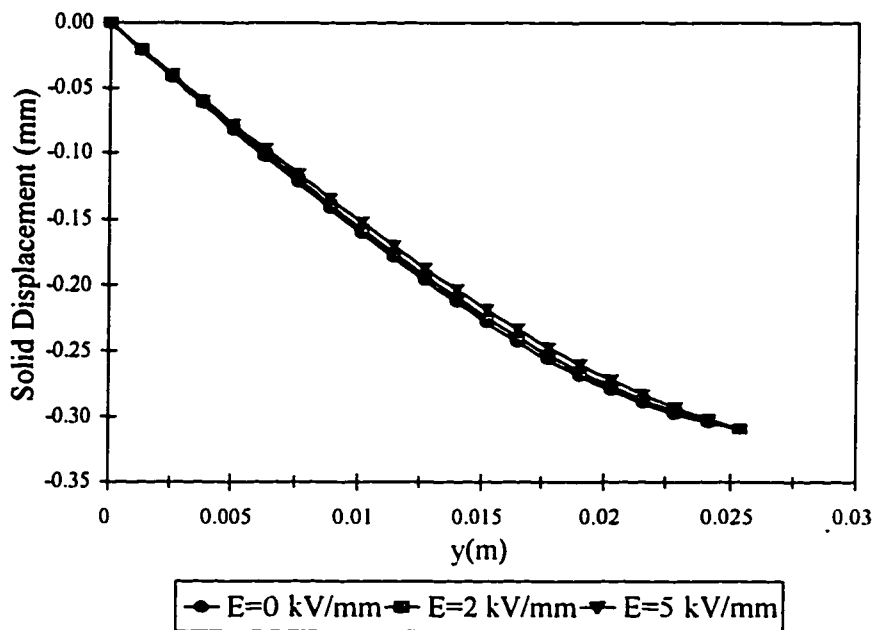


Fig. 5.10. Variation of solid displacement with electric field (ERF II)

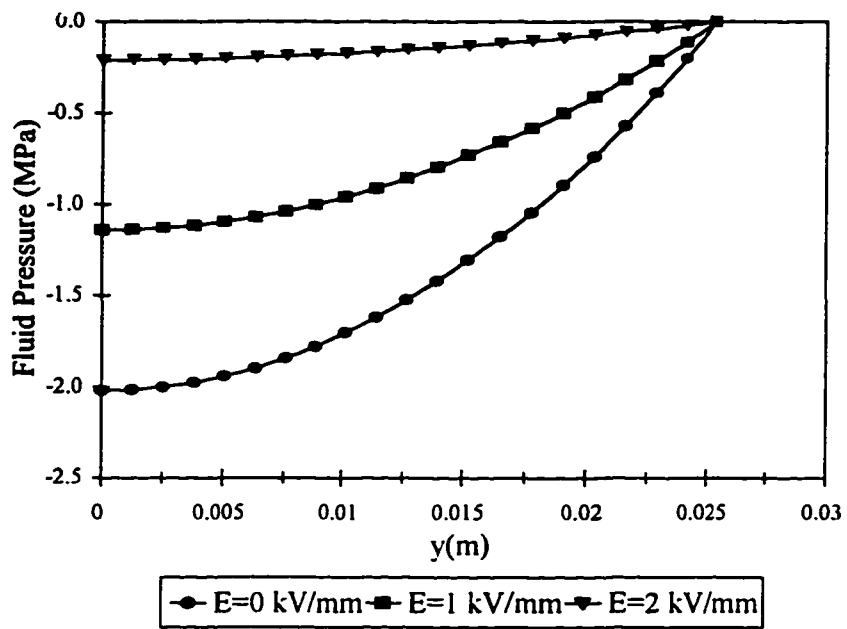


Fig. 5.11. Variation of fluid pressure with electric field (ERF I)

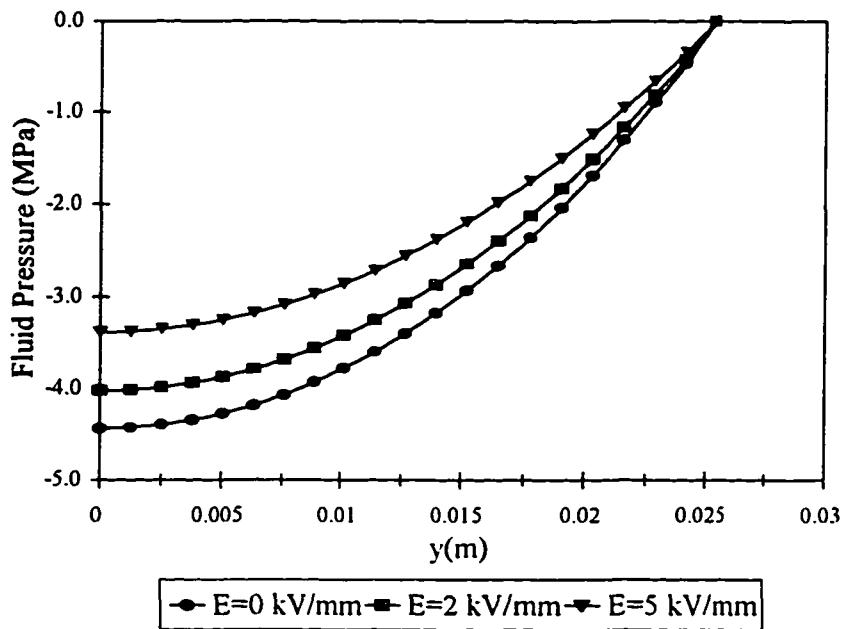


Fig. 5.12. Variation of fluid pressure with electric field (ERF II)

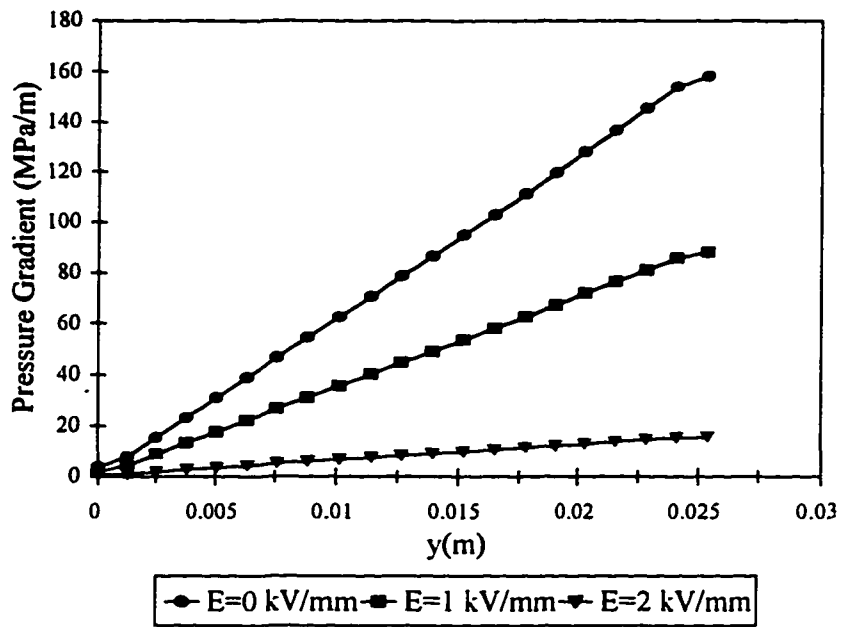


Fig. 5.13. Variation of pressure gradient with electric field (ERF I)

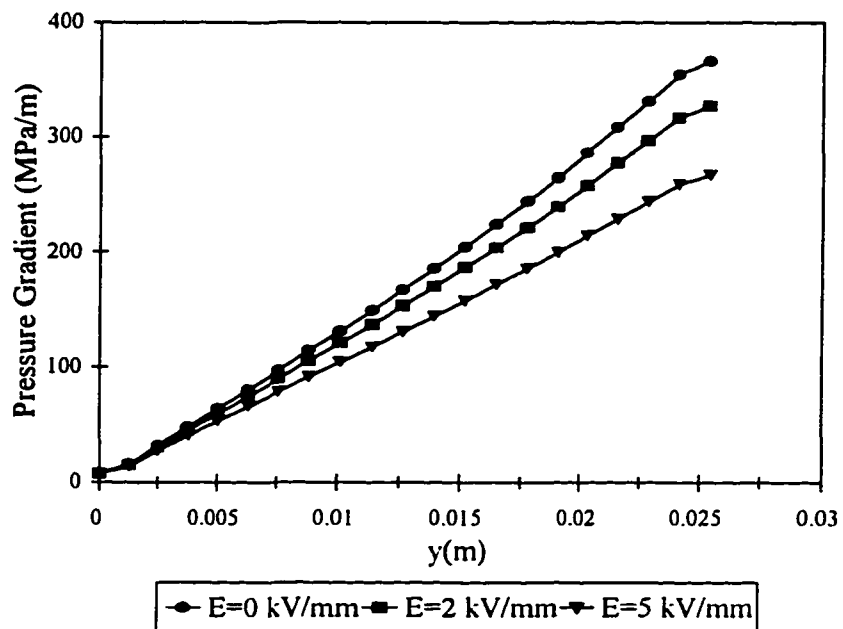


Fig. 5.14. Variation of pressure gradient with electric field (ERF II)

-0.2 MPa as the electric field is increased from 0 to 2 kV/mm as shown in Fig. 5.10. Pressure gradient also decreases with increasing electric field strength.

The complex modulus which is defined as the ratio of normal surface stress to a dimensionless surface displacement, as given by Equation (3.30), is calculated for different electric field strengths using the finite element model for the flow of ERF I and ERF II fluids in the poroelastic structure. The storage modulus and loss tangent values are plotted in Fig. 5.15, 5.16, 5.17 and 5.18 as a function of frequency.

As shown in these figures, the electric field has considerable effect on the complex modulus. When the electric field is increased the critical frequency at which the maximum dissipation occurs shifts to higher frequencies (Fig. 5.16 and 5.18) and

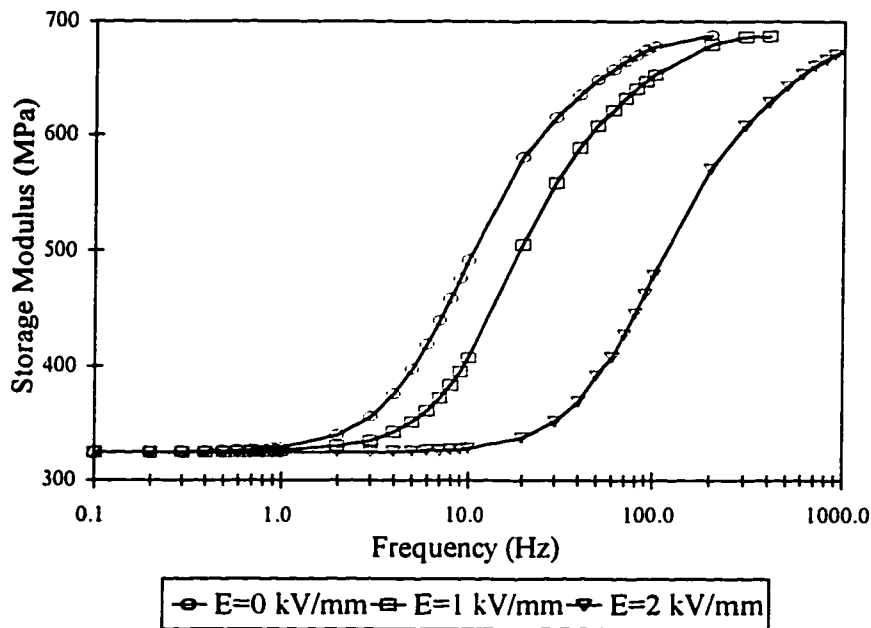


Fig. 5.15. Storage modulus calculated at different electric fields (ERF I)

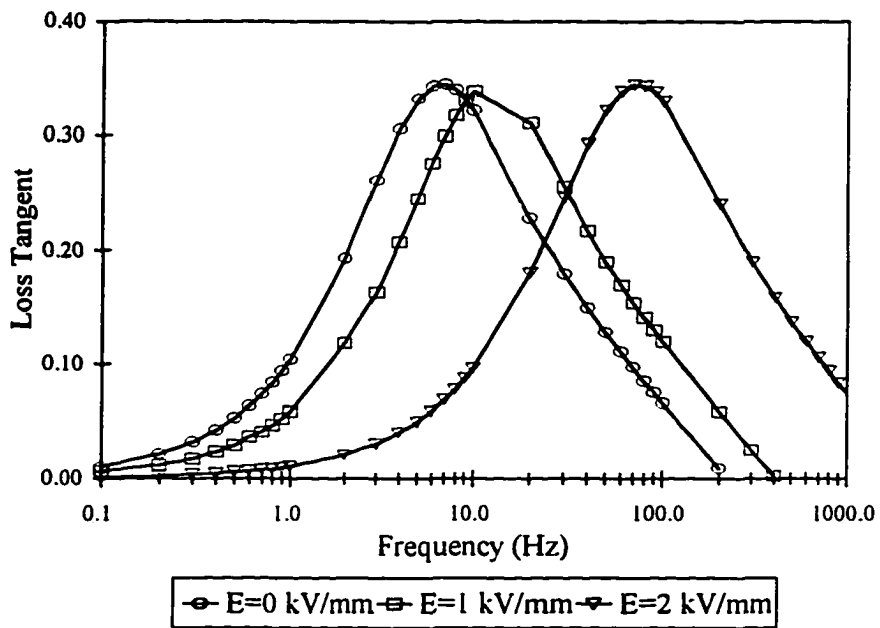


Fig. 5.16. Loss tangent calculated at different electric fields (ERF I)

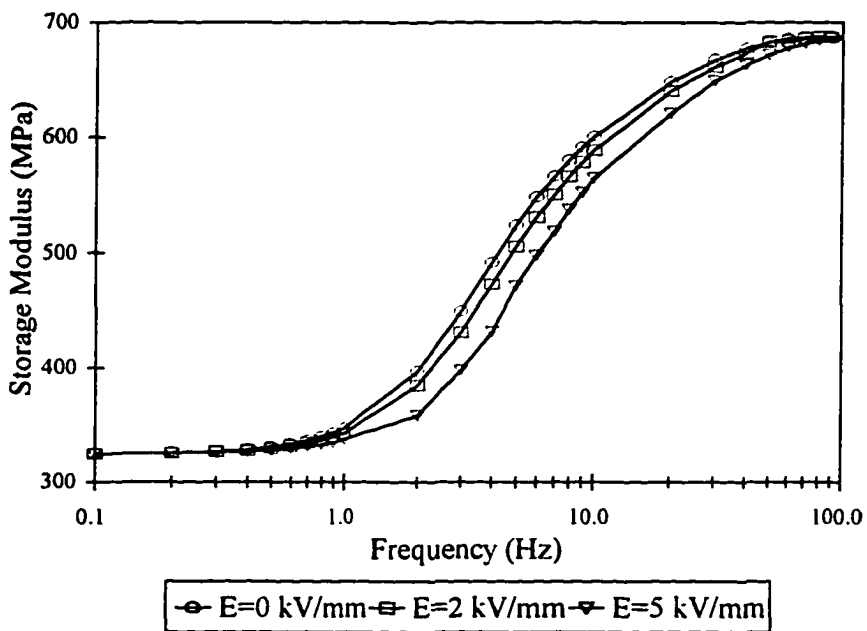


Fig. 5.17. Storage modulus calculated at different electric fields (ERF II)

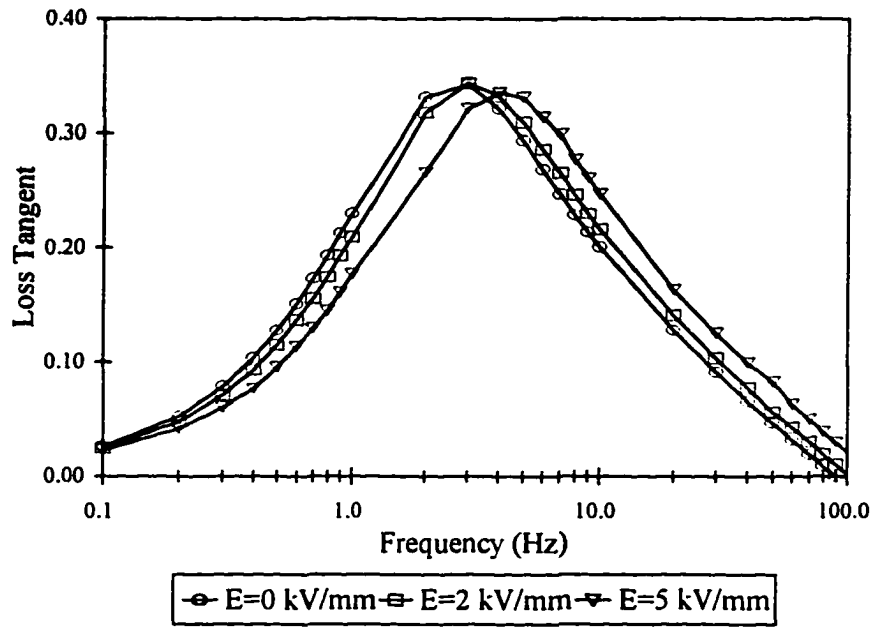


Fig. 5.18. Loss tangent calculated at different electric fields (ERF II)

rubber to glass transition behavior also occurs at higher frequencies (Fig. 5.15 and 5.17). However, electric field has no effect on the maximum amount of dissipation.

A considerable amount of change is observed in the storage modulus and loss tangent of ERF I system when the electric field is increased from 0 to 2 kV/mm while the change in the storage modulus and loss tangent of ERF II system was small even though the electric field is increased from 0 to 5 kV/mm. This is again due to the fact that ERF I has a strong electric-field-dependent plastic viscosity while the electric field dependency of ERF II is weak. As defined by Equation (5.6), the apparent viscosity becomes field dependent not only due to field dependent plastic viscosity but also due to the threshold gradient α_0 which is field dependent as well. On the other hand, the ratio $\alpha_0/\Delta P_1$ gradually decreases along the y-direction and becomes almost zero at the

surface due to increasing ΔP along the y-direction. Therefore, the field dependency of α_0 does not have a noticeable effect on the complex modulus which is defined as the ratio of the normal surface traction to the dimensionless surface displacement.

CHAPTER VI

CONCLUSIONS

In this thesis, the dynamic response to harmonic loading of a disk of poroelastic material containing non-Newtonian Bingham fluid which exhibits a yield stress is investigated. Biot's poroelasticity equations and modified Darcy's law which is derived for non-Newtonian fluids exhibiting a yield stress are combined together to obtain the nonlinear, coupled governing equations of the system. A numerical model is constructed using the finite element technique taking into account the nonlinear nature of Bingham fluid in order to calculate the response and the complex modulus of the system. As an application of the model developed, the behavior of electrorheological fluids in poroelastic media is studied. The storage modulus and loss tangent are calculated for different electric field strengths and the effect of electric field on the system response is investigated.

The constitutive equations derived are based on Biot's quasi-static theory which includes dissipation due to friction arising from the flow of fluid relative to the solid but neglects the inertia effects. It is assumed that the porous solid skeleton is linearly elastic and undergoes small deformations while the flow of fluid produced by

the deformation of the material is governed by modified Darcy's law. The governing equations are valid as long as $|\Delta P| \geq \alpha_0$ is satisfied over the entire flow field. In other words, the minimum threshold gradient should be exceeded and the flow should occur everywhere. This assumption is the result of several facts;

i) ER fluids yield at relatively low levels of strains ($< 1\%$).

ii) Lipscomb and Dean (1984) showed that yielding and flow must occur everywhere for the flow of Bingham type of fluids in confined, complex geometries. They concluded that;

- * no flow occurs anywhere until a minimum stress is reached,

- * yielding occurs over the entire flow field,

- * no plug regions exist,

- * flow occurs everywhere until the yield condition is no longer satisfied, after which flow must stop everywhere.

iii) The validity of this assumption is also somehow related to the selection of the poroelastic material/fluid combination. Using a stiff material will result in higher pressure gradient and flow velocity at each point within the structure according to the first constitutive relation given by Equation (3.25). If the purpose is to obtain maximum dissipation, it would be necessary to increase the fluid flow within the porous structure. This can be achieved by using a poroelastic material with relatively high stiffness which will also provide that $|\Delta P| \geq \alpha_0$ over the entire flow field.

In order to verify the accuracy of the numerical model, the results obtained by using the finite element model developed were compared with the analytical solution

which is available for Newtonian fluid flow through poroelastic media. The numerical results matched the analytical solution well and the accuracy was good enough even with 20 elements.

The model developed is also modified for the analysis of poroelastic materials containing ER fluids. Two different ER fluids are considered; ERF I and ERF II. ERF I has stronger field-dependent parameters compared to ERF II. In ER fluids, the yield stress and the plastic viscosity are two important parameters affected by the electric field changes most. The fluid compressibility is assumed field-independent. The following conclusions are drawn from the obtained results;

i) The analysis shows that the poroelastic system exhibits the rubber to glass transition frequency behavior typical of viscoelastic materials as pointed out by Wijesinghe and Kingsbury (1979). As the frequency is increased, the fluid flow resistance increases, resulting in increased material stiffness and loss factor. At high frequencies, the interaction force between the fluid and the solid matrix becomes so large that the solid and fluid move together and there is no fluid flow. At these frequencies the loss modulus, due to the fluid flow, becomes zero and the storage modulus becomes its maximum. Thus as the frequency increases, the loss factor starts to increase from zero and reaches its maximum at a critical frequency and then reduces to zero again. Similarly, the storage modulus starts to increase from the matrix storage modulus and approaches its maximum value as the frequency goes to infinity.

ii) The poroelastic theory provides both methods of predicting the response of structures composed of fluid-filled porous solids and insight into the system

parameters which control the maximum value of loss modulus and the corresponding excitation frequency. The stiffness and energy dissipation characteristics of the systems can be related to the elastic properties of the fluid phase, solid phase, and the solid skeleton, as well as the fluid viscosity and the flow resistance (resistivity) of the skeleton. Damping and stiffness are frequency dependent quantities. Although the frequency at which damping is maximum depends upon the fluid viscosity, the maximum value of the damping depends only on the bulk moduli of fluid, solid and skeleton. By using ER fluid whose viscosity can be altered, the dynamic response of a poroelastic system could be tailored to provide optimum stiffness and damping over a range of operating conditions. The critical frequency, for example, could be made to coincide with a resonance or excitation frequency by adjusting the electric field strength. However, the maximum value of damping does not change with the electric field since the fluid bulk modulus is a weak function of field strength.

iii) The electric field dependencies of the plastic viscosities of ERF I and ERF II are different. ERF I has a strong field-dependent plastic viscosity; however, the plastic viscosity of ERF II does not change much with field strength. By comparing complex moduli of two ER fluids, as shown in Fig. 5.15, 5.16, 5.17, and 5.18, it can be concluded that the field dependency of plastic viscosity is a very important factor in the response of the system. Apparent viscosity changes not only due to the field-dependent plastic viscosity but also because of the field-dependent yield stress. However, the yield stress term in the definition of apparent viscosity gradually decreases along y-direction due to increasing pressure gradient and the apparent

viscosity becomes almost equal to plastic viscosity at the surface. Therefore, the field dependency of the yield stress does not have a considerable effect on the complex modulus which is defined as the ratio of the normal surface traction to the dimensionless surface displacement.

iv) Under these circumstances, it is possible to use ER fluid-poroelastic solid device as a semi-active vibration isolation system to provide optimum stiffness and damping as excitation or resonant frequencies change. For the applications in which small but accurate frequency changes are desired, ERF II type of systems would be suitable since they could provide small but accurate changes in the complex modulus with a wide range of electric field changes. On the other hand, ERF I type of systems would be more convenient for the applications in which large but less precise frequency changes are desired since a small change in the electric field results in a considerable change in the complex modulus of these systems.

BIBLIOGRAPHY

- Adriani, P.M., A.P. Gast, "A Microscopic Model of Electrorheology", *Phys. Fluids*, v31 n10, 1988, pp2757-2768.
- Al-Fariss, Tariq F., "Flow of Polymer Solutions Through Porous Media", *Ind. Eng. Chem. Res.*, v29, October 1990, pp2159-2160.
- Al-Fariss, T.F., K.L. Pinder, "Flow Through Porous Media of a Shear-Thinning Liquid with Yield Stress", *The Canadian Journal of Chemical Engineering*, v65, 1987, pp391-405.
- Al-Fariss, T.F., "A New Correlation for Non-Newtonian Flow Through Porous Media", *Computers and Chemical Engineering*, v13 n3-4, 1989, pp475-482.
- Atkin, R.J., Xiao Shi, W.A. Bullough, "Solutions of the Constitutive Equations for the Flow of an Electrorheological Fluid in Radial Configuration", *J. Rheol.* v35 n7, October 1991, pp 1441-1461.
- Beris, A.N., J.A. Tsamopoulos, R.C. Armstrong, R.A. Brown, "Creeping Motion of a Sphere Through a Bingham Plastic", *J. Fluid Mech.*, v158, 1985, pp219-244.
- Bhadra, D.K., W.B. Thompson, "Distributed Anechoic System Using Electrically Active Fluid", *Int. J. Modern Phys. B*, v6 n15-16, 1992, pp2749-2762.
- Biot, M.A., "General Theory of Three Dimensional Consolidation", *J. Appl. Phys.*, v12, 1941, pp155-164.
- Biot, M.A., "Theory of Elasticity and Consolidation for a Porous Anisotropic Solid", *J. Appl. Phys.*, v26, 1955, pp182-185.
- Biot, M.A., "General Solutions of the Equations of Elasticity and Consolidation for a Porous Material", *J. Appl. Phys.*, v23, 1956, pp91-96.
- Biot, M.A., "The Elastic Coefficients of the Theory of Consolidation", *Journal of Applied Mechanics*, v24, 1957, pp594-601.
- Block, H., J.P. Kelly, "Electro-rheology", *Journal of Physics. D, Applied Physics*, v21, 1988, pp1661-1677.

- Bonnecaze, R.T., J.F. Brady, "Yield Stresses in Electrorheological Fluids", *J. Rheol.*, v36 n1, January 1992, pp 73-43.
- Bonnecaze, R.T., J.F. Brady, "Dynamic Simulation of an Electrorheological Fluid", *Journal of Chemical Physics*, v96 n3, 1992, pp2183-2202.
- Boutin, C., J.L. Auriault, "Dynamic Behavior of Porous media saturated by a viscoelastic fluid. Application to bituminous concretes", *Int. Journal of Engn. Sci.*, v28 n11, 1990, pp1157-1181.
- Brooks, D., J. Goodwin, C. Hjelm, L. Marshall, C. Zukoski, "Visco-elastic Studies on an Electro-rheological Fluid", *Coolids and Surfaces*, v18, 1986, pp293-312.
- Ceccio, S.L., A.S. Wineman, "Influence of Orientation of Electric Field on Shear Flow of Electrorheological Fluids", *J. of Rheology*, v38 n3, 1994, pp453-463.
- Chen, Tian-jie, Xuesong Zhang, R.N. Zitter, R. Tao, "Deformation of an Electrorheological Chain Under Flow", *J. Appl. Phys.*, v74, July 15, 1993, pp942-945.
- Cohen, Yoram, F.R. Christ, "Polymer Retention and Adsorption in the Flow of Polymer Solutions Through Porous Media", *SPE Reservoir Engineering*, v1, 1986, pp113-118.
- Coleman, C.J., "A Finite Element Routine for Analysing Non-Newtonian Flows, Part II: The Extrusion of a Maxwell Fluid", *J. of Non-Newtonian Fluid Mechanics*, v8, 1981, pp261-270.
- Conrad, H., A.F. Sprecher, Y. Choi, Y. Chen, "The Temperature Dependence of the Electrical Properties and Strength of Electrorheological Fluids", *J. Rheol.* v35 n7, October 1991, pp1393-1410.
- Conrad, H., A.F. Sprecher, Y. Chen, "The Strength of Electrorheological (ER) Fluids", *Int. J. Modern Phys. B*, v6 n15-16, 1992, pp2575-2594.
- Conrad, H., A.F. Sprecher, "Characteristics and Mechanisms of Electrorheological Fluids", *Journal of Statistical Physics*, v64 n5-6, 1991, pp1073-1091.
- Coulter, J.P., T.G. Duclos, "Application of Electrorheological Materials in Vibration Control", *Proceedings of the Second International Conference on Electrorheological Fluids*, J.D. Carlson, A.F. Sprecher, H. Conrad, eds. Lancaster: Technomic Publishing Company, Inc., pp300-325.
- Coulter, J.P., K.D. Weiss, J.D. Carlson, "Electrorheological Materials and Their Usage in Intelligent Material Systems and Structures, Part II: Applications",

Proceedings of the Recent Advances in Adaptive and Sensory Materials and Their Applications, C.A. Rogers, ed. Lancaster: Technomic Publishing Company, Inc., 1992, 17 pages.

Covey, G.H., B.R. Stanmore, "Use of the Parallel-Plate Plastometer for the Characterization of Viscous Fluids with a Yield Stress", *J. of Non-Newtonian Fluid Mechanics*, v8, 1981, pp249-260.

Desai, C.S., "Finite Element Methods for Flow in Porous Media", Chapter 8 in *Finite Elements in Fluids* (eds Gallagher, R.H. et al.) John Wiley & Sons, U.K., 1975, pp157-182.

Desai, C.S., "Free Surface Flow Through Porous Media Using a Residual Procedure", Chapter 18 in *Finite Elements in Fluids* (eds Gallagher, R.H. et al.) John Wiley & Sons, U.K., 1984, pp377-392.

Duclos, Theodore G., "Electrorheological Fluids and Devices", *Automotive Engineering*, v96, December 1988, pp 45-52.

Duclos, T.G., "Design of Devices Using Electrorheological Fluids", *SAE Technical Paper Series*, Paper No. 881134, 1988, 5 pages.

Ehrgott, R.C., S.F. Masri, "Experimental Characterization of an Electrorheological Material Subjected to Oscillatory Shear Strains", *Journal of Vibration and Acoustics*, v116 n1, 1994, pp53-60.

Ehrgott, R.C., S.F. Masri, "Modeling the Oscillatory Dynamic Behaviour of Electrorheological Materials in Shear", *Smart Materials and Structures*, v1 n4, 1992, pp275-285.

Fujita, T., J. Mochizuki, I.J. Lin, "Viscosity of Electrorheological Magneto-dielectric Fluid Under Electric and Magnetic Fields", *Journal of Magnetism and Magnetic Materials*, v122 n1-3, 1993, pp29-33.

Gale, J.E., "Flow in Rocks with Deformable Fractures", *Finite Element Methods in Flow Problems* (Oden et al.), Huntsville, Ala., UAH Press, 1974, pp583-598.

Gamota, D.R., F.E. Filisko, "High Frequency Dynamic Mechanical Study of an Alumino silicate Electrorheological Material", *J. Rheol.*, v35 n7, October 1991, pp1411-1415.

Gamota, D.R., F.E. Filisko, "Dynamic Mechanical Studies of Electrorheological Materials: Moderate Frequencies", *J. Rheol.*, v35 n3, April 1991, pp399-425.

- Gamota, D.R., F.E. Filisko, "Linear/nonlinear Mechanical Properties of Electrorheological Materials", *Int. J. Modern Phys. B*, v6 n15-16, 1992, pp2595-2607.
- Gamota, D.R., A.S. Wineman, F.E. Filisko, "Fourier Transform Analysis: Nonlinear Dynamic Response of an Electrorheological Material", *J. Rheol.*, v37 n5, 1993, pp919-933.
- Gartling, D.K., N. Phan-Thien, "A Numerical Simulation of a Plastic Fluid in a Parallel- Plate Plastometer", *Journal of Non-Newtonian Fluid Mechanics*, v14, 1984, pp347-360.
- Gent, A.N. and K.C. Rush, "Viscoelastic Behavior of Open-Cell Foams", *Rubber Chem. Tech.*, v39, 1966, pp389.
- Goldstein, Gina, "Electrorheological Fluids: Applications Begin to Gel", *Mechanical Engineering*, v112, October 1990, pp48-52.
- Hartsock, D.L., R.F. Novak, G.J. Chaundy, "ER Fluid Requirements for Automotive Devices", *J. Rheol.*, v35 n7, October 1991, pp1305-1326.
- Hejri, Shahab, G.P. Willhite, D.W. Green, "Development of Correlations to Predict Biopolymer Mobility in Porous Media", *SPE Reservoir Engineering*, v6 n1, 1991, pp91-98.
- Irobe, M., T. Akagi and H. Itoh, "Finite Element Analysis of Consolidation of Unsaturated Soil", *Finite Element Methods in Flow Problems* (Oden et al.), Huntsville, Ala., UAH Press, 1974, pp757-767.
- Jordan, T.C., M.T. Shaw, "Viscoelastic Response of Electrorheological Fluids. II. Field Strength and Strain Dependence", *J. Rheol.*, v36 n3, April 1992, pp441-463.
- Keentok, M., "The Measurement of the Yield Stress of Liquids", *Rheologica Acta*, v21, 1982, pp325-332.
- Keentok, M., J.F. Milthorpe and E. O'Donovan, "On the Shearing Zone Around Rotating Vanes in Plastic Liquids: Theory and Experiment", *Journal of Non-Newtonian Fluid Mechanics*, v17, 1985, pp23-35.
- Kim, Y.S., K.W. Wang, H.S. Lee, "Feedback Control of ER-Fluid-Based Structures for Vibration Suppression", *Smart Materials and Structures*, v1, 1992, pp139-145.

- Kim Y.K., H.B. Kingsbury, "Dynamic Characterization of Poroelastic Materials", *Experimental Mechanics*, v19, 1979, pp252-258.
- Kingsbury, H.B., "Determination of Material Parameters of Poroelastic Media", *Fundamentals of Transport Phenomena in Porous Media*, J. Bear and M. Corapcioglu, eds., M. Nijhoff, Dordrecht, 1984, pp581-609.
- Klass, D.L., T.W. Martinek, "Electroviscous Fluids. I. Rheological Properties", *J. Appl. Phys.*, v38 n1, January 1967, pp67-74.
- Klass, D.L., T.W. Martinek, "Electroviscous Fluids. II. Electrical Properties", *J. Appl. Phys.*, v38 n1, January 1967, pp75-80.
- Klaus, E.E., J.A. O'Brien, "Precise Measurement and Prediction of Bulk-Modulus Values for Fluids and Lubricants", *ASME Journal of Basic Engineering*, v86, 1964, pp469-474.
- Kordonsky, V.I., E.V. Korobko, T.G. Lazareva, "Electrorheological Polymer-Based Suspensions", *J. Rheol.*, v35 n7, October 1991, pp1427-1439.
- Korobko, E.V., V.E. Dreval, Z.P. Shulman, "Peculiar Features in the Rheological Behavior of Electrorheological Suspensions", *Rheologica Acta*, v33 n2, 1994, pp117-124.
- Lewis, R.W., R.W. Garner, "A Finite Element Solution of Coupled Electrokinetic and Hydrodynamic Flow in Porous Media", *Int. J. for Num. Meth. in Eng.*, v5, 1972, pp41-55.
- Kudallur, Suresh B., Gary H. Conners, Keith W. Buffinton, "Damping and Stiffness Control in a Mount Structure Using Electrorheological (ER) Fluids", *Electrorheological Flows and Measurement Uncertainty*, ASME 1994, pp57-67.
- Lipscomb, G.G., M.M. Denn, "Flow of Bingham Fluids in Complex Geometries", *Journal of Non-Newtonian Fluid Mechanics*, v14, 1984, pp337-346.
- Lou, Yuejin, J.M. Peden, "Flow of Non-Newtonian Fluids Through Eccentric Annuli", *SPE Prod. Eng.*, v5, February 1990, pp91-96.
- Lou, Zheng, Robert D. Ervin, Frank E. Filisko, "The Influence of Viscometer Dynamics on the Characterization of an Electrorheological Fluid Under Sinusoidal Electric Excitation", *J. Rheol.*, v37 n1, Jan./Feb. 1993, pp55-70.
- Margolis, D.L., Nader Vahdati, "The Control of Damping in Distributed Systems Using ER-Fluids", *Proceedings of the Second International Conference on*

- Electrorheological Fluids, J.D. Carlson, A.F. Sprecher, H. Conrad, eds. Lancaster: Technomic Publishing Company, Inc., pp326-348.
- Marshall, R.J. , A.B. Metzner, "Flow of Viscoelastic Fluids Through Porous Media", *Ind. Eng. Chem. Fundam.*, v6 n3, 1967, pp393-400.
- McLeish, T.C.B., "Viscoelastic Response of Electrorheological Fluids. I. Frequency Dependence", *J. Rheol.*, v35 n3, April 1991, pp427-448.
- Monkman, G.J., "Addition of Solid Structures to Electrorheological Fluids", *J. Rheol.*, v35 n7, October 1991, pp1385-1393.
- Munson, B.R., D.F. Young, T.H. Okiishi, *Fundamentals of Fluid Mechanics*, John Wiley & Sons, Newyork, 1994.
- Pinkos, Andrew, Emil Shtarkman, Thomas Fitzgerald, "Active Damping Using ERM Fluids", *Automotive Eng.*, v101, June 1993, pp19-23.
- O'Donovan, E.J., R.I. Tanner, "Numerical Study of the Bingham Squeeze Film Problem", *Journal of Non-Newtonian Fluid Mechanics*, v15, 1984, pp75-83.
- Okuna, A., H.B. Kingsbury, "Dynamic Modulus of Poroelastic Materials", *ASME Journal of Applied Mechanics*, v56, 1989, pp535-540.
- Ota, Montonori, Tetsuo Miyamoto, "Many-body effect in the static yield stress of electro rheological fluid", *J. Applied Phys.*, v74, July 15, 1993, pp938-978.
- Otsubo, Yasufumi, Masahiro Sekine, Shingo Katayama, "Electrorheological Properties of Silica Suspensions", *J. Rheol.*, v36 n3, April 1992, pp479-496.
- Papanastasiou, A.C., C.W. Macosko, L.E. Scriven, "Streamlined Finite Elements and Transit Times", *Finite Elements in Fluids*, v6, R.H. Gallagher, G.F. Carey, J.T. Oden, O.C. Zienkiewicz, eds., John Wiley and Sons, NewYork, 1985, p263.
- Papanastasiou, T.C., "Flows of Materials with Yield", *J. Rheol.*, v31, 1987, pp385-404.
- Pascal, H., "Rheological Behaviour Effect of Non-Newtonian Fluids on Steady and Unsteady Flow Through a Porous Medium", *Int. J. for Num. and Anal. Meth. in Geomechanics*, v7, 1983, pp289-303.
- Pascal, H., "Nonsteady Flow of Non-Newtonian Fluids Through a Porous Medium", *Int. J. Engng Sci.*, v21 n3, 1983, pp199-210.

- Pascal, H., "Rheological Behaviour Effect of Non-Newtonian Fluids on Dynamic of Moving Interface in Porous Media", *Int. J. Engng Sci.*, v22 n3, 1984, pp227-241.
- Pascal, H., "Rheological Effects of Non-Newtonian Fluids on Gravitational Segregation Mechanism in a Porous Medium", *Int. J. Engng Sci.*, v22 n7, 1984, pp857-866.
- Pascal, H., "Some Problems Related to the Quantitative Evaluation of Physical Properties of the Porous Medium From Flow Tests with Non-Newtonian Fluids", *Int. J. Engng Sci.*, v23 n3, 1985, pp307-317.
- Pascal, H., "Dynamics of Moving Interface in Porous Media for Power Law Fluids with Yield Stress", *Int. J. Engng Sci.*, v22 n5, 1984, pp577-590.
- Pascal, H., "A Theoretical Analysis on Stability of a Moving Interface in a Porous Medium for Bingham Displacing Fluids and its Application in Oil Displacement Mechanism", *The Canadian Journal of Chemical Engineering*, v64, 1986, pp375-379.
- Pascal, H., F. Pascal, "Flow of Non-Newtonian Fluid Through Porous Media", *Int. J. Engng Sci.*, v23 n5, 1985, pp571-585.
- Pascal, H., "Nonsteady Flow Through Porous Media in the Presence of a Threshold Gradient", *Acta Mechanica*, v39, 1981, pp207-224.
- Pascal, H., "Stability of a Moving Interface in Porous Medium for Non-Newtonian Displacing Fluids and its Applications in Oil Displacement Mechanism", *Acta Mechanica*, v58, 1986, pp81-91.
- Pascal, H. and F. Pascal, "On Viscoelastic Effects in Non-Newtonian Steady Flows Through Porous Media", *Transport in Porous Media*, v4, 1989, pp17-35.
- Pascal, H., F. Pascal, "On Viscoelastic effect in Non-Newtonian Steady Flows Through Porous Media", *Transport in Porous Media*, v4, 1989, pp17-35.
- Powell, J.A., "The Mechanical Properties of an Electrorheological Fluid Under Oscillatory Dynamic Loading", *Smart Materials and Structures*, v2 n4, 1993, pp217-231.
- Rajagopal, K.R., A.S. Wineman, "Flow of Electro-rheological Materials", *Acta Mechanica*, v91 n1-2, pp57-75.
- Rusch, K.C., "Dynamic Behavior of Flexible Open-Cell Foams", Ph.D. Thesis, Un. of Akron, Akron, Ohio, 1965.

- Sandhu, R.S., E.L. Wilson, "Finite-Element Analysis of Seepage in Elastic Media", *Journal of Engineering Mechanics Division, ASCE*, v95 n3, 1969, pp641-652.
- Savins, J.G., "Non-Newtonian Flow Through Porous Media", *Ind. Eng. Chem.*, v61, 1969, pp118-147.
- See, Howard, Masao Doi, "Shear Resistance of Electrorheological Fluids Under Time-Varying Electric Fields", *J. Rheol.*, v36 n6, August 1992, pp1143-1163.
- See, H., H. Tamura, M. Doi, "The Role of Water Capillary Forces in Electrorheological Fluids", *J. Phys. D: Appl. Phys.*, v26, 1993, pp746-752.
- Sharabi, M.N., "Nonlinear Response of Coupled Flow-Stress Problems", *J. Eng. Mech.*, v110, 1984, pp1303-1319.
- Shulman, Z.P., E.V. Korobko, Yu.G. Yanovskii, "The Mechanism of the Viscoelastic Behaviour of Electrorheological Suspensions", *Journal of Non-Newtonian Fluid Mechanics*, v33 n2, 1989, pp181-196.
- Song, H.S., E.E. Klaus, J.L. Duda, "Prediction of Bulk Moduli for Mineral Oil Based Lubricants, Polymer Solutions, and Several Classes of Synthetic Fluids", *J. of Tribology*, v113, October 1991, pp675-680.
- Sprecher, A.F., J.D. Carlson, H. Conrad, "Electrorheology at Small Strains and Strain Rates of Suspensions of Silica Particles in Silicone Oil", *Materials Science and Engineering*, v95, 1987, pp187-197.
- Sproston, J.L., S.G. Rigby, E.W. Williams, R. Stanway, "A Numerical Simulation of Electrorheological Fluids in Oscillatory Compressive Squeeze-Flow", *Journal of Physics D: Applied Physics*, v27 n2, 1994, pp338-343.
- Sproston, J.L., S.G. Rigby, E.W. Williams, R. Stanway, "The Electrorheological Automotive Engine Mount", *Journal of Electrostatics*, v32 n3, 1994, pp253-259.
- Stangroom, J.E., "Basic Considerations in Flowing Electrorheological Fluids", *Journal of Statistical Physics*, v64 n5-6, 1991, pp1059-1072.
- Stanway, R., J. Sproston, R. Firoozian, "Identification of the Damping Law of an Electro-rheological Fluid: A Sequential Filtering Approach", *Journal of Dynamic Systems, Measurement and Control*, v111, March 1989, pp91-96.

- Stanway, R., J.L. Sproston, N.G. Stevens, "Non-linear modelling of an Electro-rheological Vibration Damper", *Journal of Electrostatics*, v20, 1987, pp167-184.
- Stanway, R., J.L. Sproston, M.J. Prendergast, J.R. Case, C.E. Wilne, "ER Fluids in the Squeeze-flow Mode: An Application to Vibration Isolation", *Journal of Electrostatics*, v28, 1992, pp89-94.
- Tamura, H., H. See, M. Doi, "Model of porous particles containing water in electro-rheological fluids", *J. Phys. D: Appl. Phys.*, v26, August 14, 1993, pp1181-1187.
- Terzaghi, K., "Endbaumechanik auf bodenphysikglischer grundlage", F Denticke, Leipzig, Germany, 1925.
- Terzaghi, K., *Theoretical Soil Mechanics*, John Wiley & Sons, N.Y., 1943.
- Thurston, G.B., E.B. Gaertner, "Viscoelasticity of Electrorheological Fluids During Oscillatory Flow in a Rectangular Channel", *J. Rheol.*, v35 n7, October 1991, pp1327-1343.
- Valliappan, S., I.K. Lee and P. Boonlualohr, "Finite Element Analysis of Consolidation Problem", *Finite Element Methods in Flow Problems* (Oden et al.), Huntsville, Ala., UAH Press, 1974, pp741-755.
- Vinogradov, G.V., Z.P. Shul'man, Yu G. Yanovskii, V.V. Barancheeva, E.V. Korobko, I.V. Bukovich, "Viscoelastic Behavior of Electrorheological Suspensions", *J. Eng. Phys.* 50, 1986, pp429-432.
- Vradis, George C., Angelos L. Protopapas, "Macroscopic Conductivities for Flow of Bingham Plastics in Porous Media", *J. Hydraulic Eng.*, v119, January 1993, pp95-108.
- Walton, I.C., S.H. Bittleston, "The Axial Flow of a Bingham Plastic in a Narrow Eccentric Annulus", *J. Fluid Mech.*, v222, January 1991, pp39-60.
- Wang, K.C., R. McLay, G.F. Carey, "ER Fluid Modelling", *Proceedings of the Second International Conference on Electrorheological Fluids*, J.D. Carlson, A.F. Sprecher, H. Conrad, eds. Lancaster: Technomic Publishing Company, Inc., pp41-52..
- Weiss, K.D., J.P. Coulter, J.D. Carlson, "Electrorheological Materials and Their Usage in Intelligent Material Systems and Structures, Part I: Mechanisms, Formulations and Properties", *Proceedings of the Recent Advances in*

Adaptive and Sensory Materials and Their Applications, C.A. Rogers, ed. Lancaster: Technomic Publishing Company, Inc., 1992, 17 pages.

- Weiss, K.D., J.D. Carlson, D.A. Nixon, "Viscoelastic Properties of Magneto- and Electro-Rheological Fluid", *Journal of Intelligent Material Systems and Structures*, v5, November 1994, pp772-775.
- Whittle, M., "Computer Simulation of an Electrorheological Fluid", *Journal of Non-Newtonian Fluid Mechanics*, v37 n2-3, 1990, pp233-263.
- Wijesinghe, A.M., H.B. Kingsbury, "On the Dynamic Behavior of Poroelastic Materials", *J. of Acous. Soc. of America*, v65, January 1979, pp90-95.
- Williams, E.W., S.G. Rigby, J.L. Sproston, R. Stanway, "Electrorheological Fluids Applied to an Automotive Engine Mount", *Journal of Non-Newtonian Fluid Mechanics*, v47, 1993, pp221-238.
- Winslow, W.M., Patent 2,417,850, March 25, 1947.
- Winslow, W.M., "Induced Fibration of Suspensions", *Journal of Applied Physics*, v20, 1949, pp1137-1140.
- Wissler, E.H., "Viscoelastic Effects in the Flow of Non-Newtonian Fluids through a Porous Medium", *Ind. Eng. Chem. Fundam.*, v10 n3, 1971, pp411-417.
- Wood, R.H., J.R. Quint, "Compressibility of a Fluid Substance in an Electrostatic Field", *J. Phys. Chem.*, v93, 1989, pp936-937.
- Wu, Yu-Shu, "Theoretical Studies of Non-Newtonian and Newtonian Fluid Flow through Porous Media", Ph.D. Thesis, Un. of California, February 1990.
- Xu, Yuan-Ze, Rui-Feng Liang, "Electrorheological Properties of Semiconducting Polymer-Based Suspensions", *J. Rheol.*, v35 n7, October 1991, pp1355-1373.
- Yen, W.S., P.J. Achorn, "A Study of the Dynamic Behavior of an Electrorheological Fluid", *J. Rheol.*, v35 n7, October 1991, pp1375-1384.

APPENDIX A

GOVERNING EQUATIONS OF POROELASTIC SYSTEMS

In this section the equations governing the flow and deformation of poroelastic systems are presented in detail. According to Biot's quasi-static poroelastic theory, there are twenty unknowns;

$\tau_{xx}, \tau_{yy}, \tau_{zz}, \tau_{yz}, \tau_{zx}, \tau_{xy}, P$ (seven stress components)

$e_{xx}, e_{yy}, e_{zz}, e_{yz}, e_{zx}, e_{xy}, \varepsilon$ (seven strain components)

$u_x, u_y, u_z, U_x, U_y, U_z$ (six displacement components)

to be determined. Also, there are seven stress-strain equations, seven strain-displacement equations and three equilibrium equations that make a total of seventeen equations. The remaining three equations necessary to complete the theory are obtained from Darcy's law.

A.1. Stress-Strain Equations

The stress tensor in a porous material is

$$\begin{Bmatrix} \sigma_{xx} + \sigma & \sigma_{xy} & \sigma_{xz} \\ \sigma_{yx} & \sigma_{yy} + \sigma & \sigma_{yz} \\ \sigma_{zx} & \sigma_{zy} & \sigma_{zz} + \sigma \end{Bmatrix} \quad (\text{A.1})$$

with the symmetry property $\sigma_{ij} = \sigma_{ji}$. If we consider a cube of unit size of the bulk material, σ represents the total normal tension force applied to the fluid part of the faces of the cube (fluid plays a purely dilatational role) as defined by the Equation (3.9). The remaining components σ_{xx} , σ_{xy} , etc., of the stress tensor are the forces applied to that portion of the cube faces occupied by the solid.

The strain energy function V of a poroelastic system can be written as

$$2V = \sigma_{xx}e_{xx} + \sigma_{yy}e_{yy} + \sigma_{zz}e_{zz} + \sigma_{yz}\gamma_{yz} + \sigma_{zx}\gamma_{zx} + \sigma_{xy}\gamma_{xy} + \sigma\varepsilon \quad (\text{A.2})$$

where γ_{ij} are the shear strains for solid phase which is defined as

$$\gamma_{ij} = \left(\frac{\partial u_i}{\partial x_j} + \frac{\partial u_j}{\partial x_i} \right) \quad (\text{A.3})$$

The relation between γ_{ij} and the general strain tensor e_{ij} which is given by Equation (3.12) can be written as

$$\gamma_{ij} = 2e_{ij} \quad (\text{A.4})$$

Assuming the seven stress components are linear functions of the seven strain components the expression $2V$ is a homogeneous quadratic function of the strain with twenty-eight distinct coefficients. The stress components are obtained from the partial derivatives of V as follows;

$$\begin{aligned} \sigma_{xx} &= \frac{\partial V}{\partial e_{xx}} , & \sigma_{yy} &= \frac{\partial V}{\partial e_{yy}} , & \sigma_{zz} &= \frac{\partial V}{\partial e_{zz}} \\ \sigma_{yz} &= \frac{\partial V}{\partial \gamma_{yz}} , & \sigma_{zx} &= \frac{\partial V}{\partial \gamma_{zx}} , & \sigma_{xy} &= \frac{\partial V}{\partial \gamma_{xy}} \\ & & \sigma &= \frac{\partial V}{\partial \varepsilon} \end{aligned} \quad (\text{A.5})$$

This can be written in a matrix form as

$$\begin{Bmatrix} \sigma_{xx} \\ \sigma_{yy} \\ \sigma_{zz} \\ \sigma_{yz} \\ \sigma_{zx} \\ \sigma_{xy} \\ \sigma \end{Bmatrix} = \begin{bmatrix} C_{11} & C_{12} & C_{13} & C_{14} & C_{15} & C_{16} & C_{17} \\ & C_{22} & C_{23} & C_{24} & C_{25} & C_{26} & C_{27} \\ & & C_{33} & C_{34} & C_{35} & C_{36} & C_{37} \\ & & & C_{44} & C_{45} & C_{46} & C_{47} \\ & & & & C_{55} & C_{56} & C_{57} \\ & & & & & C_{66} & C_{67} \\ & & & & & & C_{77} \end{bmatrix} \begin{Bmatrix} e_{xx} \\ e_{yy} \\ e_{zz} \\ 2e_{yz} \\ 2e_{zx} \\ 2e_{xy} \\ \varepsilon \end{Bmatrix} \quad (\text{A.6})$$

In the case of complete isotropy the strain energy function, given by Equation (A.2), becomes

$$2V = (A + 2N)(e_{xx} + e_{yy} + e_{zz})^2 + N(\gamma_{yz}^2 + \gamma_{zx}^2 + \gamma_{xy}^2 - 4e_{yy}e_{zz} - 4e_{zz}e_{xx} - 4e_{xx}e_{yy}) + 2Q(e_{xx} + e_{yy} + e_{zz})\varepsilon + R\varepsilon^2 \quad (\text{A.7})$$

Then, the stress-strain relations calculated from Equation (A.5) will be

$$\begin{Bmatrix} \sigma_{xx} \\ \sigma_{yy} \\ \sigma_{zz} \\ \sigma_{yz} \\ \sigma_{zx} \\ \sigma_{xy} \\ \sigma \end{Bmatrix} = \begin{bmatrix} 2N + A & A & A & 0 & 0 & 0 & Q \\ A & 2N + A & A & 0 & 0 & 0 & Q \\ A & A & 2N + A & 0 & 0 & 0 & Q \\ 0 & 0 & 0 & N & 0 & 0 & 0 \\ 0 & 0 & 0 & 0 & N & 0 & 0 \\ 0 & 0 & 0 & 0 & 0 & N & 0 \\ Q & Q & Q & 0 & 0 & 0 & R \end{bmatrix} \begin{Bmatrix} e_{xx} \\ e_{yy} \\ e_{zz} \\ 2e_{yz} \\ 2e_{zx} \\ 2e_{xy} \\ \varepsilon \end{Bmatrix} \quad (\text{A.8})$$

where A, N, Q, and R are four independent elastic constants. It is also possible and more convenient for some cases to represent stress-strain equations with alternative variables. A second form [Biot (1957)] which employs the total stress τ_{ij} as given in Equation (3.16) and (3.17) can be re-written as

$$\tau_{xx} = 2\mu^* e_{xx} + (\lambda^* + \alpha^2 M)e - \alpha M\zeta$$

$$\tau_{yy} = 2\mu^* e_{yy} + (\lambda^* + \alpha^2 M)e - \alpha M\zeta$$

$$\begin{aligned}
\tau_{zz} &= 2\mu^* e_{zz} + (\lambda^* + \alpha^2 M)e - \alpha M\zeta \\
\tau_{yz} &= \mu^* (2e_{yz}) \\
\tau_{zx} &= \mu^* (2e_{zx}) \\
\tau_{xy} &= \mu^* (2e_{xy}) \\
P &= -\alpha Me + M\zeta
\end{aligned} \tag{A.9}$$

It is more convenient to use the second form of the stress-strain relations, given by Equation (A.9), with the constants μ^* , λ^* , α , and M in problems which neglect the inertia forces while the other form employing the constants A , N , Q , and R have been introduced in connection with wave propagation.

A.2. Strain-Displacement Equations

The average displacement vector of the solid has the components u_x , u_y , u_z , and that of the fluid has the components U_x , U_y , U_z . The solid strain components given in a general form in Equation (3.12) and the fluid dilatation ε can be re-written as

$$e_{xx} = \frac{\partial u_x}{\partial x}$$

$$e_{yy} = \frac{\partial u_y}{\partial y}$$

$$e_{zz} = \frac{\partial u_z}{\partial z}$$

$$\gamma_{yz} = \frac{\partial u_y}{\partial z} + \frac{\partial u_z}{\partial y} = 2e_{yz} \quad (\text{A.10})$$

$$\gamma_{zx} = \frac{\partial u_z}{\partial x} + \frac{\partial u_x}{\partial z} = 2e_{zx}$$

$$\gamma_{xy} = \frac{\partial u_x}{\partial y} + \frac{\partial u_y}{\partial x} = 2e_{xy}$$

$$\varepsilon = \frac{\partial U_x}{\partial x} + \frac{\partial U_y}{\partial y} + \frac{\partial U_z}{\partial z}$$

Equation (A.10) is the seven strain-displacement relations for a poroelastic system.

A.3. Equilibrium Equations

The stress field given by Equation (A.1) of the bulk material satisfies the equilibrium equations given by

$$\begin{aligned} \frac{\partial}{\partial x}(\sigma_{xx} + \sigma) + \frac{\partial \sigma_{xy}}{\partial y} + \frac{\partial \sigma_{xz}}{\partial z} + \rho X &= 0 \\ \frac{\partial \sigma_{yx}}{\partial x} + \frac{\partial}{\partial y}(\sigma_{yy} + \sigma) + \frac{\partial \sigma_{yz}}{\partial z} + \rho Y &= 0 \\ \frac{\partial \sigma_{zx}}{\partial x} + \frac{\partial \sigma_{zy}}{\partial y} + \frac{\partial}{\partial z}(\sigma_{zz} + \sigma) + \rho Z &= 0 \end{aligned} \quad (\text{A.11})$$

where ρ is the mass density of the bulk material and X, Y, Z are the body forces per unit mass.

In the absence of body forces, the three equilibrium equations can be written in terms of the total stress τ_{ij} as

$$\begin{aligned}\frac{\partial \tau_{xx}}{\partial x} + \frac{\partial \tau_{xy}}{\partial y} + \frac{\partial \tau_{xz}}{\partial z} &= 0 \\ \frac{\partial \tau_{yx}}{\partial x} + \frac{\partial \tau_{yy}}{\partial y} + \frac{\partial \tau_{yz}}{\partial z} &= 0 \\ \frac{\partial \tau_{zx}}{\partial x} + \frac{\partial \tau_{zy}}{\partial y} + \frac{\partial \tau_{zz}}{\partial z} &= 0\end{aligned}\tag{A.12}$$

A.4. Darcy's Law

A generalized form of Darcy's law for a nonisotropic material is

$$\begin{pmatrix} -\frac{\partial P}{\partial x} + \rho_f X \\ -\frac{\partial P}{\partial y} + \rho_f Y \\ -\frac{\partial P}{\partial z} + \rho_f Z \end{pmatrix} = \begin{bmatrix} b_{xx} & b_{xy} & b_{xz} \\ b_{yx} & b_{yy} & b_{yz} \\ b_{zx} & b_{zy} & b_{zz} \end{bmatrix} \cdot \begin{pmatrix} \dot{U}_x - \dot{u}_x \\ \dot{U}_y - \dot{u}_y \\ \dot{U}_z - \dot{u}_z \end{pmatrix}\tag{A.13}$$

where ρ_f is the mass density of the fluid. The matrix b_{ij} constitutes a generalization of Darcy's constant if the viscosity coefficient is included in it. The average velocities of the fluid and solid are denoted by \dot{U} and \dot{u} , respectively.

In the case of complete isotropy the equations of flow contain a single coefficient b . In the absence of body forces Darcy's law can be simplified to

$$\begin{aligned} -\frac{\partial P}{\partial x} &= b(\dot{U}_x - \dot{u}_x) \\ -\frac{\partial P}{\partial y} &= b(\dot{U}_y - \dot{u}_y) \\ -\frac{\partial P}{\partial z} &= b(\dot{U}_z - \dot{u}_z) \end{aligned} \tag{A.14}$$

APPENDIX B

GALERKIN WEIGHTED-RESIDUAL METHOD

The method of weighted-residual provides an analyst with a very powerful approximate solution procedure that is applicable to a wide variety of problems. It is a method for finding approximate solutions for linear and nonlinear problems by using a set of trial functions which are defined piecewise over each element.

Let us consider the differential equation for the state variable ϕ as

$$\Gamma(\phi) = g \quad (\text{B.1})$$

where Γ is a differential operator and g is a known function of independent variables.

The first step in the Galerkin method is to assume an approximate solution as

$$\bar{\phi} = \sum_{i=1}^n \alpha_i N_i \quad (\text{B.2})$$

where N_i 's are the trial functions and a_i 's are the values of ϕ at the nodal points. The approximate solution must satisfy the boundary conditions. If the approximate solution is substituted into the governing differential equation, then it will result in an error called the residual as

$$R = \Gamma \left(\sum_{i=1}^n a_i N_i \right) - g \quad (\text{B.3})$$

For exact solution, the residual should be zero at all points. For an approximate solution the residual should be small at all points of the solution domain. Different weighted-residual methods employ different criteria for the determination of a_i so that a weighted average of R vanishes. In Galerkin method, the trial functions N_i themselves are used as the weighting functions. Therefore, a_i 's are obtained from

$$\int_D N_i \cdot R \cdot dD = 0 \quad i = 1, 2, 3, \dots, n \quad (\text{B.4})$$

where D is the domain.

APPENDIX C

ELEMENTAL COEFFICIENT MATRICES AND RIGHT-HAND-SIDE VECTORS

In this section the derivation of the elemental coefficient matrices and RHS vectors for the element Ω_e will be presented. The derivations are based on the definitions given by Equations (4.20)-(4.26).

The trial functions $N_A(\xi)$ and $N_B(\xi)$ shown in Fig. 4.2 and the derivative functions can be re-written as

$$N_A(\xi) = 1 - \frac{\xi}{h} \quad (\text{C.1})$$

$$N_B(\xi) = \frac{\xi}{h} \quad (\text{C.2})$$

$$N'_A(\xi) = -\frac{1}{h} \quad (\text{C.3})$$

$$N'_B(\xi) = \frac{1}{h} \quad (\text{C.4})$$

C.1. Derivation of $[K_e^u]$

Recalling the definition of coefficient matrix $[K_{ij}^u]$ as

$$[K_{ij}^u] = \int_0^d (\lambda^* + 2\mu^*) \frac{dN_i}{dy} \frac{dN_j}{dy} dy \quad (C.5)$$

Substituting Equations (C.1)-(C.4) in the definition, the elemental matrix $[K_e^u]$ can be obtained as given below.

$$K_{AA}^u = (\lambda^* + 2\mu^*) \int_A^B N'_A N'_A d\xi = (\lambda^* + 2\mu^*) \int_A^B \frac{1}{h^2} d\xi = (\lambda^* + 2\mu^*) \frac{1}{h} \quad (C.6)$$

$$K_{AB}^u = (\lambda^* + 2\mu^*) \int_A^B N'_A N'_B d\xi = (\lambda^* + 2\mu^*) \int_A^B \frac{-1}{h^2} d\xi = (\lambda^* + 2\mu^*) \frac{-1}{h} \quad (C.7)$$

$$K_{BA}^u = K_{AB}^u = (\lambda^* + 2\mu^*) \frac{-1}{h} \quad (C.8)$$

$$K_{BB}^u = (\lambda^* + 2\mu^*) \int_A^B N'_B N'_B d\xi = (\lambda^* + 2\mu^*) \int_A^B \frac{1}{h^2} d\xi = (\lambda^* + 2\mu^*) \frac{1}{h} \quad (C.9)$$

$$[M_e^u] = \begin{bmatrix} K_{AA}^u & K_{AB}^u \\ K_{BA}^u & K_{BB}^u \end{bmatrix} = (\lambda^* + 2\mu^*) \begin{bmatrix} 1/h & -1/h \\ -1/h & 1/h \end{bmatrix} \quad (C.10)$$

C.2. Derivation of $[K_e^{P1}]$

Recalling the definition of coefficient matrix $[K_{ij}^{P1}]$ as

$$[K_{ij}^{P1}] = \int_0^d \alpha N_i \frac{dN_j}{dy} dy \quad (C.11)$$

Substituting Equations (C.1)-(C.4) in the definition, the elemental matrix $[K_e^{P1}]$ can be obtained as given below.

$$K_{AA}^{P1} = \alpha \int_A^B N_A N_A' d\xi = \alpha \int_A^B \left(\frac{-1}{h} + \frac{\xi}{h^2} \right) d\xi = \frac{-\alpha}{2} \quad (C.12)$$

$$K_{AB}^{P1} = \alpha \int_A^B N_A N_B' d\xi = \alpha \int_A^B \left(\frac{1}{h} - \frac{\xi}{h^2} \right) d\xi = \frac{\alpha}{2} \quad (C.13)$$

$$K_{BA}^{P1} = \alpha \int_A^B N_B N_A' d\xi = \alpha \int_A^B \left(\frac{-\xi}{h^2} \right) d\xi = \frac{-\alpha}{2} \quad (C.14)$$

$$K_{BB}^{P1} = \alpha \int_A^B N_B N_B' d\xi = \alpha \int_A^B \left(\frac{\xi}{h^2} \right) d\xi = \frac{\alpha}{2} \quad (C.15)$$

$$[M_e^{P1}] = \begin{bmatrix} K_{AA}^{P1} & K_{AB}^{P1} \\ K_{BA}^{P1} & K_{BB}^{P1} \end{bmatrix} = \alpha \begin{bmatrix} -1/2 & 1/2 \\ -1/2 & 1/2 \end{bmatrix} \quad (C.16)$$

C.3. Derivation of $[K_e^{P2}]$

Recalling the definition of coefficient matrix $[K_{ij}^{P2}]$ as

$$[K_{ij}^{P2}] = \int_0^d \left[\frac{dN_i}{dy} \frac{dN_j}{dy} - \left(\mu_a \frac{\partial}{\partial y} \left(\frac{1}{\mu_a} \right) \right) N_i \frac{dN_j}{dy} \right] dy \quad (C.17)$$

The apparent viscosity μ_a is not constant and a function of pressure gradient in y -direction. A linear variation of apparent viscosity is assumed over the element Ω_e with the nodal values of μ_A and μ_B as shown in Fig. C.1.

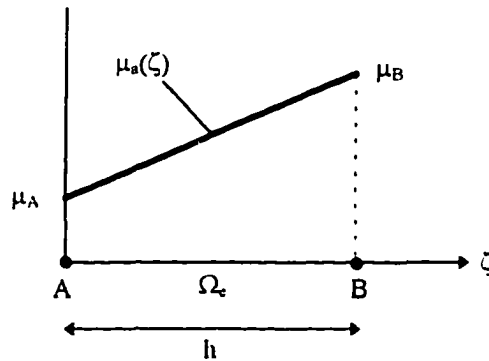


Fig. C.1. Variation of apparent viscosity over the element Ω_e

This linear variation of the apparent viscosity for an element can be written as

$$\mu_a(\xi) = \left(\frac{\mu_B - \mu_A}{h} \right) \xi + \mu_A \quad (C.18)$$

Then, substituting Equations (C.1)-(C.4) and (C.18) in the definition, the elemental matrix $[K_e^{P2}]$ can be obtained as given below.

$$[K_{AA}^{P2}] = \int_A^B \left[N'_A N'_A - \left(\mu_a \frac{\partial}{\partial \xi} \left(\frac{1}{\mu_a} \right) \right) N'_A N'_A \right] d\xi \quad (C.19)$$

$$[K_{AA}^{P2}] = \int_A^B \left\{ \frac{1}{h^2} - \left[\left(\frac{\mu_B - \mu_A}{h} \right)^2 \xi + \left(\frac{\mu_B \mu_A - \mu_A^2}{h} \right) \right] \left[\frac{-1}{h} + \frac{1}{h^2} \xi \right] \right\} d\xi \quad (C.20)$$

simplifying and integrating,

$$[K_{AA}^{P2}] = \frac{1}{h} + \frac{\mu_B^2 - 2\mu_A^2 + \mu_B \mu_A}{6h} \quad (C.21)$$

similarly,

$$[K_{AB}^{P2}] = \frac{-1}{h} + \frac{-\mu_B^2 + 2\mu_A^2 - \mu_B \mu_A}{6h} \quad (C.22)$$

$$[K_{BA}^{P2}] = \frac{-1}{h} + \frac{2\mu_B^2 - \mu_A^2 - \mu_B \mu_A}{6h} \quad (C.23)$$

$$[K_{BB}^{P2}] = \frac{1}{h} + \frac{-2\mu_B^2 + \mu_A^2 + \mu_B \mu_A}{6h} \quad (C.24)$$

$$[K_e^{P2}] = \begin{bmatrix} \frac{1}{h} + \frac{\mu_B^2 - 2\mu_A^2 + \mu_B \mu_A}{6h} & \frac{-1}{h} + \frac{-\mu_B^2 + 2\mu_A^2 - \mu_B \mu_A}{6h} \\ \frac{-1}{h} + \frac{2\mu_B^2 - \mu_A^2 - \mu_B \mu_A}{6h} & \frac{1}{h} + \frac{-2\mu_B^2 + \mu_A^2 + \mu_B \mu_A}{6h} \end{bmatrix} \quad (C.25)$$

C.4. Derivation of $[M_e^k]$

Recalling the definition of coefficient matrix $[M_{ij}^k]$ as

$$[M_{ij}^k] = \int_0^d [\mu_a] \beta_1 N_i \frac{dN_j}{dy} dy \quad (C.26)$$

Substituting Equations (C.1)-(C.4) and (C.18) in the definition, the elemental matrix $[M_e^k]$ can be obtained as given below.

$$[M_{AA}^k] = \beta_1 \int_A^B [(\mu_a) N_A N_A'] d\xi \quad (C.27)$$

$$[M_{AA}^k] = \beta_1 \int_A^B \left[\left(\frac{\mu_B - \mu_A}{h} \xi + \mu_A \right) \left(\frac{-1}{h} + \frac{1}{h^2} \xi \right) \right] d\xi \quad (C.28)$$

Simplifying and integrating,

$$[M_{AA}^k] = \beta_1 \frac{-2\mu_A - \mu_B}{6} \quad (C.29)$$

Similarly,

$$[M_{AB}^k] = \beta_1 \frac{2\mu_A + \mu_B}{6} \quad (C.30)$$

$$[M_{BA}^u] = \beta_1 \frac{-2\mu_B - \mu_A}{6} \quad (C.31)$$

$$[M_{BB}^u] = \beta_1 \frac{2\mu_B + \mu_A}{6} \quad (C.32)$$

$$[M_e^u] = \frac{\beta_1}{6} \begin{bmatrix} -2\mu_A - \mu_B & 2\mu_A + \mu_B \\ -2\mu_B - \mu_A & 2\mu_B + \mu_A \end{bmatrix} \quad (C.33)$$

C.5. Derivation of $[M_e^{\dot{p}}]$

Recalling the definition of coefficient matrix $[M_{ij}^{\dot{p}}]$ as

$$[M_{ij}^{\dot{p}}] = \int_0^d [\mu_a] \beta_2 N_i N_j dy \quad (C.34)$$

Substituting Equations (C.1)-(C.4) and (C.18) in the definition, the elemental matrix $[M_e^{\dot{p}}]$ can be obtained as given below.

$$[M_{AA}^{\dot{p}}] = \beta_2 \int_A^B [(\mu_a) N_A N_A] d\xi \quad (C.35)$$

$$[M_{AA}^{\dot{p}}] = \beta_2 \int_A^B \left[\left(\frac{\mu_B - \mu_A}{h} \xi + \mu_A \right) \left(1 - \frac{2}{h} \xi + \frac{1}{h^2} \xi^2 \right) \right] d\xi \quad (C.36)$$

Simplifying and integrating,

$$\left[M_{AA}^{\dot{p}} \right] = \beta_2 h \frac{\mu_B + 3\mu_A}{12} \quad (\text{C.37})$$

Similarly,

$$\left[M_{AB}^{\dot{p}} \right] = \beta_2 h \frac{\mu_B + \mu_A}{12} \quad (\text{C.38})$$

$$\left[M_{BA}^{\dot{p}} \right] = \beta_2 h \frac{\mu_B + \mu_A}{12} \quad (\text{C.39})$$

$$\left[M_{BB}^{\dot{p}} \right] = \beta_2 h \frac{3\mu_B + \mu_A}{12} \quad (\text{C.40})$$

$$\left[M_e^{\dot{p}} \right] = \frac{\beta_2 h}{12} \begin{bmatrix} \mu_B + 3\mu_A & \mu_B + \mu_A \\ \mu_B + \mu_A & 3\mu_B + \mu_A \end{bmatrix} \quad (\text{C.41})$$

C.6. Derivation of $\{F_e^1\}$

Recalling the definition of RHS vector $\{F_e^1\}$ as

$$\{F_i^1\} = (\lambda^* + 2\mu^*) N_i \frac{\partial u}{\partial y} \Big|_0^d \quad (\text{C.42})$$

Substituting Equations (C.1)-(C.4) in the definition, the elemental vector $\{F_e^1\}$ can be

obtained as given below.

$$\{F_A^1\} = -(\lambda^* + 2\mu^*)N_i \frac{\partial u}{\partial y} \Big|_{y=0} \quad (C.43)$$

$$\{F_B^1\} = (\lambda^* + 2\mu^*)N_i \frac{\partial u}{\partial y} \Big|_{y=d} \quad (C.44)$$

$$\{F_e^1\} = \left\{ \begin{array}{l} -(\lambda^* + 2\mu^*)N_i \frac{\partial u}{\partial y} \Big|_{y=0} \\ (\lambda^* + 2\mu^*)N_i \frac{\partial u}{\partial y} \Big|_{y=d} \end{array} \right\} \quad (C.45)$$

In Equations (C.43) and (C.44), N_i is used instead of N_A or N_B since it is not defined over an element (N_i is not in an integration).

C.7. Derivation of $\{F_e^2\}$

Recalling the definition of RHS vector $\{F_e^2\}$ as

$$\{F_i^2\} = N_i \frac{\partial P}{\partial y} \Big|_0^d \quad (C.46)$$

Substituting Equations (C.1)-(C.4) in the definition, the elemental vector $\{F_e^2\}$ can be obtained as given below.

$$\{F_A^2\} = -N_i \frac{\partial P}{\partial y} \Big|_{y=0} \quad (\text{C.47})$$

$$\{F_B^2\} = N_i \frac{\partial P}{\partial y} \Big|_{y=d} \quad (\text{C.48})$$

$$\{F_e^2\} = \left\{ \begin{array}{l} -N_i \frac{\partial P}{\partial y} \Big|_{y=0} \\ N_i \frac{\partial P}{\partial y} \Big|_{y=d} \end{array} \right\} \quad (\text{C.49})$$

Again, in Equations (C.47) and (C.48), N_i is used instead of N_A or N_B since it is not defined over an element (N_i is not in an integration).

APPENDIX D

NUMERICAL CODE

The finite element model developed for the numerical analysis of the flow of non-Newtonian Bingham fluid through poroelastic medium is explained in Chapter 4. The following is the numerical code, written in Fortran 77, of this model.

PROGRAM FEM

```
INTEGER NEND,WNUM,COUNW
REAL*8 FTIMER(500),FTIMEI(500)
REAL*8 MEMO(500,500),LOSS(500,1000),L(500),VRATIO
COMPLEX ERRO11(250),ERRO12(250),ERRO21(250),ERRO22(250)
COMPLEX*16 SUM,DISP,ERRO1(250),ERRO2(250)
COMPLEX TAUYY(500,1000),KCOMPLEX(500,1000),K(500)
CHARACTER FINP*20,FOUT*20,F2OUT*20,F5OUT*20,F6OUT*20
CHARACTER F7OUT*20,F8OUT*20,F9OUT*20
INTEGER ND,NX,NN,NE,E(500,5),BC(500),COUNT,NTIME,ICON
REAL*8 PI,LAMDA,MU,ALPHA,D,H,BETA1,BETA2,W,T,V0,ALPHA0
REAL*8 YIN,DX,Y(500),TINI,DT,TEND,WINI,WDT,WEND
REAL*8 A(500,500),B(500,500),MTIME(500,500)
REAL*8 META1,META2
REAL*8 VISCO1(250),VISCO2(250),RESIST(250)
```

```

REAL*8 PORO,PVISCO,BULKMOD,PERME,YIELD
REAL*8 VMEMO(250)
COMPLEX U(20,500),FBC(500),FTIME(500),F(500)
COMPLEX PG(20,500),VELO(250)
COMMON /A/ ND,NX,NN,NE,E,BC,COUNT,NTIME
COMMON /B/PI,LAMDA,MU,ALPHA,D,H,BETA1,BETA2, W,T,VO,
      ALPHA0
COMMON YIN,DX,Y,TINI,DT,TEND,WINI,WDT,WEND
COMMON A,B,MTIME
COMMON /C/ U,FBC,FTIME,F
COMMON /D/ META1,META2
COMMON /E/ VISCO1,VISCO2,RESIST
COMMON /F/ PORO,PVISCO,BULKMOD,PERME,YIELD
C **** INPUT FILE
      FINP='SIL.INP'
C **** OUTPUT FILES
      FOUT='DISP.OUT'
      F5OUT='PGRAD.OUT'
      F6OUT='VISCO.OUT'
      F7OUT='REAL.OUT'
      F9OUT='MODULUS.OUT'
32  FORMAT(A20)
      OPEN(2,FILE=FINP,STATUS='OLD')
      OPEN(3,FILE=FOUT,STATUS='UNKNOWN')
      OPEN(7,FILE=F5OUT,STATUS='UNKNOWN')
      OPEN(8,FILE=F6OUT,STATUS='UNKNOWN')
      OPEN(9,FILE=F7OUT,STATUS='UNKNOWN')
      OPEN(11,FILE=F9OUT,STATUS='UNKNOWN')
      CALL DATAIN
      WNUM=(WEND-WINI)/WDT+1

```

```

NEND=NTIME
WRITE(11,*) 'COMPLEX MODULUS AS A FUNCTION OF W(rad/s)'
WRITE(11,*) ' w(rad/s) K(w) (Pa) Loss Tan'
WRITE(11,*) ' -----'
DO 101 COUNW=1,WNUM
W=WINI+(COUNW-1)*WDT
CALL INIT
C **** STRESS IN Y DIRECTION at y=d for I.C. (T=0)
TAUYY(COUNW,1)=((LAMDA+2.0*MU)*((U(1,NN)-
U(1,NN-1))/H)-ALPHA*U(1,2*NN))
C **** COMPLEX MODULUS FOR INITIAL CONDITIONS (T=0)
KCOMPLEX(COUNW,1)=TAUYY(COUNW,1)/(DISP(0.0,V0,W)/D)
LOSS(COUNW,1)=AIMAG(KCOMPLEX(COUNW,1))/
REAL(KCOMPLEX(COUNW,1))
TEND=(6.2831853)/W
DT=TEND/NTIME
ICON=NEND+1
DO 100 COUNT=2,NEND+1
T=TINI+(COUNT-1)*DT
MM=1
WRITE (8,*) 'VISCOSITIES FOR TIME=',T
140 DO 142 I=1,NN
RESIST(I)=(VISCO1(I)*PORO)/PERME
142 CONTINUE
META1=(ALPHA)/(PERME*PORO)
META2=1.0D0/(BULKMOD*PERME*PORO)
WRITE(8,*) 'ITERATION #=',MM
99 CALL APPBOUN
CALL ASSEMBLY
CALL BOUNDARY

```



```

DO 166 JJ=1,2*NN
FTIMER(JJ)=REAL(FTIME(JJ))
FTIMEI(JJ)=AIMAG(FTIME(JJ))
166 CONTINUE
DO 168 II=1,2*NN
DO 168 JJ=1,2*NN
MEMO(II,JJ)=MTIME(II,JJ)
168 CONTINUE
CALL GAUSSJ(MEMO,2*NN,500,FTIMEI,1,1)
CALL GAUSSJ(MTIME,2*NN,500,FTIMER,1,1)
DO 63 I=1,2*NN
U(COUNT,I)=CMPLX(FTIMER(I),FTIMEI(I))
63 CONTINUE
C *** OBTAIN PRESSURE GRADIENT FROM THE PRESSURE VALUES
C *** OBTAIN dP FOR THE FIRST & LAST NODES USING FORWARD &
C *** BACKWARD DIFFERENCE
PG(COUNT,1)=(1.0/H)*(U(COUNT,NN+2)-U(COUNT,NN+1))
PG(COUNT,NN)=(1.0/H)*(U(COUNT,2*NN)-U(COUNT,2*NN-1))
C *** OBTAIN dP FOR THE OTHER NODES USING CENTRAL DIFFERENCE
117 DO 854 IP=2,NE
PG(COUNT,IP)=(1.0/(2.0*H))*(U(COUNT,IP+NN+1)
-U(COUNT,IP+NN-1))
854 CONTINUE
DO 855 IP=1,NN
C *** OBTAIN THE VELOCITY USING MODIFIED DARCY'S LAW
VELO(IP)=(-PERME/VISCO1(IP))*PG(COUNT,IP)
C *** CALCULATE APPARENT VISCOSITY
VISCO2(IP)=PVISCO/(1-(ALPHA0/ABS(REAL(PG(COUNT,IP))))))
C *** To verify with exact solution & to avoid singularity, use;
C VISCO2(IP)=VISCO1(IP)

```

```

C *****
      WRITE(8,851) VISCO1(IP),VISCO2(IP),VISCO1(IP)/VISCO2(IP)
851  FORMAT(2x,E14.7,3x,E14.7,5x,E14.7)
      VMEMO(IP)=VISCO1(IP)
      VISCO1(IP)=(VISCO2(IP)+VMEMO(IP))/2.0
      WRITE(7,*) PG(COUNT,IP)
855  CONTINUE
      MM=MM+1
      WRITE(3,*) '**** U & P FOR T=',T,' ****'
C *** MM IS THE # OF ITERATIONS
      IF (MM.GT.50) GOTO 111
      GOTO 140
111  WRITE(9,*) '*** RESULTS FOR W=',W,' T=',TINI+(COUNT-1)*DT
      WRITE(9,*) 'Displacem. Pressure Pres.Grad. Viscosity1
                Viscosity2'
      WRITE(9,*) "-----  -----  -----  -----
                -----"
C *** Check if visco converges & if it doesn't skip that time step
C *** Calculate average modulus
      DO 69 II=1,NN
      VRATIO=VMEMO(II)/VISCO2(II)
      IF((VRATIO.GT.1.00001).OR.(VRATIO.LT.0.99).OR.
        (VISCO2(NN).LT.0.0)) THEN
      ICON=ICON-1
      GOTO 113
      ELSE
      GOTO 69
      ENDIF
69  CONTINUE
C *** STRESS IN Y DIRECTION AT y=d FOR TIME T

```

```

    TAUYY(COUNW,COUNT)=(LAMDA+2.0*MU)*((U(COUNT,NN)-
        U(COUNT,NN-1))/H)-ALPHA*U(COUNT,2*NN)
C *** COMPLEX MODULUS FOR TIME T
    KCOMPLEX(COUNW,COUNT)=TAUYY(COUNW,COUNT)/
        (DISP(T,V0,W)/D)
    LOSS(COUNW,COUNT)=AIMAG(KCOMPLEX(COUNW,COUNT))/
        REAL(KCOMPLEX(COUNW,COUNT))
113 DO 76 I=1,NN
    WRITE(9,424) REAL(U(COUNT,I)),REAL(U(COUNT,NN+I)),REAL(PG
        (COUNT,I)),VMEMO(I),VISCO2(I),VMEMO(I)/VISCO2(I)
424 FORMAT(1x,E10.4,2x,F10.1,3x,F12.1,2x,E12.6,2x,E12.6,2x,F7.5)
    76 CONTINUE
    100 CONTINUE
C *** OBTAIN AVERAGE STORAGE AND LOSS MODULUS
    K(COUNW)=CMPLX(0.0,0.0)
    L(COUNW)=0.0
    DO 108 I=1,NEND+1
    K(COUNW)=K(COUNW)+KCOMPLEX(COUNW,I)
    L(COUNW)=L(COUNW)+LOSS(COUNW,I)
108 CONTINUE
    K(COUNW)=K(COUNW)/(ICON)
    L(COUNW)=L(COUNW)/(ICON)
    WRITE(11,138) W,REAL(K(COUNW)),L(COUNW)
138 FORMAT(3x,F9.4,2x,E14.6,2x,F9.6)
101 CONTINUE
    STOP
    END

COMPLEX*16 FUNCTION DISP(T,V0,W)
REAL*8 T,V0,W

```

```

DISP=CMPLX(V0*COS(W*T),V0*SIN(W*T))
RETURN
END

```

SUBROUTINE INIT

```

INTEGER ND,NX,NN,NE,E(500,5),BC(500),COUNT,NTIME
REAL*8 PI,LAMDA,MU,ALPHA,D,H,BETA1,BETA2,W,T,V0,ALPHA0
REAL*8 YIN,DX,Y(500),TINI,DT,TEND,WINI,WDT,WEND
REAL*8 A(500,500),B(500,500),MTIME(500,500)
COMPLEX U(20,500),FBC(500),FTIME(500),F(500)
REAL*8 META1,META2
REAL*8 VISCO1(250),VISCO2(250),RESIST(250)
REAL*8 PORO,PVISCO,BULKMOD,PERME,YIELD
REAL*8 RO
COMPLEX*16 OMEGA,C1,C2
COMMON /A/ ND,NX,NN,NE,E,BC,COUNT,NTIME
COMMON /B/ PI,LAMDA,MU,ALPHA,D,H,BETA1,BETA2,W,T,V0,
      ALPHA0
COMMON YIN,DX,Y,TINI,DT,TEND,WINI,WDT,WEND
COMMON A,B,MTIME
COMMON /C/ U,FBC,FTIME,F
COMMON /D/ META1,META2
COMMON /E/ VISCO1,VISCO2,RESIST
COMMON /F/ PORO,PVISCO,BULKMOD,PERME,YIELD
C *** INITIAL CONDITIONS FOR DISPLACEMENT AND PRESSURE
BETA1=(PVISCO*ALPHA)/(PERME*PORO)
BETA2=PVISCO/(BULKMOD*PERME*PORO)
RO=BETA2+(BETA1*ALPHA)/(LAMDA+2.0*MU)
OMEGA=CMPLX(1.0,1.0)*DSQRT(0.5*RO*W)
C2=(V0/D)/((BETA2/BETA1)*(EXP(OMEGA*D))+EXP(-OMEGA*D))+

```

```

      (ALPHA/((LAMDA+2.0*MU)*OMEGA*D))*(EXP(OMEGA*D)
      -EXP(-OMEGA*D)))
C1=(-C2)*(EXP(OMEGA*D)+EXP(-OMEGA*D))
DO 31 II=1,NN
U(1,II)=(-BETA2/BETA1)*C1*(H*(II-1))+(ALPHA/((LAMDA+2.0*MU)*
      OMEGA))*C2*(EXP(OMEGA*(H*(II-1)))-EXP(-OMEGA*(H*(II
      -1))))
U(1,II)=U(1,II)*CMPLX(1.0,0.0)
U(1,II+NN)=C1+C2*(EXP(OMEGA*(H*(II-1)))+EXP(-OMEGA*
      (H*(II-1))))
U(1,II+NN)=U(1,II+NN)*CMPLX(1.0,0.0)
31 CONTINUE
END

```

SUBROUTINE DATAIN

```

COMPLEX SUM,DISP
INTEGER ND,NX,NN,NE,E(500,5),BC(500),COUNT,NTIME
REAL*8 PI,LAMDA,MU,ALPHA,D,H,BETA1,BETA2,W,T,V0,ALPHA0
REAL*8 YIN,DX,Y(500),TINI,DT,TEND,WINI,WDT,WEND
REAL*8 A(500,500),B(500,500),MTIME(500,500)
COMPLEX U(20,500),FBC(500),FTIME(500),F(500)
REAL*8 META1,META2
REAL*8 VISCO1(250),VISCO2(250),RESIST(250)
REAL*8 PORO,PVISCO,BULKMOD,PERME,YIELD,FIELD
COMMON /A/ ND,NX,NN,NE,E,BC,COUNT,NTIME
COMMON /B/ PI,LAMDA,MU,ALPHA,D,H,BETA1,BETA2,W,T,V0,
      ALPHA0
COMMON YIN,DX,Y,TINI,DT,TEND,WINI,WDT,WEND
COMMON A,B,MTIME
COMMON /C/ U,FBC,FTIME,F

```

```

COMMON /D/ META1,META2
COMMON /E/ VISCO1,VISCO2,RESIST
COMMON /F/ PORO,PVISCO,BULKMOD,PERME,YIELD
C ND : # OF NODES IN AN ELEMENT
C NX : # OF NODES IN X-DIRECTION
C NN : # OF NODES IN THE DOMAIN (NN=ND FOR 1D)
C YIN : INITIAL Y COORDINATE
C DX : MESH SIZE IN Y DIRECTION
C NE : # OF ELEMENTS
C Y(I) : COORDINATES OF NODE POINTS
C E(I,J) : NODE NUMBERS IN THE ELEMENT
C BC(I) : BOUNDARY CONDITION INDEX
C FBC(I) : BOUNDARY CONDITION VECTOR
C D : HEIGHT
C V0 : AMPLITUDE OF DISPLACEMENT INPUT
C W : FREQUENCY OF DISPLACEMENT INPUT
C T : TIME
C *** SET CONSTANTS
      PI=3.1415927D0
      LAMDA=1.29D08
      MU=9.79D07
      ALPHA=0.98D0
      D=0.0254D0
      T=0.0D0
      PORO=0.48D0
      PERME=3.62D-12
      FIELD=1.0
      PVISCO=0.05D0-0.02273D0*FIELD
      YIELD=103.0D0*(FIELD**2)
      BULKMOD=5.58D08

```

```

C *** SET ELEMENTAL DATA
  ND=2
  READ(2,*) TINI,NTIME
  READ(2,*) WINI,WDT,WEND
  READ(2,*) V0
  READ(2,*) NE
  NN=NE+1
  H=D/NE
  DX=D/NE
  YIN=0.0
  DO 141 I=1,NN
  VISCO1(I)=PVISCO
141 CONTINUE
  ALPHA0=(0.001/DSQRT(PERME))*YIELD
C *** SET MASTER VECTORS TO ZERO
  DO 88 I=1,2*NN
  F(I)=0.0D0
  DO 88 J=1,2*NN
  A(I,J)=0.0D0
  B(I,J)=0.0D0
 88 CONTINUE
C *** GENERATE NODAL COORDINATES
  DO 10 I=1,NN
  Y(I)=YIN+(I-1)*DX
 10 CONTINUE
C *** GENERATE ELEMENTAL NODES
  DO 11 I=1,NE
  E(I,1)=I
  E(I,2)=I+1
 11 CONTINUE

```

```

C *** SET BOUNDARY CONDITIONS & BC INDEX TO ZERO
      DO 12 I=1,2*NN
      FBC(I)=CMPLX(0.0,0.0)
      BC(I)=0
12   CONTINUE
      END

C *** APPLY BOUNDARY CONDITIONS
      SUBROUTINE APPBOUN
      COMPLEX SUM,DISP
      INTEGER ND,NX,NN,NE,E(500,5),BC(500),COUNT,NTIME
      REAL*8 PI,LAMDA,MU,ALPHA,D,H,BETA1,BETA2,W,T,V0,ALPHA0
      REAL*8 YIN,DX,Y(500),TINI,DT,TEND,WINI,WDT,WEND
      REAL*8 A(500,500),B(500,500),MTIME(500,500)
      COMPLEX U(20,500),FBC(500),FTIME(500),F(500)
      REAL*8 META1,META2
      REAL*8 VISCO1(250),VISCO2(250),RESIST(250)
      REAL*8 PORO,PVISCO,BULKMOD,PERME,YIELD
      COMMON /A/ ND,NX,NN,NE,E,BC,COUNT,NTIME
      COMMON /B/ PI,LAMDA,MU,ALPHA,D,H,BETA1,BETA2,W,T,V0,
           ALPHA0
      COMMON YIN,DX,Y,TINI,DT,TEND,WINI,WDT,WEND
      COMMON A,B,MTIME
      COMMON /C/ U,FBC,FTIME,F
      COMMON /D/ META1,META2
      COMMON /E/ VISCO1,VISCO2,RESIST
      COMMON /F/ PORO,PVISCO,BULKMOD,PERME,YIELD
C *** RESET THE SOLUTION VECTOR (U)
      DO 93 I=1,2*NN
      U(COUNT,I)=CMPLX(0.0,0.0)

```


93 CONTINUE

C *** SET BOUNDARY CONDITIONS INDEX

C *** INDEX=0 IF BC IS NOT SPECIFIED FOR THE NODE

C *** INDEX=1 IF FUNCTION ITSELF IS SPECIFIED FOR THE NODE

C *** INDEX=2 IF DERIVATIVE OF FUNCTION IS SPECIFIED FOR THE

C *** NODE

C *****

C *** BC INDEX & BC FOR DISPLACEMENT FIELD

BC(1)=1

FBC(1)=CMPLX(0.0,0.0)

U(COUNT,1)=CMPLX(0.0,0.0)

BC(NN)=1

FBC(NN)=DISP(T,V0,W)

U(COUNT,NN)=DISP(T,V0,W)

BC(2*NN)=1

FBC(2*NN)=CMPLX(0.0,0.0)

U(COUNT,2*NN)=CMPLX(0.0,0.0)

C *** BC INDEX & BC FOR PRESSURE FIELD

C *** FOR DERIVATIVE B.C.; F(I)=B.C.

BC(NN+1)=2

FBC(NN+1)=CMPLX(0.0,0.0)

F(NN+1)=FBC(NN+1)

END

SUBROUTINE COEFF(AE1,AE2,AE3,AE4,BE1,BE2,BE3,BE4)

REAL*8 AE1(2,2),AE2(2,2),AE3(2,2),AE4(2,2)

REAL*8 BE1(2,2),BE2(2,2),BE3(2,2),BE4(2,2)

REAL*8 FE(2)

COMPLEX SUM,DISP

INTEGER ND,NX,NN,NE,E(500,5),BC(500),COUNT,NTIME

```

REAL*8 PI,LAMDA,MU,ALPHA,D,H,BETA1,BETA2,W,T,V0,ALPHA0
REAL*8 YIN,DX,Y(500),TINI,DT,TEND,WINI,WDT,WEND
REAL*8 A(500,500),B(500,500),MTIME(500,500)
COMPLEX U(20,500),FBC(500),FTIME(500),F(500)
REAL*8 META1,META2
REAL*8 VISCO1(250),VISCO2(250),RESIST(250)
REAL*8 PORO,PVISCO,BULKMOD,PERME,YIELD
COMMON /A/ ND,NX,NN,NE,E,BC,COUNT,NTIME
COMMON /B/ PI,LAMDA,MU,ALPHA,D,H,BETA1,BETA2,W,T,V0,
      ALPHA0
COMMON YIN,DX,Y,TINI,DT,TEND,WINI,WDT,WEND
COMMON A,B,MTIME
COMMON /C/ U,FBC,FTIME,F
COMMON /D/ META1,META2
COMMON /E/ VISCO1,VISCO2,RESIST
COMMON /F/ PORO,PVISCO,BULKMOD,PERME,YIELD
C** AE1 : 2X2 ELEMENTAL DISPL. & PRESS. COEFF. MATRIX (Mu)
C** AE2 : 2X2 ELEMENTAL DISPL. & PRESS. COEFF. MATRIX (Mp1)
C** AE3 : 2X2 ELEMENTAL DISPL. & PRESS. COEFF. MATRIX (zero)
C** AE4 : 2X2 ELEMENTAL DISPL. & PRESS. COEFF. MATRIX (Mp2)
C** BE1 : 2X2 ELEMENTAL DISPL. & PRESS. DERIV. COEFF. MATRIX (zero)
C** BE2 : 2X2 ELEMENTAL DISPL. & PRESS. DERIV. COEFF. MATRIX (zero)
C** BE3 : 2X2 ELEM. DISPL. & PRESS. DERIV. COEFF. MATRIX (MuDOT)
C** BE4 : 2X2 ELEM. DISPL. & PRESS. DERIV. COEFF. MATRIX (MpDOT)
C** A1 : PART OF ELEMENTAL DISPL. & PRESS. COEFF. MATRIX (Mu)
C** A2 : PART OF ELEMENTAL DISPL. & PRESS. COEFF. MATRIX (Mp1)
C** A3 : PART OF ELEMENTAL DISPL. & PRESS. COEFF. MATRIX (zero)
C** A4 : PART OF ELEMENTAL DISPL. & PRESS. COEF. MATRIX (Mp2)
C** B1 : PART OF ELEM. DISPL. & PRESS. DERIV. COEF. MATRIX (zero)
C** B2 : PART OF ELEM. DISPL. & PRESS. DERIV. COEF. MATRIX (zero)

```

C B3 : PART OF ELEM. DISPL. & PRESS. DERIV. COEF. MATRIX (MuDOT)**

C B4 : PART OF ELEM. DISPL. & PRESS. DERIV. COEF. MATRIX (MpDOT)**

C A : DISPLACEMENT & PRESSURE COEFFICIENT MATRIX**

C B : DISPLACEMENT & PRESSURE DERIVATIVES COEFF. MATRIX**

$$AE1(1,1)=(LAMDA+2.0D0*MU)/H$$

$$AE1(1,2)=-LAMDA+2.0D0*MU)/H$$

$$AE1(2,1)=AE1(1,2)$$

$$AE1(2,2)=(LAMDA+2.0D0*MU)/H$$

$$AE2(1,1)=-ALPHA)/2.0D0$$

$$AE2(1,2)=ALPHA)/2.0D0$$

$$AE2(2,1)=-ALPHA)/2.0D0$$

$$AE2(2,2)=ALPHA)/2.0D0$$

$$AE3(1,1)=0.0D0$$

$$AE3(1,2)=0.0D0$$

$$AE3(2,1)=0.0D0$$

$$AE3(2,2)=0.0D0$$

$$AE4(1,1)=1.0D0/H$$

$$AE4(1,2)=-1.0D0/H$$

$$AE4(2,1)=-1.0D0/H$$

$$AE4(2,2)=1.0D0/H$$

$$BE1(1,1)=0.0D0$$

$$BE1(1,2)=0.0D0$$

$$BE1(2,1)=0.0D0$$

$$BE1(2,2)=0.0D0$$

$$BE2(1,1)=0.0D0$$

$$BE2(1,2)=0.0D0$$

$$BE2(2,1)=0.0D0$$

$$BE2(2,2)=0.0D0$$

$$FE(1)=0.0D0$$

$$FE(2)=0.0D0$$

END

SUBROUTINE ASSEMBLY

REAL*8 AE1(2,2),AE2(2,2),AE3(2,2),AE4(2,2),AE44(2,2)

REAL*8 A1(250,250),A2(250,250),A3(250,250),A4(250,250)

REAL*8 BE1(2,2),BE2(2,2),BE3(2,2),BE4(2,2)

REAL*8 B1(250,250),B2(250,250),B3(250,250),B4(250,250)

REAL*8 FE(2)

COMPLEX SUM,DISP

INTEGER ND,NX,NN,NE,E(500,5),BC(500),COUNT,NTIME

REAL*8 PI,LAMDA,MU,ALPHA,D,H,BETA1,BETA2,W,T,V0,ALPHA0

REAL*8 YIN,DX,Y(500),TINI,DT,TEND,WINI,WDT,WEND

REAL*8 A(500,500),B(500,500),MTIME(500,500)

COMPLEX U(20,500),FBC(500),FTIME(500),F(500)

REAL*8 META1,META2

REAL*8 VISCO1(250),VISCO2(250),RESIST(250)

REAL*8 PORO,PVISCO,BULKMOD,PERME,YIELD

REAL*8 FACTOR,TETE

COMMON /A/ ND,NX,NN,NE,E,BC,COUNT,NTIME

COMMON /B/ PI,LAMDA,MU,ALPHA,D,H,BETA1,BETA2,W,T,V0,
ALPHA0

COMMON YIN,DX,Y,TINI,DT,TEND,WINI,WDT,WEND

COMMON A,B,MTIME

COMMON /C/ U,FBC,FTIME,F

COMMON /D/ META1,META2

COMMON /E/ VISCO1,VISCO2,RESIST

COMMON /F/ PORO,PVISCO,BULKMOD,PERME,YIELD

C *** RESET COEFFICIENT MATRICES

DO 20 I=1,NN

DO 20 J=1,NN

```

A1(I,J)=0.0D0
A2(I,J)=0.0D0
A3(I,J)=0.0D0
A4(I,J)=0.0D0
B1(I,J)=0.0D0
B2(I,J)=0.0D0
B3(I,J)=0.0D0
B4(I,J)=0.0D0
20 CONTINUE
C *** CONSTRUCT 4 PARTS OF MAJOR MATRICES A & B
DO 30 L=1,NE
CALL COEFF(AE1,AE2,AE3,AE4,BE1,BE2,BE3,BE4)
AE44(1,1)=(1.0/(6.0*H))*((VISCO1(L+1)**2)-2.0*(VISCO1(L)**2)
      +VISCO1(L+1)*VISCO1(L))
AE44(1,2)=-AE44(1,1)
AE44(2,1)=(1.0/(6.0*H))*(2.0*(VISCO1(L+1)**2)-(VISCO1(L)**2)
      -VISCO1(L+1)*VISCO1(L))
AE44(2,2)=-AE44(2,1)
BE3(1,1)=(-META1/6.0)*(2.0*VISCO1(L)+VISCO1(L+1))
BE3(1,2)=-BE3(1,1)
BE3(2,1)=(-META1/6.0)*(2.0*VISCO1(L+1)+VISCO1(L))
BE3(2,2)=-BE3(2,1)
BE4(1,1)=((META2*H)/12.0)*(VISCO1(L+1)+3.0*VISCO1(L))
BE4(1,2)=((META2*H)/12.0)*(VISCO1(L+1)+VISCO1(L))
BE4(2,1)=BE4(1,2)
BE4(2,2)=((META2*H)/12.0)*(VISCO1(L)+3.0*VISCO1(L+1))
DO 30 I=1,ND
IB=E(L,I)
DO 30 J=1,ND
JB=E(L,J)

```

```

A1(IB,JB)=A1(IB,JB)+AE1(I,J)
A2(IB,JB)=A2(IB,JB)+AE2(I,J)
A3(IB,JB)=A3(IB,JB)+AE3(I,J)
A4(IB,JB)=A4(IB,JB)+AE4(I,J)+AE44(I,J)
B1(IB,JB)=B1(IB,JB)+BE1(I,J)
B2(IB,JB)=B2(IB,JB)+BE2(I,J)
B3(IB,JB)=B3(IB,JB)+BE3(I,J)
B4(IB,JB)=B4(IB,JB)+BE4(I,J)
30 CONTINUE
C *** ASSEMBLE MAJOR MATRICES A AND B FROM 4 PARTS
DO 44 I=1,NN
DO 44 J=1,NN
A(I,J)=A1(I,J)
A(I,J+NN)=A2(I,J)
A(I+NN,J)=A3(I,J)
A(I+NN,J+NN)=A4(I,J)
B(I,J)=B1(I,J)
B(I,J+NN)=B2(I,J)
B(I+NN,J)=B3(I,J)
B(I+NN,J+NN)=B4(I,J)
44 CONTINUE
C *** OBTAIN MTIME & FTIME MATRICES USING TIME DEPENDENCY
C TETE=0 ==> Forward Difference Scheme (Gives Singularity in B(I,J))
C TETE=1/2 ==> Central (Improved Euler, Crank-Nicholsan) Difference Scheme
C TETE=1 ==> Backward Difference Scheme
C TETE=2/3 ==> Galerkin finite element
TETE=2.0/3.0
DO 71 I=1,2*NN
SUM=CMPLX(0.0,0.0)
DO 72 J=1,2*NN

```

```

MTIME(I,J)=B(I,J)+TETE*DT*A(I,J)
SUM=SUM+(B(I,J)-(1.0-TETE)*DT*A(I,J))*U((COUNT-1),J)
72 CONTINUE
FTIME(I)=DT*F(I)+SUM
71 CONTINUE
END

```

SUBROUTINE BOUNDARY

```

COMPLEX SUM,DISP
INTEGER ND,NX,NN,NE,E(500,5),BC(500),COUNT,NTIME
REAL*8 PI,LAMDA,MU,ALPHA,D,H,BETA1,BETA2,W,T,V0,ALPHA0
REAL*8 YIN,DX,Y(500),TINI,DT,TEND,WINI,WDT,WEND
REAL*8 A(500,500),B(500,500),MTIME(500,500)
COMPLEX U(20,500),FBC(500),FTIME(500),F(500)
REAL*8 META1,META2
REAL*8 VISCO1(250),VISCO2(250),RESIST(250)
REAL*8 PORO,PVISCO,BULKMOD,PERME,YIELD
COMMON /A/ ND,NX,NN,NE,E,BC,COUNT,NTIME
COMMON /B/ PI,LAMDA,MU,ALPHA,D,H,BETA1,BETA2,W,T,V0,
ALPHA0
COMMON YIN,DX,Y,TINI,DT,TEND,WINI,WDT,WEND
COMMON A,B,MTIME
COMMON /C/ U,FBC,FTIME,F
COMMON /D/ META1,META2
COMMON /E/ VISCO1,VISCO2,RESIST
COMMON /F/ PORO,PVISCO,BULKMOD,PERME,YIELD
DO 51 I=1,2*NN
IF (BC(I).EQ.0) GOTO 51
IF (BC(I).EQ.2) GOTO 51
DO 52 J=1,2*NN

```

```

      IF (I.NE.J) GOTO 49
      MTIME(I,J)=1.0D0
      GOTO 52
49    FTIME(J)=FTIME(J)-MTIME(J,I)*U(COUNT,I)
      MTIME(I,J)=0.0D0
      MTIME(J,I)=0.0D0
52    CONTINUE
      FTIME(I)=FBC(I)
51    CONTINUE
      END

```

C* SOLUTION OF THE ALGEBRAIC EQUATIONS**

SUBROUTINE GAUSSJ(A,N,NP,B,M,MP)

PARAMETER (NMAX=500)

INTEGER IPIV(NMAX),INDXR(NMAX),INDXC(NMAX)

REAL *8 A(NP,NP),B(NP,NP)

REAL *8 BIG,DUM,PIVINV

DO 11 J=1,N

IPIV(J)=0

11 CONTINUE

DO 22 I=1,N

BIG=0.0D0

DO 13 J=1,N

IF(IPIV(J).NE.1)THEN

DO 12 K=1,N

IF (IPIV(K).EQ.0) THEN

IF (ABS(A(J,K)).GE.BIG)THEN

BIG=ABS(A(J,K))

IROW=J

ICOL=K


```

    ENDIF
    ELSE IF (IPIV(K).GT.1) THEN
    PAUSE 'Singular matrix'
    ENDIF
12  CONTINUE
    ENDIF
13  CONTINUE
    IPIV(ICOL)=IPIV(ICOL)+1
    IF (IROW.NE.ICOL) THEN
    DO 14 L=1,N
    DUM=A(IROW,L)
    A(IROW,L)=A(ICOL,L)
    A(ICOL,L)=DUM
14  CONTINUE
    DO 15 L=1,M
    DUM=B(IROW,L)
    B(IROW,L)=B(ICOL,L)
    B(ICOL,L)=DUM
15  CONTINUE
    ENDIF
    INDXR(I)=IROW
    INDXC(I)=ICOL
    IF (A(ICOL,ICOL).EQ.0.) PAUSE 'Singular matrix.'
    PIVINV=1.0D0/A(ICOL,ICOL)
    A(ICOL,ICOL)=1.0D0
    DO 16 L=1,N
    A(ICOL,L)=A(ICOL,L)*PIVINV
16  CONTINUE
    DO 17 L=1,M
    B(ICOL,L)=B(ICOL,L)*PIVINV

```

```

17  CONTINUE
    DO 21 LL=1,N
      IF(LL.NE.ICOL)THEN
        DUM=A(LL,ICOL)
        A(LL,ICOL)=0.0D0
        DO 18 L=1,N
          A(LL,L)=A(LL,L)-A(ICOL,L)*DUM
18  CONTINUE
        DO 19 L=1,M
          B(LL,L)=B(LL,L)-B(ICOL,L)*DUM
19  CONTINUE
        ENDIF
21  CONTINUE
22  CONTINUE
    DO 24 L=N,1,-1
      IF(INDXR(L).NE.INDXC(L))THEN
        DO 23 K=1,N
          DUM=A(K,INDXR(L))
          A(K,INDXR(L))=A(K,INDXC(L))
          A(K,INDXC(L))=DUM
23  CONTINUE
        ENDIF
24  CONTINUE
    RETURN
    END

```